UNIVERSITY OF OKLAHOMA

GRADUATE COLLEGE

CONVERSION OF ALICYCLIC COMPOUNDS FOR IMPROVEMENT OF FUEL PROPERTIES

A DISSERTATION

SUBMITTED TO THE GRADUATE FACULTY

in partial fulfillment of the requirement for the

degree of

Doctor of Philosophy

By

MALEE SANTIKUNAPORN
Norman, Oklahoma
2006

CONVERSION OF ALICYCLIC COMPOUNDS FOR
IMPROVEMENT OF FUEL PROPERTIES

A DISSERTATION APPROVED FOR THE
SCHOOL OF CHEMICAL, BIOLOGICAL AND MATERIAL ENGINEERING

BY

_____
Daniel E. Resasco

_____
Lance L. Lobban

_____
Richard G. Mallinson

_____
George B. Richter-Addo

_____
Walter E. Alvarez

ACKNOWLEDGMENTS

First of all, I would like to express my deep appreciation and admiration to my advisor, Dr. Daniel E. Resasco, for his generous guidance and encouragement, and for a partial financial support. I am grateful to Dr. Walter E. Alvarez, Dr. Lance L. lobban, and Dr. Richard G. Mallinson for their valuable contributions and for serving on my doctoral committees. In addition, thank you to Dr. George B. Richter-Addo for serving as member of my doctoral committee and for providing an enjoyable course.

I would like to thank my colleagues both in the OU Heterogeneous catalysis group and in the OU Nanotube group as well as my friends (both Thai and other countries) from outside the work place for their help and friendship. Their friendship means a lot when I am in Norman without my family. Particular thank to Dr. Jongpatiwut, Dr. Sergio, Phuong, Steven, and Roboto for their company and enjoyable time in the lab. Special Dr. Beltramone has given support when frustrations and discouragements appeared. Also, I would like to express appreciation to “Jim” -ConocoPhillips” for finding me equipments, especially a high pressure pump when I first started this project, “Jim”-glass blower and “Laura”-chemical store for their friendly conversations, and “staff” of the School of Chemical, Biological, and Materials Engineering for their assistant me in many ways such as filing paperwork, ordering chemicals and equipment, and fixing some equipments.

Particular thanks to the Energy Policy and Planning Office of the Ministry of Energy of the Royal Thai Government for Thai scholars studying abroad. I also would like to thank Oklahoma Center for Advancement of Science and Technology (OCAST) and ConocoPhillips for financial support of the ConocoPhillips Catalysis Lab at the University of Oklahoma.

Finally, I would like to thank my parents for their continuous encouragement and moral support in many ways. I also want to thank my sisters and my brothers who have taken good care of our parents during my study time in the United States and for their individual ways for encourage and support me: “P’Nie for visiting me many times in Norman, “P’Noi” for providing me a financial support for many years, “Nut” for supplying me delicious Thai food, “Nee” for making me laugh over the phone, “Porn” for being good taking care of me and taking me with her all the time when we were young and for telling me her incredible stories, “Jubjang” for staying here with me for a year, and “N’Chan and N’Chai” for being good younger brothers. Special thank to my best friend “Lek” who encourage me to study aboard. Last but not least, I would like to thank “P’Gong” who gives me an overwhelming support, patience, and encouragement during my Ph.D. studying time.

TABLE OF CONTENTS

ACKNOWLEDGMENTS iv

TABLE OF CONTENTS vi

LIST OF TABLES xi

LIST OF FIGURES xiv

ABSTRACT xxiii

CHAPTERS

I. INTRODUCTION

1.1 Introduction 1

1.2 Literature Review 8

1.2.1 Ring Opening of Cyclic Compounds on Acid and Bifuctional Catalysts 9

1.2.2 Ring Opening of Non-Aromatic Compounds on Metal Catalysts 21

1.3 Motivation 27

II. EXPERIMENTAL SETUP

2.1 Catalyst Preparation 29

2.1.1 Acidic Zeolite Catalysts 29

2.1.2 Pt-Supported Zeolite Catalysts 30

2.1.3 Metal Catalysts 33

2.2 Catalyst Characterization 33
2.2.1 Temperature Programmed Desorption (TPD) of Adsorbed Ammonia 33
2.2.2 Fourier Transform Infrared (FTIR) of Adsorbed Pyridine 34
2.2.3 Extened X-ray Adsorption Fine Structure (EXAFS) 35
2.2.4 Hydrogen (H_2)Chemisorption 36
2.2.5 Carbon monoxide (CO) Chemisorption 36
2.2.6 Atomic Absorption Spectrometer (AAS) 37
2.2.7 Transmission Electron Microscopy (TEM) 37
2.2.8 Temperature Programmed Oxidation (TPO) 38
2.3 Catalytic Activity Tests 39
2.3.1 Catalytic Activity Test for the Deaction Reaction 39
2.3.1.1 Continuous Flow System 39
2.3.1.2 Pulse System 40
2.3.2 Catalytic Activity Test for the Tetralin Reaction 41
2.3.3 Catalytic Activity Test for the Methylcyclohexane Reaction 42
2.4 Product Analysis 44
2.4.1 The Decalin and Tetralin Reactions 44
2.4.2 The Methylcyclohexane Reaction 47

III. RING OPENING OF DECALIN AND TETRALIN ON HY AND Pt/HY ZEOLITE CATALYSTS

3.1 Introduction 51
3.2 Experimental 55
3.3 Results and Discussion 55

3.3.1 Characterization of Catalysts 55
3.3.2 Catalytic Activity Measurement 57
3.3.2.1 Conversion of Decalin over HY and Metal-HY Catalysts 57
3.3.2.2 Conversion of Isomerically Pure *Cis*- and *Trans*-Decalin 70
3.3.2.3 Conversion of Tetralin 73
3.3.2.4 Tetralin Conversion on Physical Mixtures and Segregated Beds of Pt/SiO_2 and HY Catalysts 78
3.4 Conclusion 83

IV. ENHANCING THE SELECTIVITY OF DECALIN RING CONTRACTION VS. RING OPENING BY TAILORING THE ACID DENSITY AND Pt PARTICLE LOCATION IN Pt/HY CATALYSTS

4.1 Introduction 86
4.2 Experimental 90
4.3 Results and Discussion 91
4.3.1 Characterization of Catalysts 91
4.3.2 Catalytic Activity Measurements 93
4.3.2.1 Conversion of Decalin over HY and Metal-HY Catalysts 93
4.3.2.2 Conversion of Decalin over a Series of Proton-Form Zeolites 102
4.3.2.3 Influence of Metal on the Stereoisomer of Decalin 107

4.4 Conclusion 111

V. RING CONTRACTION AND SELECTIVE RING OPENING OF NAPHTHENIC MOLECULES FOR OCTANE NUMBER IMPROVEMENT

5.1 Introduction 114
5.2 Experimental 121
5.3 Results and Discussion 122
5.3.1 Characterization of Catalysts 122
5.3.2 Catalytic Activity Measurements 124
5.3.2.1 Conversion of Methylcyclohexane over HY and Pt/HY Catalysts 124
5.3.2.2 Evolution of Product Distribution with Conversion 128
5.3.2.3 Conversion of Methylcyclohexane over Ir/SiO_2 Catalyst 146
5.3.2.4 Conversion of Methylcyclohexane on Physical Mixtures and Segregated Beds of Pt/HY and Ir/SiO_2 Catalysts 149
5.4 Conclusion 159

VI. HYDROISOMERIZATION OF METHYLCYCLOHEXANE ON MFI, BEA, FAU ZEOLITES WITH AND WITHOUT Pt METAL

6.1 Introduction 162
6.2 Experimental 166

6.3 Results and Discussion 167
6.3.1 Characterization of Catalysts 167
6.3.2 Catalytic Activity Measurements 173
6.3.2.1 Influence of the Acidic Strength and Pore Structure of Zeolites on the MCH Reaction 173
6.3.2.2 Effect of metal (Pt) on RC Isomers over Pt/MFI, Pt/BEA and Pt/FAU Zeolites 187
6.3.2.3 Effect of the Reaction Temperatures on RC Isomers 203
6.3.2.4 Effect of Acid Density on RC Isomers 205
6.4 Conclusion 211

LITERATURE CITED 213

PUBLICATIONS, PRESENTATIONS AND POSTERS 221

APPENDIX Additional Results for the Decalin Reaction 224

LIST OF TABLES

Table 2.1	A List of catalysts used in the decalin, tetralin, and methylcyclohexane reactions	31
Table 2.2	Structures of some ring contraction and ring opening products	47
Table 2.3	Product names and their research octane number (RON), motor octane number (MON) and specific gravity (Sp. Gr.).	49
Table 3.1	Characterization of acidity of fresh catalysts	56
Table 3.2	Product distribution and conversion of decalin over HY zeolites and Pt/HY catalysts	58
Table 3.3	Conversion of pure *cis*- and *trans*-decalin in pulse reactor on HY3 zeolite	72
Table 3.4	Conversion of tetralin over HY zeolites and Pt/HY catalyst	74
Table 3.5	Conversion of tetralin on physical mixtures of Pt/SiO_2 and HY3 Catalysts.	79
Table 4.1	Characterization of the fresh Pt-containing HY zeolites	91
Table 4.2	Characterization of acidity of fresh catalysts and coke contents of spent catalysts	94

Table 4.3A	Conversion of decalin on HY zeolite and Pt catalysts at two times on stream	97
Table 4.3B	Some RC and RO products from the reaction of decalin on HY zeolite and Pt catalysts after 90 min.	98
Table 4.4	The RC/RO ratio of two different Pt catalysts (PtHY) and PtIE) with almost the same conversion level.	101
Table 4.5A	Conversion of decalin on various HY zeolite with different acid densities at two times on stream	102
Table 4.5B	Some RC and RO products from the reaction of decalin on various HY zeolite after 90 min.	103
Table 4.6A	Conversion of decalin on different Pt supported Y zeolites with different acid densities at two times on stream	108
Table 4.6B	Some RC and RO products from the reaction of decalin on different Pt supported Y zeolites after 90 min.	109
Table 5.1	Acidity of HY and Pt/HY catalysts	122
Table 5.2	Hydrogen chemisorption of Pt/HY and Ir/SiO_2 catalysts	123
Table 5.3	Product distribution of methylcyclohexane reaction on acid catalysts and metal catalyst for two times on stream	126

Table 5.4	Product distribution of methylcyclohexane reaction over Pt/HY catalyst at different temperatures	139
Table 5.5	Product distribution of methylcyclohexane reaction at different reaction system configurations	152
Table 6.1	Characterization of fresh catalysts	168
Table 6.2	The catalytic conversion of methylcyclohexane over various zeolites for two times on stream	175
Table 6.3	The catalytic conversion of methylcyclohexane over various Pt catalysts at 533 K and 563 K.	204
Table 6.4	The catalytic conversion of methylcyclohexane over acidic and bifunctional catalysts	206

LIST OF FIGURES

FIGURE 1.1	Cetane number of naphthalene and its hydrogenation products	4
FIGURE 1.2	Cetane number of decalin and some relavant C_{10} products	6
FIGURE 1.3	Octane number of various low molecular weight hydrocarbons	7
FIGURE 1.4	A proposed reaction network of direct ring opening of decalin reaction over acidic zeolites at 723 K and 0.1 MPa	11
FIGURE 1.5	A proposed reaction network of isomerization and ring opening of decalin reaction over acidic zeolite catalysts at 473-573 K and 2 MPa	13
FIGURE 1.6a	A proposed mechanism for methylcyclohexane reaction on metal catalysts	15
FIGURE 1.6b	A proposed mechanism for methylcyclohexane reaction on acidic catalysts	15
FIGURE 1.6c	A proposed mechanism for methylcyclohexane reaction on bifunctional catalysts	16
FIGURE 1.7	Three major reaction paths for hydrocracking of tetralin	18

FIGURE 1.8	A reaction pathway for hydroconversion of tetralin on bifunctional Pt/zeolite catalyts	20
FIGURE 1.9	Two types of methylcyclopentane adsorption over Pt(111) surface	22
FIGURE 1.10	A dissociative flat adsorption of cyclopentane	23
FIGURE 1.11	A dissociative edgewise adsorption of cyclopentane	24
FIGURE 1.12	A metallocyclobutane intermediate of methylcyclopentane	25
FIGURE 1.13	Hydrogenolysis products of methylcyclopentane	27
FIGURE 2.1	A schematic diagram of the experimental setup of decalin reaction in flow system	40
FIGURE 2.2	A schematic diagram of the experimental setup of decalin reaction in pulse system	41
FIGURE 2.3	A schematic diagram of different catalytic bed configurations for tetralin reaction	42
FIGURE 2.4	A schematic diagram of different catalytic bed configurations for methylcyclohexane reaction	44
FIGURE 3.1	Cetane number of decalin and some relevant products	53
FIGURE 3.2	Total conversion of decalin on various catalysts	60

FIGURE 3.3	Product distribution of decalin ring opening on HY3 at different space velocities	63
FIGURE 3.4	Ring opening (RO) and ring contraction (RC) products of decalin ring opening on various catalysts at varying conversions	65
FIGURE 3.5	RC/RO ratio of decalin ring opening on HY zeolites and Pt/HY at different conversions	66
FIGURE 3.6	Yield of two relevant products as a function of conversion	69
FIGURE 3.7	Pure *cis*- and *trans*-decalin in flow mode on (a) HY3 and (b) Pt/HY	71
FIGURE 3.8	Product distribution of tetralin ring opening on Pt/HY	75
FIGURE 3.9	RC/RO ratio of tetralin ring opening on HY3 and Pt/HY	77
FIGURE 4.1	Cetane number of some C_{10} compounds	86
FIGURE 4.2	A strategy for improving cetane number or octane number from aromatics	88
FIGURE 4.3	Effect of metal supported catalysts on the turnover frequency for decalin ring opening	95

FIGURE 4.4	RC/RO ratio of decalin ring opening on the HY zeolite and metal (Pt) supported on HY zeolites at different conversions	100
FIGURE 4.5	Total conversion of decalin on various catalysts	104
FIGURE 4.6	Effect of Brønsted acid site over proton-form zeolites on RC/RO ratio at the same conversion	106
FIGURE 4.7	Comparison between the Pt supported on zeolites and the bare zeolites on the *trans/cis*-decalin ratio on various conversions	110
FIGURE 5.1	Possible products from methylcyclohexane and their research octane number (RON) and their motor octane number (MON)	116
FIGURE 5.2	Hydrogenolysis products on metal catalysts from ring opening reactions of C_7 ring contraction compounds and their corresponding research octane number (RON) and motor octane number (MON)	118
FIGURE 5.3	TEM images of the Pt/HY and Ir/SiO2 samples	124
FIGURE 5.4a	Product distribution of methylcyclohexane reaction over HY as a function of conversion	129
FIGURE 5.4b	Product distribution of methylcyclohexane reaction over Pt/HY as a function of conversion	130

FIGURE 5.5	Isomerized RC products of methylcyclohexane reaction over HY (solid symbols) and Pt/HY (open symbols) at varying conversion	132
FIGURE 5.6a	Selectivities of isomerized RC products on HY and Pt/HY at the same conversion (~16%)	134
FIGURE 5.6b	Selectivities of isomerized RC products on HY and Pt/HY at the same conversion (~30%)	135
FIGURE 5.7	Carbocation chemistry for the ring contraction reactions	137
FIGURE 5.8	Hydride transfer paths involving C_5-ring carbocation intermediates	137
FIGURE 5.9a	Product distributions of methylcyclohexane reaction over Pt/HY at different reaction temperatures	140
FIGURE 5.9b	Selecitivities to ring contraction products of methylcyclohexane reaction over Pt/HY at different reaction temperatures	141
FIGURE 5.10a	Research octane number (RON) of the product mixture as a function of methylcyclohexane reaction	144
FIGURE 5.10b	Motor octane number (MON) of the product mixture as a function of methylcyclohexane reaction	145
FIGURE 5.11a	Product distributions of methylcyclohexane reaction over Ir/SiO_2 at different reaction temperatures	147

FIGURE 5.11b	The distribution of ring opening and cracking products of methylcyclohexane reaction over Ir/SiO_2 at different reaction temperatures	148
FIGURE 5.12	Schematic reaction system configurations	150
FIGURE 5.13a	Research octane number (RON) of the product mixture as a function of methylcyclohexane reaction	154
FIGURE 5.13b	Motor octane number (MON) of the product mixture as a function of methylcyclohexane reaction	155
FIGURE 5.14a	Research octane number (RON) of the product mixture as a function of corresponding specific volume	157
FIGURE 5.14b	Motor octane number (MON) of the product mixture as a function of corresponding specific volume	158
FIGURE 6.1	A proposed reaction scheme for the hydroconversion of methylcyclohexane and their research (RON) and motor (MON) octane numbers.	164
FIGURE 6.2a	TPD profiles of ammonia for MFI and Pt/MFI catalysts	170
FIGURE 6.2b	TPD profiles of ammonia for BEA and Pt/BEA catalysts	171

FIGURE 6.2c	TPD profiles of ammonia for FAU and Pt/FAU catalysts	172
FIGURE 6.3	The ratio of CR and RO products to RC products on various zeolites at the same conversion (~3%)	177
FIGURE 6.4a	Selectivity to RC products as a function of methylcyclohexane conversion over MFI zeolite at different space velocities	180
FIGURE 6.4b	Selectivity to RC products as a function of methylcyclohexane conversion over BEA zeolite at different space velocities	181
FIGURE 6.4c	Selectivity to RC products as a function of methylcyclohexane conversion over FAU zeolite at different space velocities	182
FIGURE 6.5	Carbocation chemistry for the ring contraction reactions	184
FIGURE 6.6	The DMCP/ECP ratio over MFI, BEA, and FAU zeolites	185
FIGURE 6.7a	Selectivity to RC products as a function of methylcyclohexane conversion over Pt/MFI catalyst at different space velocities	190
FIGURE 6.7b	Selectivity to RC products as a function of methylcyclohexane conversion over Pt/BEA catalyst at different space velocities	191

FIGURE 6.7c	Selectivity to RC products as a function of methylcyclohexane conversion over Pt/FAU catalyst at different space velocities	192
FIGURE 6.8a	Selectivity to some RC products (*trans*-1,2-dimethylcyclopentane, *t*-1,2-DMCP and 1,3-diemthylcyclopentane, 1,3-DMCP) as a function of methylcyclohexane conversion over Pt/MFI, Pt/BEA, and Pt/FAU catalysts	195
FIGURE 6.8b	Selectivity to some RC products (1,1-dimethylcyclopentane, 1,1-DMCP and ethylcyclopentane, ECP) as a function of methylcyclohexane conversion over Pt/MFI, Pt/BEA, and Pt/FAU catalysts	196
FIGURE 6.9a	The 1,3-DMCP/(1,2-DMCP+1,1-DMCP) ratio over MFI, BEA and FAU zeolites at the same conversion (~3%)	198
FIGURE 6.9b	The 1,3-DMCP/(1,2-DMCP+1,1-DMCP) ratio over Pt/MFI, Pt/BEA and Pt/FAU catalysts at the same conversion (~13%)	199
FIGURE 6.10a	The *cis*-1,3-DMCP/*trans*-1,3-DMCP ratio over MFI, BEA, and FAU zeolites a the same conversion (~3%)	201
FIGURE 6.10b	The *cis*-1,3-DMCP/*trans*-1,3-DMCP ratio over Pt/MFI, Pt/BEA, and Pt/FAU zeolites a the same conversion (~13%)	202

FIGURE 6.11a	Selectivity to some RC products (ethylcyclopentane, ECP and 1,3-diemthylcyclopentane, 1,3-DMCP) as a function of methylcyclohexane conversion over CBV400 (solid) and CBV720 (open) zeolites	207
FIGURE 6.11b	Selectivity to some RC products (1,1-dimethylcyclopentane, 1,1-DMCP and *trans*-1,2-dimethylcyclopentane, *t*1,2-DMCP) as a function of methylcyclohexane conversion over CBV400 (solid) and CBV720 (open) catalysts	208
FIGURE 6.12a	Selectivity to some RC products (ethylcyclopentane, ECP and 1,3-diemthylcyclopentane, 1,3-DMCP) as a function of methylcyclohexane conversion over Pt/CBV400 (solid) and Pt/CBV720 (open) catalysts	209
FIGURE 6.12b	Selectivity to some RC products (1,1-dimethylcyclopentane, 1,1-DMCP and *trans*-1,2-dimethylcyclopentane, *t*1,2-DMCP) as a function of methylcyclohexane conversion over Pt/CBV400 (solid) and Pt/CBV720 (open) catalysts	210

ABSTRACT

High demand for transport fuels (both diesel and gasoline) and the increasingly stringent environmental legislation associated with clean fuels have stimulated intense research for a development of new catalytic systems in order to produce high quality fuels with less negative environmental impact. Environmental regulations set limits in the content of (poly)aromatics in diesel and gasoline so that imposes a challenge to refiners who need to maintain high quality (cetane number for diesel and octane numbers for gasoline) while decreasing the (poly)aromatic content.

An interesting possibility to remove (poly)aromatics is the opening of naphthenic rings derived from the saturation of aromatics (hydrogenation of aromatics) to produce molecules of higher cetane numbers (i.e., aromatics < naphthenics, *i*-paraffins < *n*-paraffins). In this contribution, the ring opening reaction of decalin over a series of HY and Pt/HY catalysts of varying acidity densities and the ring opening reaction of tetralin over different catalytic system configurations of Pt/SiO_2 and HY catalysts (Pt>>HY, HY>>Pt, and Pt+HY) under high hydrogen/feed molar ratio were investigated. Under these conditions, mainly ring-contraction and one-ring opening reactions take place over these catalysts. These products are important intermediates for high cetane number compounds. The results of this investigation show that HY zeolites with an optimum acidity can be effective catalysts for the ring-contraction and one-ring-opening of decalin in order to give

high conversion, but slow deactivation**.** In addition, *cis*-decalin shows higher reactivity to ring-opening than *trans*-decalin.

The presence of Pt improves the production of ring-contraction and ring-opening products from tetralin due to hydrogenation of tetralin to decalin. In addition, the location of metal (Pt) affects the ratio of RC/RO on the decalin reaction. The results show that the ratio of RC/RO increases over Pt located on the inside of the zeolite structure resulting from the enhancement of the RC desorption rate. Inversely, the ratio of RC/RO decreases over catalysts with high acidity.

Similarly to diesel fuel, aromatics in gasoline fuel have to decrease, even though they have a high octane number (ON). In this study, the ring-contraction reaction followed by selective ring-opening is proposed. The reaction of methylcyclohexane is investigated over various catalysts (HY, Pt and Ir/SiO_2) and different catalytic system configurations with high hydrogen/feed molar ratio. Under these conditions, skeletal isomerization (ring-contraction) is the primary reaction in both HY and Pt/HY catalysts. The octane numbers of the RC product mixtures result in high RON, but show little or negative effect on MON and the specific volume. However, the octane numbers (RON and MON), including specific volume of product mixtures were found to be improved in the methylcyclohexane reaction over segregated beds of Pt/HY and Ir/SiO_2 catalysts due to better control of the selective breaking of C-C bonds of RC isomers, which produces high iso-alkanes yield.

To maximize RC isomers with a high degree of branching (high ON precursors), the effects of acid strength, structure, and pore sizes of zeolites were

investigated in the methylcyclohexane reaction over acidic and Pt supported zeolites (MFI, BEA, and FAU) in mild reaction conditions. The shape selectivity effect was noted for the methylcyclohexane reaction over a medium pore zeolite (MFI), especially for *trans*-1,2-dimethylcyclopentane (the most bulky isomer). In addition, the acidic strength of supports can alter the selectivity to RC isomers in the products.

The presence of Pt was found to enhance the stability of the catalyst, and also greatly altered the distribution of RC products and approached equilibrium, enhancing 1,1-dimethylcyclopentane. This can be explained in terms of a higher rate of hydride transfer. Moreover, it was found that the acid density seems to have a less important effect in the product distribution than the acidic strength. The acid density has a strong influence on activity but has a minor or no influence on selectivity.

CHAPTER I

INTRODUCTION

1.1 Introduction

The current high demand for transport fuels (diesel and gasoline) and the stringent environmental legislation associated with clean fuels [1-5] have highlighted the need for a development of new technologies in order to produce high quality of fuels and less environmental risk [6-8]. The primary regulations for fuels involve the reduction of sulfur, nitrogen, aromatics, olefins, and volatility. During the combustion, sulfur and nitrogen compounds contribute to the emission of sulfur dioxide (SO_2) and nitrogen oxide (NO_x), with particulate matters (PM) that damage human organs, especially the lung. In addition, sulfur dioxide and nitrogen oxides are the primary causes of acid rain. The reduction of sulfur content prolongs engine life due to a decrease the formation of acids in engine combustion chambers [9]. Aromatic compounds, especially polyaromatics, produce particulates [10] and NO_x in the exhaust gases and are known as human carcinogens [11]. Due to the air pollution and health concerns, environmental regulations set limits in the content of (poly)aromatics—even though a small amount of aromatics help prevent the solidifying of paraffins from pluging in a filter for diesel in the winter.

There are two basic types of transport engines: diesel engines (the compression ignition; CI), and gasoline engines (the spark ignition; SI). Diesel engines ingest the air into the cylinders. The air is compressed to a high pressure and temperature in the cylinder in the piston. The fuel is injected directly into the hot, high-pressure air inside the cylinder where it ignites and burns as it mixes with the air. Unlike the diesel engines, the gasoline engines require an external spark for the ignition. First, the fuel and air are mixed together, then ducted into the engine's cylinders. The fuel/air mixture is compressed by the piston moving upward to the top dead center (TDC), and after that it is ignited by an external spark from a spark plug. It then burns and releases the chemical energy stored in the fuel. The fuel should resist the ignition before the external spark occurs. Gasoline engines are used in automobiles, vans, light trucks, and light busses, while diesel engines are typically used in medium and heavy trucks [12].

To ensure that both gasoline and diesel fuels meet the minimum requirements of the legislation and to allow manufacturers to design engines for specific fuel properties, standards for these fuels have been established. For gasoline engines, some properties are considered such as octane number, heating value, vapor pressure, density, and the blending of additives. For diesel engines, their characteristics are cetane number, heating value, sulfur content, viscosity, volatility, cloud point, and flash point [12].

A cetane number is the readiness of a diesel fuel to ignite spontaneously under the temperature and pressure conditions in the combustion chamber of the engine. The higher the cetane number, the shorter the delay between injection and ignition. For gasoline fuel, its quality normally is defined by using at least two different octane parameters, Research Octane Number (RON) and Motor Octane number (MON). The Research Octane Number is tested with low-speed, relatively mild driving conditions, whereas the Motor Octane Number is tested under high-speed, high severity condition. Both RON and MON are the volume percentage of isooctane (very high resistance to knock) in a blend with *n*-heptane (extremely low resistance to knock) that shows the same antiknock performance as the test fuel when tested in a standard engine under standard conditions.

Both cetane and octane qualities are related to the chemical structure of hydrocarbon. The introduction of the side chains (i.e. methyl group) and/or double bonds in the straight chain has greatly effect on decreasing the cetane number. Aromatic compounds have the lowest cetane number (poor ignition property) compared with other hydrocarbon classes at the same number of carbon atoms in molecule. Unlike cetane number, the octane number of compounds increases with increasing the number of the side chains and/or double bonds. From the octane number point of view, aromatic compounds have high octane number (high resistant to engine knocking).

Regarding environmental and health concerns, stringent environmental regulations require a high quality of transport fuels, gasoline, and diesel. A significant requirement for both gasoline and diesel is the reduction of aromatic concentration. Two methods used without adding additives or cetane boosters—aromatic saturation (ASAT) and hydrocracking—currently remove polynuclear aromatics resulting in the improvement of the diesel quality [13,14]. However, both methods have limitations.

Aromatic saturation (ASAT) is an essential process in refineries. Hydrogen is added to the hydrogenation of aromatics. Products from hydrogenation are environmental friendly and have higher cetane number than aromatics. However, the increasing cetane numbers from fully hydrogenation is not enough for the tightening legislation of fuel quality. Fig. 1.1 shows the cetane numbers of aromatic model compounds found in a typical diesel fraction and its hydrogenated products.

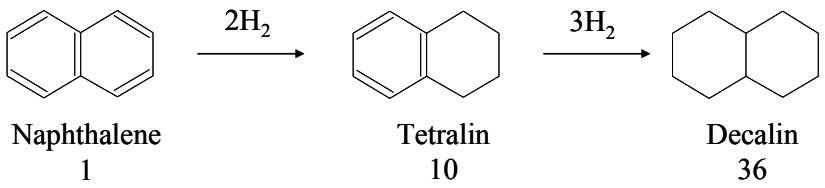

Figure 1.1 Cetane number of naphthalene and its hydrogenation products.

Hydrocracking is a catalytic cracking process assisted by the presence of an elevated partial pressure of hydrogen [15]. The products of this process are saturated hydrocarbons, which depend on the reaction conditions (temperature, pressure, catalyst activity). Hydrocracking is normally facilitated by a bifunctional catalyst that is capable of rearranging and breaking hydrocarbon chains, as well as adding hydrogen to aromatics and olefins to produce naphthenes and alkanes. Hydrocracking can produce compounds of higher cetane numbers, but it excessively reduces the molecular weight and produces lower yields in the diesel range.

An interesting alternative that has been recently proposed is a combination of deep hydrogenation and selective ring opening (SRO) of naphthenic rings to alkanes [16]. Contrary to unselective cracking, ring openings can result in a high-cetane product without the loss of reactant molecular weight. As illustrated in Fig 1.2 for some relevant C_{10} compounds, the cetane number greatly increases when a molecule such as decalin with two naphthenic rings is converted into a paraffin with a less degree of branching.

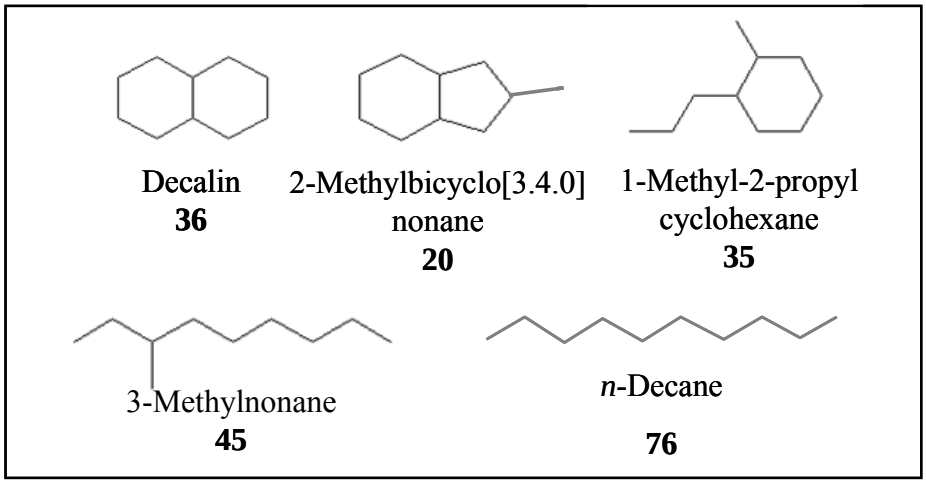

Figure 1.2 Cetane number of decalin and some relavant C_{10} products**.**

This proposed method (the combination of deep hydrogenation and the selective ring opening of naphthenic rings to paraffins), can be modified for gasoline improvement in terms of octane number (ON). The octane rating of chemical compounds [17] compared at the same number of carbon atoms in a molecule, is as follows: olefins > aromatics > naphthenes > iso-paraffins > *n*-paraffins. Additionally, the octane number decreases with an increase in molecular weight, except for aromatics, as presented in Fig. 1.3.

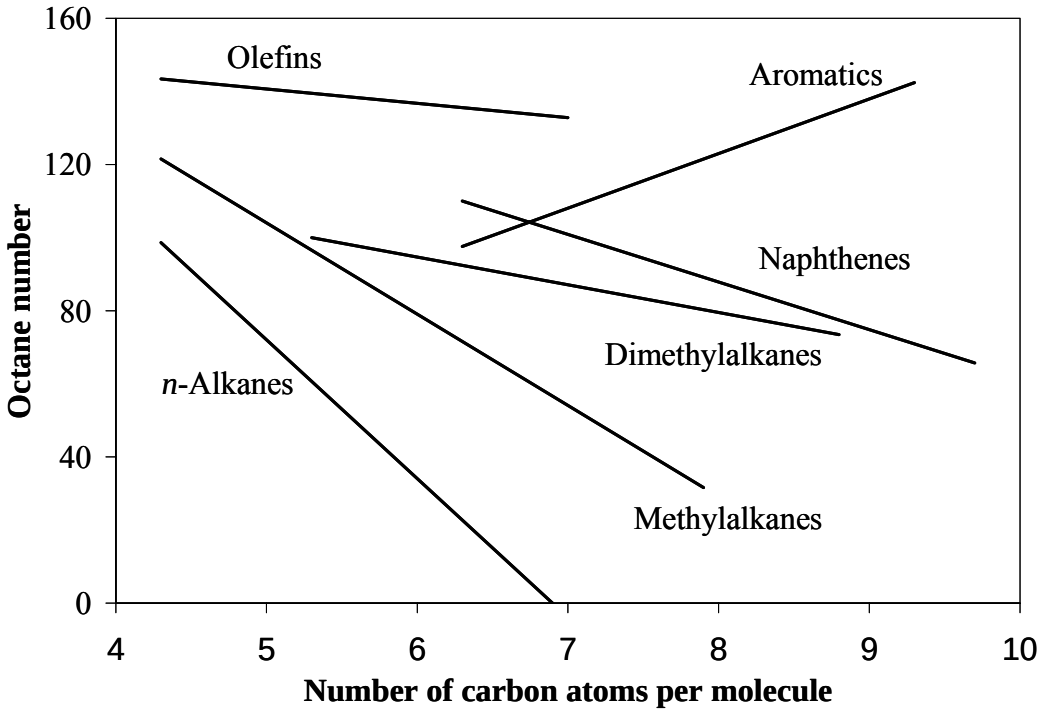

Figure 1.3 Octane number of various low molecular weight hydrocarbons [17].

An increase in either the olefins or aromatics concentration routes is unfavorable due to engine problems and environmental concerns. Therefore, the desired route is to maximize iso-alkane concentrations. Formerly, an isomerization of *n*-alkanes to iso-alkanes drew the attention of researchers who sought a new catalytic system in order to have high selectivity to multibranched alkanes; not only the isomerization of C_6, but C_7, and C_8. As described, this proposed method is an interesting alternative to produce high-octane branched paraffins to gasoline from aromatics and naphthenic ring compounds, or both. The advantage of this method is to turn excess aromatics, which are limited in gasoline by the stringent environmental legislation, to high branched naphthenes and paraffins that can be use in gasoline and even more high octane numbers.

1.2 Literature Review

As a consequence of environmental concern, reducing (poly)aromatic content is generally desirable with respect to diesel fuel quality, as aromatic reductions increase cetane levels and generally improve combustion characteristics [18]. In addition, aromatics content (e.g. benzene and tolutene) in gasoline has to be dramatically decreased while keeping a high octane number. Reducing aromatics can be achieved by several methods such as aromatic saturation (ASAT), and hydrocracking. However, these have limitations. While ASAT preserves the diesel

range molecular size, it cannot yield the high cetane numbers required in the near future. Similarly, hydrocracking can produce compounds of higher cetane number, but it excessively reduces the molecular weight and produces lower yields in the diesel range. Recently, an alternative pathway that combines hydrogenation and a selective ring opening is proposed for a reduction of aromatics concentration, and at the same time preserves the molecular weight size as the reactant. .

1.2.1 Ring Opening of Cyclic Compounds on Acidic and Bifunctional Catalysts.

Although the opening of a ring can be accomplished on either acid or metal catalysts, the combination of the two functions is much more effective than each of them alone [19,20]. The opening of small ring cycloparaffins on solid acid catalysts has been studied for many years [21]. It is widely accepted that molecules with three and four-member rings have a significant ring strain, and consequently, are more easily opened than the larger rings. As a result, cyclopropane and cyclobutane can be ring-opened at much lower temperatures than molecules, such as cyclopentane and cyclohexane [22]. It has been proposed [4] that on acidic zeolites, the activation of six-member rings can occur on Brønsted sites via an initiation step described as a protolytic cracking (PC). Subsequent steps follow the typical carbenium ion reactions, such as ring contraction (RC), β-scission cracking, and alkylation. Alternatively, the formation of olefinic intermediates via-H transfer could produce the carbenium ion without involvement of a PC step [23].

The majority of the ring-opening investigations found in relevant literature refer to single-ring molecules. While two-fused-ring compounds, such as decalin (decahydronaphthalene), tetralin (tetrahydronaphthalene), and naphthalene, are much more relevant to LCO upgrading. Detailed studies with these feedstocks are far less common. Only recently have a few interesting studies have attempted to gain insight on the complex mechanisms responsible for the different reactions undergone by two-fused-ring compounds [24,25]. For example, Corma et al. [4] studied the conversion of decalin and tetralin over proton-form zeolites of different pore sizes. They emphasized the role of the pore size and zeolite topology in determining the product distribution. Zeolites with large pores such as HY seem to be the most appropriate for selective ring opening. In the discussion of the possible mechanism of decalin conversion, they proposed that the decalin activation starts with the opening of the ring via protolytic cracking (PC) as shown in Fig 1.4.

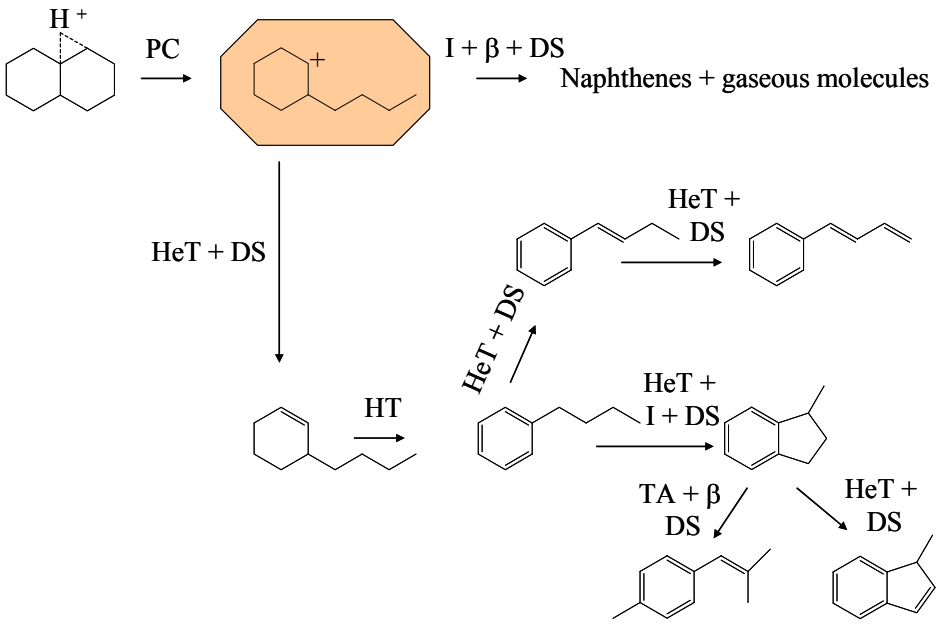

Figure 1.4 A proposed reaction network of direct ring opening of decalin reaction over acidic zeolites at 723 K and 0.1 MPa. (PC:Protolytic cracking; HeT: Hydride transfer; HT: Hydrogen transfer; I: Isomerization; β: β-scission; DS: Desorption; TA: Transalkylation) [4].

In this scheme, the products of ring-opening (RO) are primary while the products of ring-contraction isomerization (RC) are secondary. In contrast, in a more recent investigation, Kubicka et al. [26] did not observe direct ring-opening of decalin and proposed that RO is a secondary reaction, which is preceded by a step of a skeletal isomerization, ring-contraction (RC) (see in Fig. 1.5). The authors argued against the PC of decalin as an initiation step, because the RO products seem to originate only from the RC products, such as alkyl bicyclononanes (indanes) and bicyclooctanes, which acted as intermediates. The evolution of RC and RO products as a function of conversion had non-zero and zero derivatives at the zero conversion limit, respectively. This contrasting behavior strongly supports the notion that RC products are primary, while RO products are secondary and are only detected after the concentration of RC products becomes sizeable. The reaction conditions of the two studies were significantly different. Corma et al. [4] worked in a flow reactor set at atmospheric pressure (0.1 MPa), high temperatures (723 K), and with no added hydrogen. In contrast, Kubicka et al. [26] operated in a batch reactor, at higher pressures (2 MPa), lower temperatures (473-573 K), and at very low H_2/feed ratios (1:13).

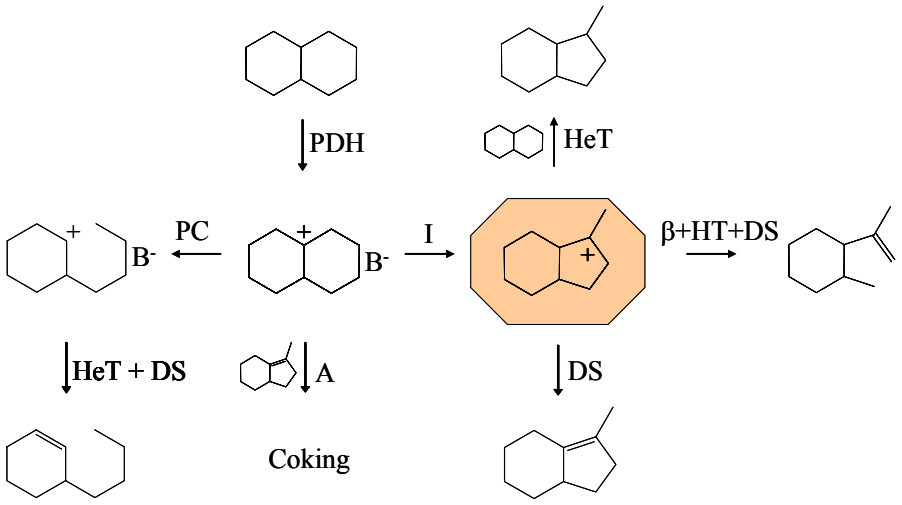

Figure 1.5 A proposed reaction network of isomerization and ring opening of decalin reaction over acidic zeolite catalysts at 473-573 K, and 2 MPa. (A: Alkylation; PC: Protolytic cracking; HeT: Hydride transfer; HT: Hydrogen transfer; I: Isomerization; β: β-scission; DS: Desorption; TA: Transalkylation) [26].

The use of metals supported on acidic zeolites for ring-opening of six-member ring naphthenics has attracted attention in recent years [27-29]. McVicker et al. [16] have shown that while alkylcyclopentanes can be readily ring-opened by low temperature hydrogenolysis over noble metals such as Ir, the corresponding ring opening of alkylcyclohexanes is close to a hundred times slower. They have proposed that the addition of an acidity function provides the catalyst for the necessary ring-contraction activity to allow selective conversion of six-membered ring naphthenes. This result is in agreement with previous observations that, on metals as well as on acid catalysts, a five-member ring opens much faster than a six-member ring [30]. Working on NiW/HY catalysts, Kustov et al. [31], found an interesting difference regarding the need for the acidic function in ring opening (see in Fig. 1.6). They determined that acidity was essential for multi-ring compounds, such as decalin, but not for the single-ring cyclohexane, which can be opened on monofunctional metal catalysts.

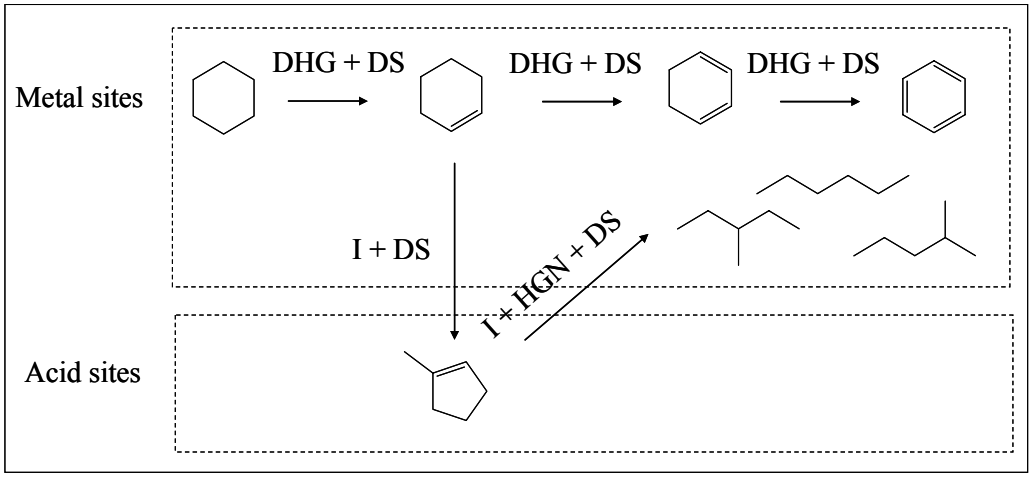

Figure 1.6a A proposed mechanism for methylcyclohexane reaction on metal catalysts. (DHG: Dehydrogenation; HG: Hydrogenation; I: Isomerization; β: β-scission; DS: Desorption) [31].

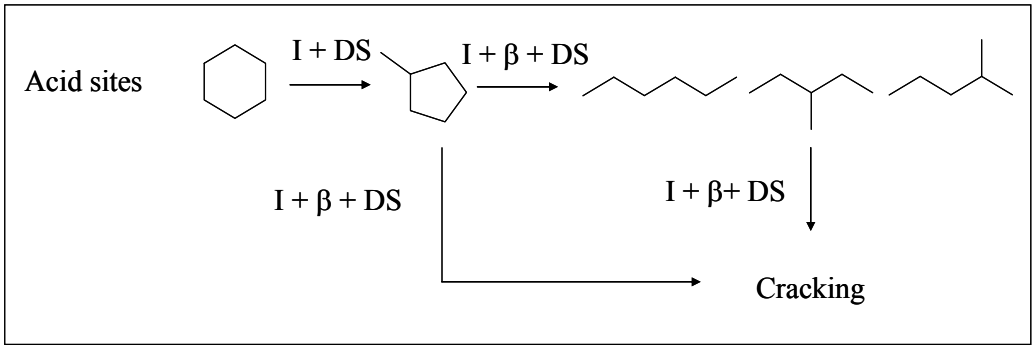

Figure 1.6b A proposed mechanism for methylcyclohexane reaction on acidic catalysts. (DHG: Dehydrogenation; HG: Hydrogenation; I: Isomerization; β: β-scission; DS: Desorption) [31].

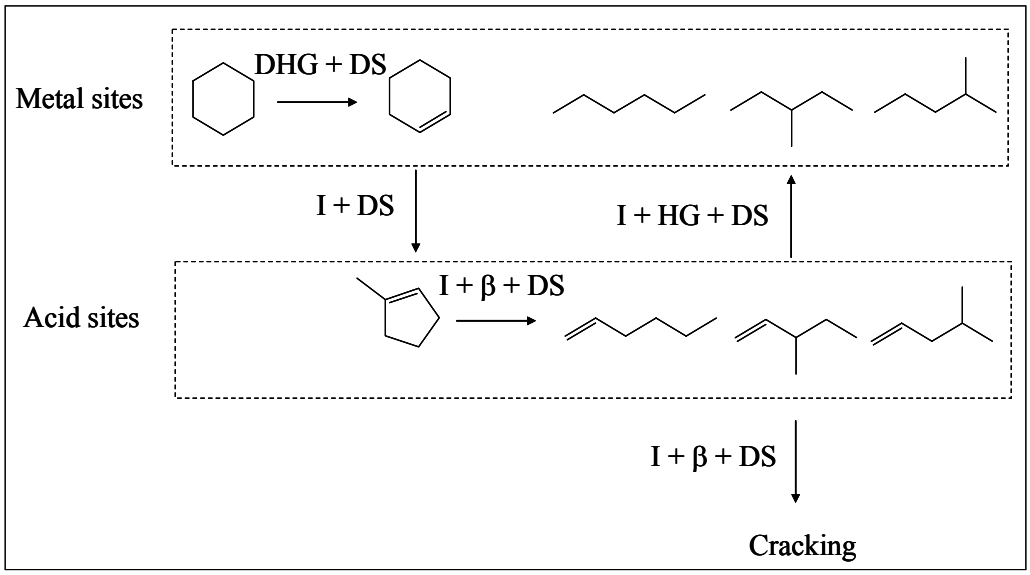

Figure 1.6c A proposed mechanism for methylcyclohexane reaction on bifuctional catalysts. (DHG: Dehydrogenation; HG: Hydrogenation; I: Isomerization; β: β-scission; DS: Desorption) [31].

Arribas et al. [27,32-34] studied the combination of hydrogenation and ring opening of tetralin and 1-methylnaphthalene over Pt catalysts supported over various supports. Their results, obtained at a H_2/feed ratio of 30:1, showed that zeolite supports resulted in concentrations of RO products higher than other supports. Among the zeolites, those with large-pore (USY, beta, mordenite) produced higher RO yields than zeolites with medium pore sizes (ZSM-5, MCM-22). The degree of easiness of undocking the reactant molecules from the pores was considered as the key parameter that determines RO selectivity. Sato et al. [24] suggested that the differences in the product distribution for hydrocracking of tetralin over NiW sulfide supported on USY and MOR results from the difference in the reaction path between USY and MOR. Three major reaction paths for hydrocracking of tetralin are as follows (Fig. 1.7): (a) ring opening via hydrogenated products of tetralin, (b) direct ring-opening of tetralin to n-butylbenzene via 1-methylindan, and (c) direct ring opening of tetralin to iso-butylbenzene via 2-methylindan. The results showed that the reaction mechanism of tetralin reaction over USY catalysts follows the pathway (a), but the tetralin reaction over MOR follows the pathways (b) and (c).

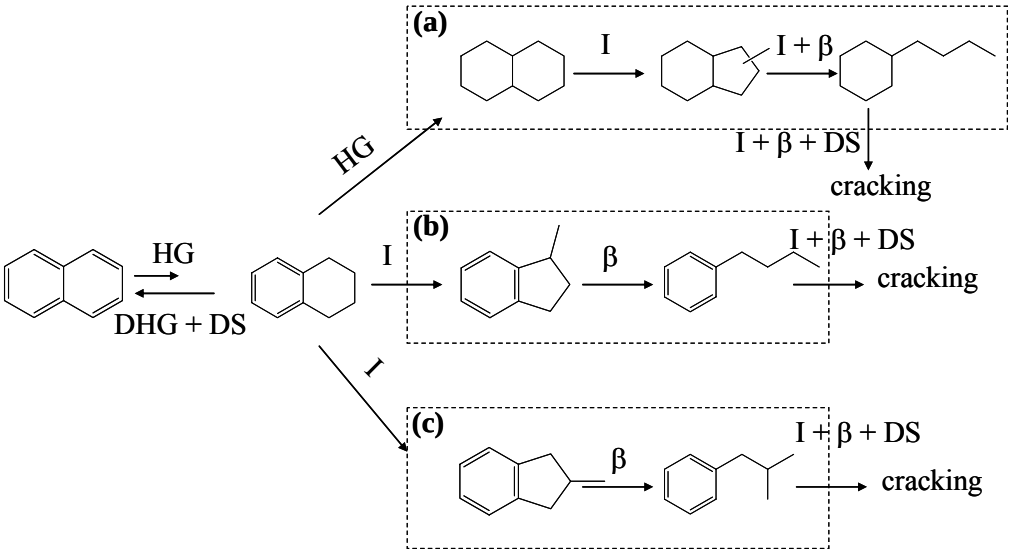

Figure 1.7 Three major reaction paths for hydrocracking of tetralin. (DHG: Dehydrogenation; HG: Hydrogenation; I: Isomerization; β: β-scission; DS: Desorption) [24].

In addition, the performance of bifunctional catalysts for hydroconversion of polyaromatics is influenced by the acidity of zeolites. Arribas and Martínez [27] found that selectivity to products with the same number of carbon atoms as feed compounds (i.e. 1-methylnaphthalene) increased with decreasing the Brønsted acidity of zeolites (i.e. USY zeolite). Beside the characteristic of supports (acidity and topology), the product distribution of hydroconversion of (poly)aromatics (e.g. tetralin and methylnaphthalene) depends on the reaction conditions, especially the reaction temperature. The higher the reaction temperature, the higher the cracking products (fewer number of carbon atoms in a molecule).

It is well known that on proton-form zeolites, the ring opening of decalin is much faster than that of tetralin [4]. In a practical application, it is conceivable that aromatics such as tetralin or naphthalene would first undergo hydrogenation, and subsequently, the fully saturated decalin would be the reactive compound for the production of ring-opening products [27,35,36]. Arribas et al. [32] have proposed the reaction pathway for hydroconversion of tetralin on bifunctional Pt/zeolite catalysts as shown in Fig. 1.8. The aromatic ring of tetralin is first hydrogenated on the metal sites (Pt) to give a mixture of *cis*- and *trans*-decalin. Decalins are then isomerized to form ring contraction products (RC), such as methyl-perhydroindanes (one C_5- and C_6-rings) and dimethyl-octahydropentalenes (two C5-rings). This step involves both the acid and the metal sites of the Pt/zeolite catalysts (bifunctional route). Ring opening products—alkylcyclohexanes and

alkylcyclopentanes—are produced from ring contraction products on the Brønsted acid sites of the bifunctional catalyst. Products containing less than 10 carbon atoms are consecutively formed from ring opening products on the acid sites.

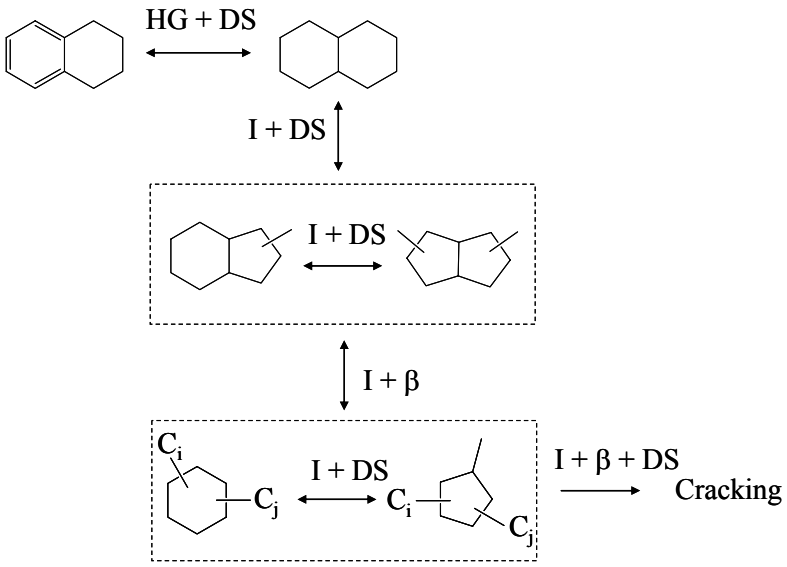

Figure 1.8 A reaction pathway for hydroconversion of tetralin on bifunctional Pt/zeolite catalysts. (DHG: Dehydrogenation; HG: Hydrogenation; I: Isomerization; β: β-scission; DS: Desorption) [32].

1.2.2 Ring Opening of Non-Aromatic Compounds on Metal Catalysts.

Noble metals, such as Pt, Pd, Ir, Ru and Rh have been found to have a high selectivity for hydrogenolysis reaction for cyclic compounds to paraffins. The activity and selectivity depends on metal catalysts, such as the nature of the metal (Pt, Pd, Ir, and Ni), supports (SiO_2, Al_2O_3, and TiO_2), and particle size (small and large), as well as the nature of the cyclic hydrocarbon compounds such as (C_4, C_5, and C_6-rings), and the size, number, and position of alkyl substituent (methyl, ethyl, and butyl), etc. Ring opening selectivities are in the following reactivity order: $C_4 > C_5 > C_7 >> C_6$. Group I, VII, and VIII metal blacks, Pt, Pd, Ir, and Rh, produced hexane isomers from methylcyclopentane with high rates at low temperature [37], whereas hexane isomers are the minor products over Co, Ni, Ru, Re and Os. Sárkány et al. [38] suggested that a flat type adsorption of the ring is found over Pt, but an edgewise type is found over Ni. The difference in selectivities to ring opening products is based on different mechanisms assuming flat or edgewise ring adsorption and associative or dissociative ring opening [39]. The nearest C-C bond of the ring to the side chain is *a*, then *b*, and then *c*.

(a) Associative flat adsorption: Liberman [40] proposed the push-pull mechanism that assumes the participation of H atoms adsorbed on the metal in the ring opening. Two kinds of the adsorptions are six (ads6-mode) and five (ads5-mode) carbon atoms attached to the surface as shown in fig. 1.9. For C_5-ring compounds, the tertiary-

secondary C-C bonds will be ruptured via ads5-mode, whereas no bonds could break for C_6-ring compounds resulting from ads6-mode [41].

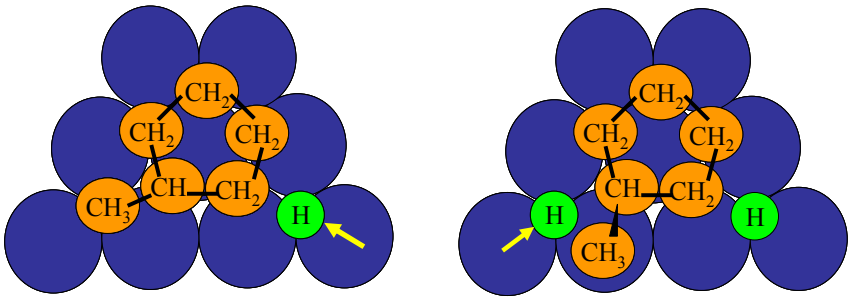

(a) 'ads6' Type (b) 'ads5' Type

Figure 1.9 Two types of methylcyclopentane adsorption over Pt(111) surface [40]. Arrows denote H atoms attacking bond in position (a).

(b) Dissociative flat adsorption: Sárkány et al. [38] suggested a ring opening of cyclopentane occurs via a flat adsorption over Pt that involves a π- or a π-allylic attachment to the catalyst surface (Fig. 1.10)

Figure 1.10 A dissociative flat adsorption of cyclopentane [38].

(c) Associative edgewise adsorption: Due to high a ratio of b/a for the ring opening of cyclopentane and cyclobutane over Rh, Ir, Ru and Os catalysts [42], this type of adsorption is known as Baladin-type doublet. There is no particular bonding involved in this mechanism. However, the ring opening at the substituted C-C bond for this type of adsorption is limited.

(d) Dissociative edgewise adsorption: Gualt et al. [43,44] proposed two mechanisms for the nonselective and selective ring opening of C5 ring compounds. Nonselective ring opening occurs over a single metal atom. An open-chain dicarbene is formed after an edgewise π

adsorption (Fig. 1.11a). Unlike nonselective ring opening, selective ring opening occurs over two contiguous metal atoms. An open-chain dicarbyne will be formed (Fig. 1.11b), resulting in the inhabitation of an adsorption at tertiary carbon atoms. In addition, Paál [45] suggested that selective ring opening would involve a flat adsorption as an intermediate, whereas nonselective ring opening involve an edgewise adsorption.

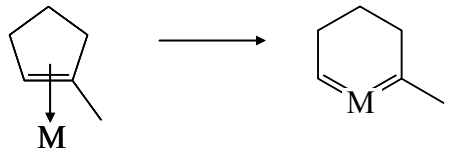

(a) An open chain dicarbene

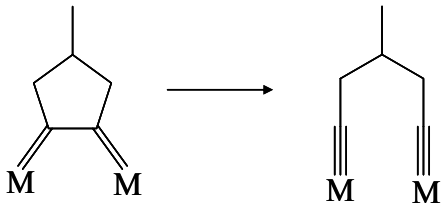

(b) An open chain dicarbyne

Figure 1.11 A dissociative edgewise adsorption of methylcyclopentane [43,44].

As described, two of the most recognized ring opening mechanisms over metal catalysts are the multiplet and the dicarbene mechanisms. The multiplet mechanism (Fig. 1.9) involves the physical adsorption via associative flat adsorption on the metal surface via associative edgewise adsorption on two metal atoms. In contrast, the dicarbene mechanism involves the chemisorption via dissociation—either flat adsorption or edgewise adsorption. In addition, this mechanism sometimes involves a partially selective hydrogenolysis, in which an alkyl substituent forms a metallocyclobutane intermediate, resulting in ring opening at the tertiary-tertiary and tertiary-seconday C-C bonds [46] (Fig. 1.12).

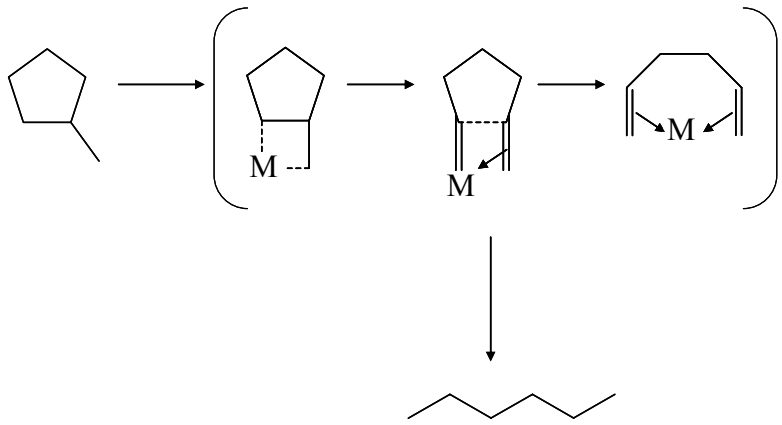

Figure 1.12 A metallocyclobutane intermediate of methylcyclopentane [46].

Fig. 1.13 demonstrates that the ring opening products of methylcyclopentane [16,43,47-49] on metal catalysts are *n*-hexane (Hx), 2-methylpentane (2-MP), and 3-methylpentane (3-MP). Products depended on the properties of catalysts. Products over Pt catalysts with less dispersion and large particle sizes (10%wt Pt/Al_2O_3) were 2-MP, 3-MP, and no Hx. Hx was found on high dispersion and small particle sizes (0.2%wt Pt/Al_2O_3). Van Senden et al. [50] reported that the particle size dependence of the catalytic properties of Ir and its sensitivity to self-poisoning are much less pronounced than with Pt, which is in agreement with other sources [16,51,52]. Mc Vicker et al. [16] have investigated that the ring opening of alkylcyclohexanes on Ir is mainly at the secondary-secondary C-C bond. Products are only 2-MP and 3-MP [51]. Furthermore, the cracking product yield is significant over other metals such as Ni, Co, and Ru [53]. Compared to C_5-ring, the ring opening of C_6-ring is much slower [16,54], so the RC isomerization step is required in order to facilitate the ring opening and keep the same number of carbon atoms as the reactant. The RC isomerization of C_6-ring can be achieved over acid catalysts as described in Section 1.2.1.

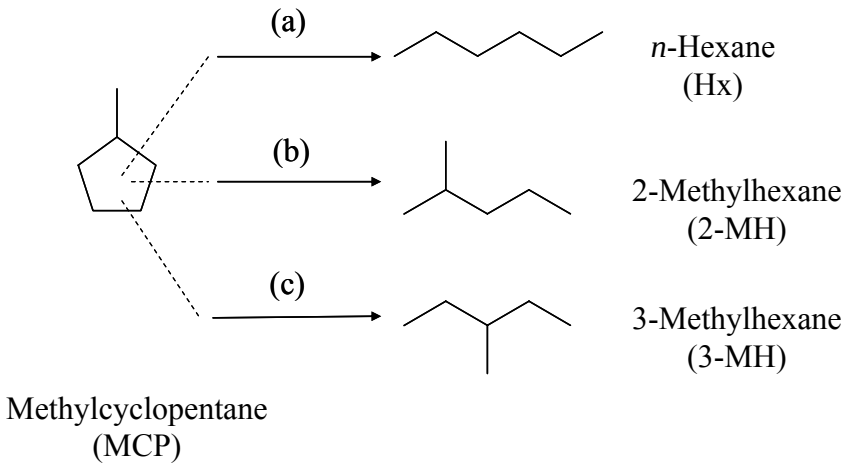

Figure 1.13 Hydrogenolysis products of methylcyclopentane.

1.3. Motivation

Environmental concerns have highlighted the development of new catalysts and catalytic processes for refineries. An interesting proposed pathway for reducing aromatic content and preserving yields of the same molecular size range is the combination of hydrogenation and selective ring opening.

Regarding the alternative pathway, I investigated the reaction of some naphthenic compounds (i.e. decalin), as well as aromatic compound (i.e. tetralin) for either cetane number aspect or octane number aspect. Tetralin, which contains one benzene ring, represents an aromatic compound that would require the hydrogenation step before the ring opening step. In addition, it is important to understand the pathway so the ring opening reaction of naphthenic compounds, such as decalin, is

also investigated over proton form zeolites and bifuctional catalysts. As described above, the acid function promotes the isomerization of a six member ring to a five member ring that would result in facilitating the ring opening step. The details of this study are described in Chapters 3 and 4.

This proposed reaction pathway is modified to increase the octane number from one naphthenic ring compound. Methylcyclohexane, which is the full hydrogenation product of methylbenzene (toluene), is used as a feed model for octane number aspect as shown in Chapters 5 and 6. The reactions were investigated with various proton form zeolites and bifunctional catalysts. In addition, the different catalyst bed configurations were also modified in order to achieve a large number of high branching alkanes that would result in a high octane number and a low density.

CHAPTER II

EXPERIMENTAL SETUP

This chapter covers the different preparation methods for catalysts, which were used in the entire study as well as the characterization techniques such as Extended X-ray Adsorption Fine Structure (EXAFS), Transmission Electron Microscopy (TEM), Temperature Programmed Desorption (TPD), Temperature Programmed Oxidation (TPO), Fourier Transform Infrared (FTIR), H_2 and CO Chemisorption that were used to determine the metal dispersion, the metal particle size, acid density and acid strength, and coke contents for these catalysts throughout this study.

2.1 Catalyst Preparation

All catalysts used in this study are listed in Table 2.1.

2.1.1 Acidic Zeolite Catalysts

Three HY zeolite catalysts with varying acidity densities were prepared by an ion-exchange of a NaY zeolite (Y54 from UOP, Si/Al=5.3). In this procedure, 100 g of NaY was added into an aqueous solution containing 120.5 g ammonium chloride dissolved in a liter of deionized water. This suspension was refluxed and stirred with a magnetic plate for 2 h. The solid was then filtered and

washed with deionized water; this solid with one ion exchange is identified as HY1. The HY2 and HY3 samples were prepared in a similar fashion, but with 2 and 4 sequential ion exchange steps, respectively. After each ion exchange step, the samples were filtered and washed. In the final step, each sample was further washed with deionized water until it was chloride-free. It was finally air dried at 383 K and kept in a desiccator. Prior to the activity measurements, the samples were calcined in a flow of oxygen at 573 K for 3 h at the heating rate of 0.5 K/min.

Another series of the faujasite zeolites with different acidic densities (CBV400, CBV720, CBV760, and CBV780) obtained from Zeolyst International and commercially available an H-MFI (Si/Al = 90) and H-BEA (Si/Al = 2.5-50) obtained from UOP were used as a catalyst and a support in this study. Prior to the activity measurements, all samples were calcined in flow of dry air at 823 K for 2 h.

2.1.2 Pt-Supported Zeolite Catalysts

The catalysts were prepared by the incipient wetness impregnation method. Pt-containing catalysts were preformed by using a HY3 as the support. Two different Pt catalysts were prepared by incipient wetness impregnation (IWI) of the HY zeolite with an appropriate Pt concentration. One was prepared with hexacloroplatinic acid (Acros) dissolved in deionized water. Another used platinum (II) acetylacetonate (Alfa Aesar) in acetone as a precursor. These two catalysts indicated as PtHY and PtAc, respectively. After impregnation, the sample was dried

at 383 K overnight, and calcined at 573 K in an oxygen flow for 3 h at a heating rate of 0.5 K/min. Prior to each activity measurement, the sample was reduced in-situ.

Table 2.1 A list of catalysts used in the decalin, tetralin, and methylcyclohexane reactions

Sample	Si/Al mole ratio	Support	Precursor	Solvent	Preparation method
HY1	5.3	-	-	-	1st ion-exchange of NaY
HY2	5.3	-	-	-	2nd ion-exchange of NaY
HY3, HY or FAU	5.3	-	-	-	4th ion-exchange of NaY
CBV400	2.5	-	-	-	-
CBV720	15	-	-	-	-
CBV760	30	-	-	-	-
CBV780	40	-	-	-	-
H-MFI	90	-	-	-	-
H-BEA	2.5-50	-	-	-	-
Pt/HY or PtHY	-	HY3	$PtCl_6^{2-}$	deionized-water	impregnated
PtIE	-	HY3	$Pt(NH_3)_4^{2+}$	deionized-water	ion-exchanged
PtAC	-	HY3	$Pt(C_5H_7O_2)_2$	acetone	impregnated
Pt/CBV400	-	CBV400	$PtCl_6^{2-}$	deionized-water	impregnated
Pt/CBV720	-	CBV720	$PtCl_6^{2-}$	deionized-water	impregnated
Pt/CBV760	-	CBV760	$PtCl_6^{2-}$	deionized-water	impregnated
Pt/CBV780	-	CBV780	$PtCl_6^{2-}$	deionized-water	impregnated
Pt/MFI	-	H-MFI	$PtCl_6^{2-}$	deionized-water	impregnated
Pt/BEA	-	H-BEA	$PtCl_6^{2-}$	deionized-water	impregnated
Pt/SiO_2	-	SiO_2	$PtCl_6^{2-}$	deionized-water	impregnated
Ir/SiO_2	-	SiO_2	$IrCl_3$	deionized-water	impregnated

Another Pt catalyst was prepared by an ion-exchange of HY zeolite, hereafter called PtIE. In this procedure, 10 g of HY zeolite powder was suspended in a liter of deionized water and stirred at 343 K for 12 h. A suspension at constant temperature (343 K) was added with a 0.01 M solution of tetraammineplatinum (II) nitrate (Acros) while continuously stirred. After the desired amount of precursor solution was added, the suspension was stirred for another 12 h and the temperature was kept constant at 343 K. In order to remove nitrate and undesired chemicals, the solid was filtered and resuspended in deionized water at room temperature. This step was repearted two times. Finally, it was dried at 353 K for 12 h and kept in a desiccator at room temperature. Before testing the catalytic activity, this catalyst was calcined at 573 K at the heating temperature of 0.2 K/min in an oxygen flow of 1 L/min. In order to flush oxygen, a flow of argon was introduced to the catalyst while a cool down process after reaching the calcination temperature.

In addition, a series of Pt-containing catalysts were prepared using the proton-form faujasite zeolites (CBVxxx) as supports. The Pt/CBVxxx catalysts were prepared by the incipient wetness impregnation (IWI) of each proton-form zeolite (CBVxxx) with hexacloroplatinic acid (Acros) of appropriate concentration to obtain a metal loading of 1.0 wt % Pt. The impregnated catalysts were dried at 383 K overnight and calcined in an oxygen flow at 573 K for 3 h, at a heating rate of 0.5 K/min. Prior to each activity measurement, the samples were reduced in-situ.

With the same preparation, the Pt metals were impregnated onto the available H-MFI and H-BEA zeolites, which were defined as Pt/MFI and Pt/BEA, respectively.

2.1.3 Metal Catalysts

The Pt/SiO_2 and Ir/SiO_2 catalysts were used as a reference for mono-functional metallic Pt and Ir. The metal loading was always 1.0 wt%. For the Pt/SiO_2 catalyst, the sample was prepared by incipient wetness impregnation of SiO_2 (Grace, grade 923, surface area 450 m^2/g) with a solution of hexachloroplatinic acid. After impregnation, the sample was dried in oven and calcined in flow of air at 573 K for 3 h. For the Ir/SiO_2 catalyst, the sample was prepared by IWI of silica powder (Hisil-210 with surface area of 120 m^2/g from Sasol) with aqueous solution of iridium chloride (AlfaAesar). The catalyst was dried overnight at 383 K before the calcination at 573 K for 2 h under air. Prior to the activity measurements, the catalysts were reduced in-situ.

2.2 Catalyst Characterization

2.2.1 Temperature Programmed Desorption (TPD) of Adsorbed Ammonia

The acidity densities of catalysts were determined by TPD of adsorbed ammonia. The test was conducted in a 1/4” quartz tube reactor containing

50 mg of catalyst that was pretreated at 773 K for 1 h in He flow. Then, the sample was cooled down in He flow to room temperature, at which point, 2 % NH_3/He was passed over the sample in an amount that greatly exceeds the total number of acid sites. To remove the excess and weakly adsorbed ammonia, the sample was purged in He flow at room temperature for 2 h. Subsequently, the sample was linearly heated to 973 K at a heating rate of 10 K/min, while the evolution of ammonia was monitored in a thermal conductivity detector. After each TPD, the amount of ammonia adsorbed was determined by a calibration curve obtained by varying volumes of 2% NH_3/He.

2.2.2 Fourier Transform Infrared (FTIR) of Adsorbed Pyridine

The distribution of acid sites on the different catalysts was determined by an infrared spectroscopic of adsorbed pyridine (Py-IR) in a Bruker Equinox 55 spectrometer. Self-supported wafers of the samples with a diameter of 2.5 cm were prepared by pressing 60 mg samples and loaded into a cell with CaF_2 windows. Before pyridine adsorption, the sample was pretreated at 773 K for 2 h in a flow of helium (He) and then cooled down to the desired temperature (423 K). A blank spectrum was taken and the samples were subsequently exposed to pyridine vapors for 2 h in order to saturate all the acid sites. A helium gas was then passed through the cell for 12 h to purge the excess pyridine. Four spectra were obtained for each sample at increasing temperatures from 423 K to 673 K. The absorption band appearing at 1545 cm^{-1} was assigned to the pyridinium ion formed on Bronsted acid

sites, while the band at 1455 cm^{-1} was assigned to pyridine coordinated to Lewis acid sites [55]. The density of both types of acid sites was quantified by integrating the corresponding absorption bands and using the molar extinction coefficients reported by Emeis [56].

2.2.3 Extended X-ray Adsorption Fine Structure (EXAFS)

The Pt L_{III} edge spectra (11564 eV) for fresh Pt/HY3 catalyst was measured at line X-11B, by the National Synchrotron Light Source (running at dedicated mode of 2.81 GeV and 100-250 mA) at the Brookhaven National Laboratory, Upton, NY. Energy was calibrated using an internal platinum foil standard. The measurements were conducted in a stainless steel sample cell that allowed in-situ pretreatments at temperature ranging from liquid nitrogen to 773 K. Prior to measurement, the fresh catalyst was reduced in-situ at 673 K (heating rate of 10 K/min) for 30 min in flowing hydrogen. After the reduction step, the sample was cooled down in flowing hydrogen. The EXAFS spectra were recorded at liquid nitrogen temperatures under hydrogen flow. The average spectrum from 6 scans was used to analyze the sample.

For the data analysis, the pre-edge background was subtracted by using power series curves, the post-edge background was then removed using a cubic spline routine, the spectra were normalized by dividing by the height of the adsorption edge, and to avoid overemphasizing the low-energy region, the data were k^3-weighted. The k-space range used for the analysis was 2-16 $Å^{-1}$. To determine

structural parameters, i.e. nearest neighbor distances and coordination numbers, curve fitting of the k-space EXAFS function and R-space Fourier transform spectra was done with EXAFSPAK suite.

2.2.4 Hydrogen (H_2) Chemisorption

The metal dispersions were estimated from volumetric H_2 chemisorption uptake measurements at 300 K in a chemisorption apparatus. Before each measurement, the catalysts were treated in H_2 at 673 K for 2 h and then evacuated for 0.5 h at 673 K. After treatment at 673 K, the samples were cooled at 300 K and H_2 chemisorption uptakes were measured in the 1-100 torr pressure range. After evacuation at room temperature, a second H_2 isotherm was performed to obtain an estimate of the reversible and irreversible uptakes. The irreversible H/M ratios were determined from the difference between the two isotherms.

2.2.5 Carbon monoxide (CO) Chemisorption

The metal dispersion of catalysts was conducted from CO chemisorption measurement. The measurement was performed in two different systems, a dynamic adsorption method and a standard volumetric method. On the dynamic adsorption, the tests were conducted in a 1/4" quartz tube reactor. In each run, the samples were first reduced in H_2 at 673 K for 1.5 h., then purged in a He flow for 30 min and finally cooled to room temperature under a He flow. Sequential pulses of 5% CO/He were injected onto the sample until the same size of the

intensity of the *m/e* = 28 mass signals were monitored by the mass spectroscopy. The dispersion of catalysts was calculated by the total amount of absorbed CO per metal sites. On the standard volumetric method, reversible and irreversible CO uptakes were measured. Before the measurement, the samples were pretreated under the same condition as on the dynamic adsorption. The first isotherm was measured at 1-100 Torr CO, and the second isotherm was obtained after the evacuation for 30 min at room temperature. The difference between these two isotherms after the extrapolation to zero CO pressure was defined as irreversible chemisorption. This value was used to determine the dispersion of metal.

2.2.6 Atomic Absorption Spectrometer (AAS)

Metal loadings of calcined catalysts (Pt supported catalysts) were determined using an atomic absorption spectrometer (AAS), a model of Varian / Spectraa-300 with a Pt lamp. The solid samples were first digested in a HF solution for 2 h, and then diluted to an appropriate concentration with deionized water. The actual amount of metal (Pt) was calibrated with the standard platinum solution.

2.2.7 Transmission Electron Microscopy (TEM)

A JOEL JSM-2000FX high resolution analytical electron microscope equipped with a field emission cathode operated at 200 keV was used to visualize the dispersion of the metal particles on the samples. For this analysis, the catalyst samples treated ex-situ were first dispersed by ultrasonication in isoproponol and for

15 min, then dropped on reveted carbon coated copper grids and dried before analysis.

2.2.8 Temperature Programmed Oxidation (TPO)

The coke content was determined as the carbon content on the spend catalysts by using a TPO reactor analyzer coupled with an FID. Prior to each run, 100 mg of dry spent catalyst was pretreated in He flow at 573 K for 1 h, to remove condensed compounds. After that the sample was cooled down to the room temperature in He flow, a continuous flow of 5% O_2/He was passed over the sample, while the temperature was linearly increased to 1173 K at a heating rate of 10 K/min. The output gas was passed to a methanation reactor using 15 wt% Ni/Al_2O_3 as a catalyst prior to FID detector. The carbon present on the catalyst sample was converted into CO_2. The amount of oxidized coke was calculated with the calibration of 100 μl pulses of pure CO_2.

2.3 Catalytic Activity Tests

2.3.1 Catalytic Activity Test for the Decalin Reaction

2.3.1.1 Continuous Flow System

A decahydronaphthalene (decalin, a mixture of *trans*- and *cis*-decalin, ratio 63/37) was obtained from Acros. The catalytic activity measurements were carried out in a continuous fixed bed stainless steel 3/8" I.D. reactor. In each run, 0.2 g of catalyst was diluted with SiC to make the volume of the catalyst bed 2.25 ml, and it was packed between the layers of quartz wool in the middle of the reactor. The top and below the quartz wool were filled with glass beads for the preheating zone. The reactor was placed in an electric furnace equipped with K-type thermocouples. The catalyst bed temperature was monitored and controlled by an Omega temperature controller. The experimental conditions were performed in the temperature range 533-600 K; at 2 MPa; the H_2/decalin molar ratio was kept constant at 65. Space velocities were systematically varied by changing either the catalyst amount or the hydrocarbon feed rate. Prior to the reaction, the catalysts were reduced in hydrogen (100ml/min) at 573 K for 2 h. The schematic diagram of the experiment setup is shown in Fig. 2.1.

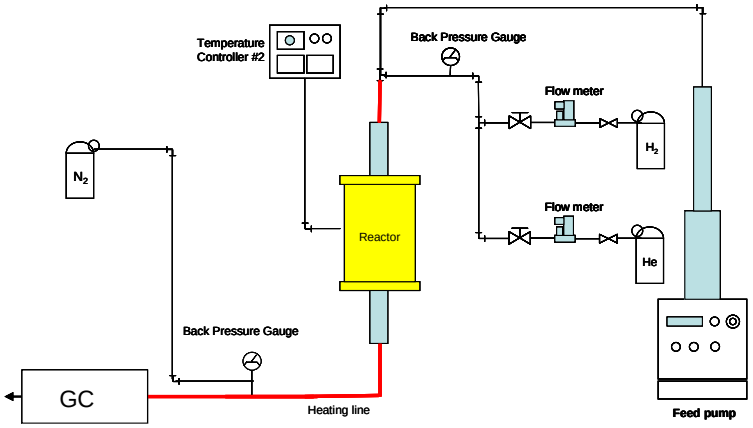

Figure 2.1 A schematic diagram of the experimental setup of decalin reaction in flow system.

2.3.1.2 Pulse System

Pure *trans*-decalin (99%) and *cis*-decalin (99%) from Alfa Aesar were tested to study the reactivity of the different isomers in the ring opening reaction. The reactions of pure isomers were conducted in the pulse system. A desired amount of catalyst was placed in a stainless steel tube between glass beads to keep the catalyst at the center of the heated zone. Before sending the hydrocarbon pulses, the catalyst was pre-treated in a 100 ml/min flow of pure H_2 at 573 K for 1 h and then heated to the selected reaction temperature (593 K or 630 K). Micro-liter pulses of either pure *cis*-decalin or pure *trans*-decalin were sent over the catalyst and the products analyzed in a GC with FID detector. The schematic diagram of the pulse experiments is shown in Fig. 2.2.

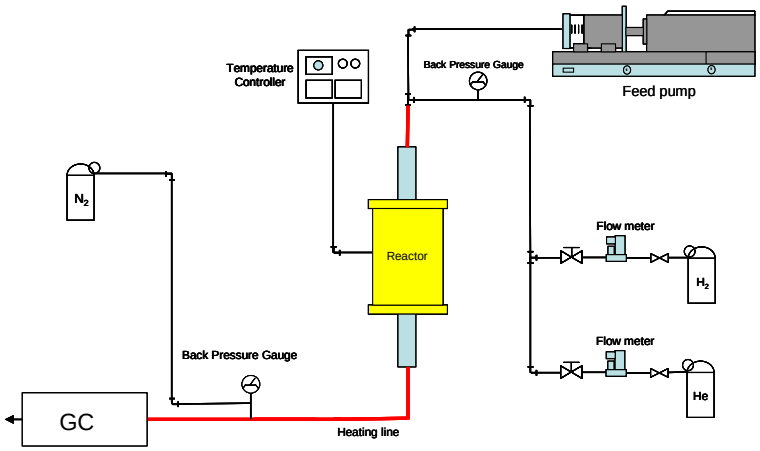

Figure 2.2 A schematic diagram of the experimental setup of decalin reaction in pulse system.

2.3.2 Catalytic Activity Test for the Tetralin Reaction

A 1,2,3,4-tetrahydronaphthalene (tetralin, 98+%) was obtained from Acros. The tetralin reactions were carried in the continuous flow system as described in Section 2.3.1.1. A set of experiments was conducted with physical mixtures of catalysts. The catalysts used in the mixtures were a conventional 1.0 wt. %Pt /SiO_2 prepared by incipient wetness impregnation and a pure HY3 zeolite. Four different physical mixtures were prepared. In two of them, the different catalysts were segregated in separate beds. In the system identified as Pt >> HY, the Pt/SiO_2 catalyst was placed in front of the HY3 zeolite. By contrast, in the system identified as HY >> Pt, the Pt/SiO_2 catalyst was placed after the HY3 zeolite. For the other two systems, the Pt/SiO_2 catalyst and the HY were intimately mixed in two different

ratios Pt + HY (1:1) and Pt + HY (1:2). The schematic diagram of a set of experiments is shown in Fig. 2.3.

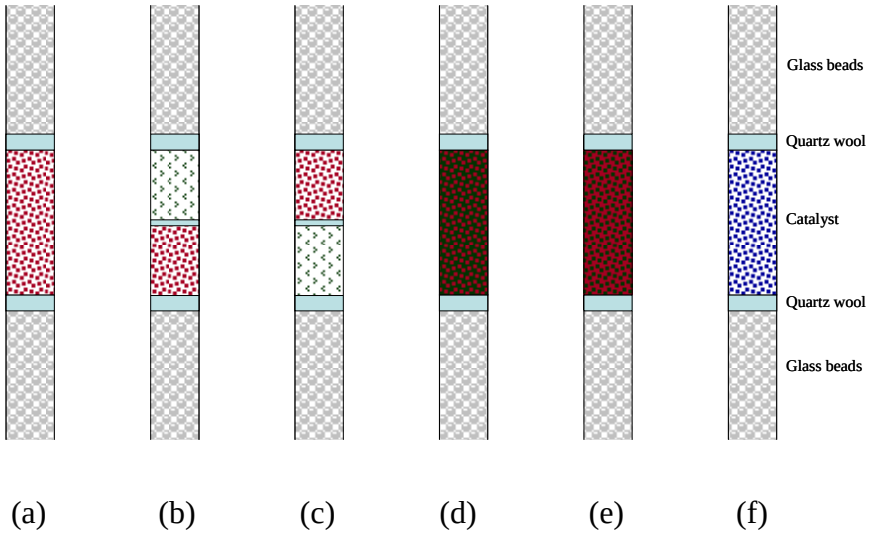

Figure 2.3 A schematic diagram of different catalytic bed configurations for tetralin reaction: (a) HY, (b) Pt/SiO_2 >> HY, (c) HY >> Pt/SiO_2, (d) Pt/SiO_2 + HY (1:1), (e) Pt/SiO_2 + HY (1:2), and (f) Pt/HY catalyst.

2.3.3 Catalytic Activity Test for the Methylcyclohexane Reaction

The methylcyclohexane reaction (MCH, Aldrich, >99%) was conducted in a 3/8" stainless steel reactor equipped with a thermowell with a thermocouple placed in the center of the bed as described in Fig. 2.1.. Prior to each experiment, the specified amount of catalysts was diluted with inert alumina to make a volume of catalyst bed of 2 ml and placed in the center of the reactor. The top and

the bottom part of the catalyst bed were filled with glass beads of 1 mm in a diameter, to ensure an effective preheating and minimize heat losses. Before starting the feed of MCH from a high-pressure liquid pump through a vaporizer, the catalysts were reduced in situ at 673 K for 2 h in flow of pure hydrogen. The catalytic activity was measured in the temperature range 513-593 K, at a total pressure of 2 MPa and at a H_2/MCH molar ratio of 40. The space velocities were systematically varied by changing either the catalyst amount or the feed rate. In each reaction with MCH, the catalysts were reduced in hydrogen at 673 K for 2 h.

In addition to the runs on individual catalysts, a set of experiments was conducted with physical mixtures of Pt/HY and Ir/SiO_2 catalysts. In two of these experiments, the two catalysts were segregated in separate beds with the Pt/HY catalyst placed in the front end and the Ir/SiO_2 catalyst in the back. In the system identified as Pt/HY > Ir/SiO_2, both catalysts were kept at the same temperature. By contrast, in the system identified as Pt/HY >> Ir/SiO_2, the Pt/HY catalyst was kept at 20 K higher temperature than the Ir/SiO_2 catalyst. In the third experiment, the Pt/HY and Ir/SiO_2 catalysts were well mixed in a weight ratio of 2:1, respectively. The details of the catalyst bed configuration are shown in Fig. 2.4. In all runs, the products were analyzed online in a HP5890 gas chromatograph with FID detector.

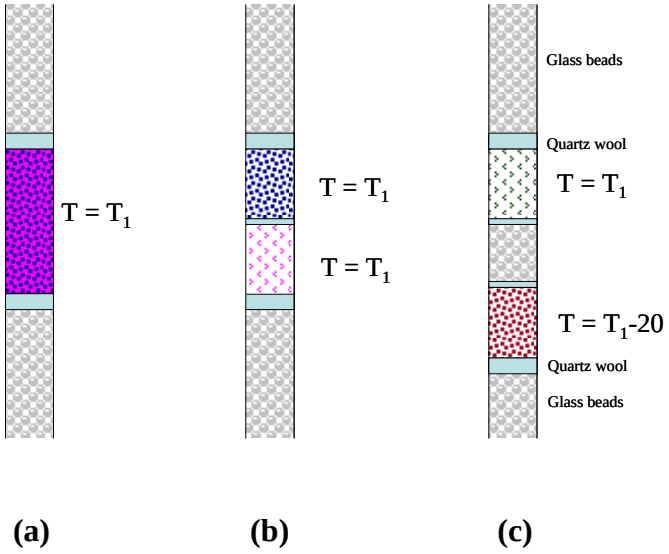

Figure 2.4 A schematic diagram of different catalytic bed configurations for methylcyclohexane reaction: (a) Pt/HY + Ir/SiO_2, (b) Pt/HY => Ir/SiO_2, and (c) Pt/HY = => Ir/SiO_2.

2.4 Product Analysis

2.4.1 The Decalin and Tetralin Reactions

The products of the decalin and tetralin reactions were analyzed online by a HP5890 II gas chromatograph with FID detector using an HP-5 and a Petrocol DH 50.2 boiling-point type columns. Then, these products was trapped by iced water (temperature kept at 273 K).Two gas chromatographs with mass spectrometer detectors (Shimadzu QP5000 and GCD HP 1800A) were used to

identify all the products formed during the reaction. More than 200 compounds were identified in the GC-MS analysis. The assignment of so many products is not a straightforward task and it must be stressed how much attention should be put into this effort to obtain a reliable analysis. To assign and quantify each product, a combination of residence time, cracking pattern, and comparison with GC standards was used. For each assignment, the relative boiling points, retention times, and cracking patterns from the NIST library were evaluated. The following Supelco GC standards were used *cis*- and *trans*-decalin, benzene, butyl-cyclohexane, cyclohexene,3-methyl-6-91-methylethyl), isoparaffin mix, n-paraffin mix (C_5-C_8 and C_7-C_{10}), aromatics mix, and naphtha standard. In addition to these comparisons we conducted reality checks to be sure that the assigned compounds behave as expected. For example, an olefin should decrease when the hydrogen pressure increases, as well as when Pt was incorporated in the HY catalyst. At the same time, the corresponding paraffin with the same skeletal structure should increase accordingly. To corroborate the analysis of the olefins present in the sample, the Bromine Index test was conducted on a couple of samples: one from the Pt/HY3 catalyst, and the other from HY3 catalyst. The former showed less than 1 wt % olefins, while the latter showed about 8 wt %, a trend that was in reasonable agreement with the results obtained from the GC analysis.

For the sake of clarity, we have grouped these products according to the number of carbon atoms in the molecule and in terms of the carbon skeleton reaction involved. These groups are as shown below:

a. Cracking products (CR): They contain two fractions, severe cracking or C1-C5 (mostly isobutane, and 2-methylbutane) and mild cracking or C6-C9 (such as methylcyclopentane, methylcyclohexane, benzene, toluene, xylenes, ethylbenzene, ethylcyclohexane and dimethylbenzene)
b. Ring contraction (RC) C10 products: They are characterized by the presence of bicyclic structure. For example, C_5-rings fused to C_6-rings (mehtylbicyclo[4.3.0]nonane, mehylbicyclo[3.3.1]nonane), two-rings connected together (such as trimethylbicyclo[4.1.0]heptane, dimethylbicyclo[3.2.1]octane, methylbicyclo[2.2.2]octane) and two-C_5-rings (1,1'-bicyclopentyl and spiro[4.5]decane).
c. Ring opening (RO) C10 products: They contains a monocyclic structure such as alkyl/alkenyl cyclopentanes, alkyl/alkenyl cyclohexanes or cyclohexenes or benzenes. Some products are butylcyclohexane, butylcyclohexene, butylbenzene, 4-methyl-1-(1-methylethyl) cyclohexene, 1-methyl-4-(1-methylethylid) cyclohexane, etc. However, it must be noted that within the RO products such as cyclohexane,1-methyl-4-(1-methylethyl) which

clearly have undergone not only RO, but also a transalkylation step [4].

d. Dehydrogenation products: a bicyclic structure containing at least one aromatic ring such as tetralin and naphthalene.

The structures of some relevant ring contraction and ring opening products from the reaction of decalin are shown in Table 2.2.

Table 2.2 Structures of some ring contraction and ring opening products

RC compound name	Structure	RO compound name	Structure
Methylbicyclo[4.3.0]nonane		Butylcyclohexane	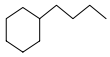
Methylcyclo[3.3.1]nonane		Methyl-4-isopropylcyclohexane	
Dimethylbicyclo[3.3.0]octane	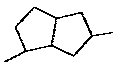	Dimethyl-3-ethylcyclohexane	
Dimethylbicyclo[2.2.2]octane		Methyl-2-isopropylcyclohexane	
Trimethylbicyclo[2.2.1]heptane	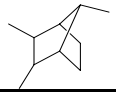	Methyl-3-isopropylcyclohexane	

2.4.2 The Methylcyclohexane Reaction

The reaction of methylcyclohexane (MCH) led to a mixture of products derived from isomerization and hydrocracking reactions with a trace dehydrogenation reaction. Products were analyzed online using a HP58900II gas

chromatograph equipped with a FID detector. To identify all the products, the standard compounds were injected into the GC for the comparison of the residence time. In addition, a gas chromatographs with mass spectrometer detector (Shimadzu QP5000) was used to provide the identification of the products as well.

In order to evaluate the products, they were classified into 4 families, regardless the catalysts as follows.

a. Ring contraction products (RC): isomerization to other napthenes, which is monobranched and dibranched cycloalkanes i.e. 1,1-dimethylcyclopentane, *trans*-1,2-dimethylcyclopentane, *trans*-1,3-dimethylcyclopentane, *cis*-1,3-dimethylcyclopentane, and ethylcyclopentane.
b. Ring opening products (RO): ring opening to alkanes with the same carbon number as the feed, i.e. *n*-heptane, 2-methylhexane, 3-methylhexane, ethylpentane, 2,3-dimethylpentane, 2,4-dimethylpentane, 2,2-dimethypentane, 3,3-diemthylpentane.
c. Cracked products (CR): hydrocracking to alkanes or cycloalkanes with less carbon atoms than the feed, i.e. hexane and cyclohexane.
d. Dehydrogenation products (HP): dehydrogenation to aromatics, i.e. toluene. However, this group was found only a trace amount because of the reaction conditions (i.e. high pressure and low temperature).

Some properties (e.g. RON, MON, and specific gravity) of compounds found in the reaction of methylcyclohexane are shown in Table 2.3.

Table 2.3 Product names and their research octane number (RON), motor octane number (MON), and specific gravity (Sp. Gr.)

Group name	Product name	Abbreviation name	RON	MON	Sp. Gr.
Feed	methylcyclohexane	MCH	73.8	73.8	0.7740
Cracking products	cyclopentane	CP	101.6	84.9	0.7505
(CR)	*n* -butane	*n* -BT	94.0	89.1	0.5844
	n -hexane	*n* -HX	24.8	26.0	0.6640
	etc				
Ring opening	2,2,3-trimethylbutane	2,2,3-TMB	100.0	100.0	0.6946
products, (RO)	3,3-dimethylpentane	3,3-DMP	80.8	86.6	0.6976
	2,2-dimethylpentane	2,2-DMP	92.8	95.6	0.6782
	2,4-dimethylpentane	2,4-DMP	83.1	83.8	0.6772
	2,3-dimethylpentane	2,3-DMP	91.1	88.5	0.6996
	n -heptane	*n* -HT	0.0	0.0	0.6882
	2-methylhexane	2-MH	42.4	46.4	0.6830
	3-methylhexane	3-MH	52.0	55.0	0.6917
	3-ethylpentane	3-EP	65.0	69.3	0.7028
Ring contraction	1,1-dimethylcyclopentane	1,1-DMCP	92.3	89.3	0.7593
products, (RC)	*cis* -1,3-dimethylcyclopentane	*c* 1,3-DMCP	79.2	73.1	0.7496
	trans -1,3-dimethylcyclopentane	*t* 1,3-DMCP	80.6	72.6	0.7537
	cis -1,2-dimethylcyclopentane	*c* 1,2-DMCP	86.5	85.8	0.7562
	trans -1,2-dimethylcyclopentane	*t* 1,2-DMCP	80.5	81.2	0.7562
	ethylcyclopentane	ECP	67.2	61.2	0.7710
Dehydrogenation	methylbenzene	Toluene	119.7	109.1	0.8719
products, (HP)	etc				

CHAPTER III

RING OPENING OF DECALIN AND TETRALIN ON HY AND Pt/HY ZEOLITE CATALYSTS[1]

Hydrogenation reaction that saturates aromatics, an interesting possibility is the opening of naphthenic rings derived from the saturation of aromatics to produce molecules of higher cetane numbers. In this contribution, we have investigated a series of HY and Pt/HY catalysts of varying acidity densities. Under the conditions of this study, mainly ring-contraction and one-ring opening reactions take place over these catalysts. Although the products from these reactions do not have cetane numbers significantly higher than those of the saturated aromatics, they can be important intermediates to high cetane number compounds, such as normal paraffins and some iso-paraffins. The results of this investigation show that HY zeolites can be effective catalysts for the ring-contraction and one-ring-opening of decalin if their acidity density is adjusted to an intermediate optimum. That is, their acidity density should be high enough to achieve conversion, but not too high which would result in fast deactivation. The low *cis*-to-*trans* ratios obtained in the products are due to both the *cis*-to-*trans* isomerization, and more importantly, to a much higher reactivity of *cis*-decalin than *trans*-decalin. Also, *cis*-decalin converts much more selectively to

---

[1] Published in Journal of Catalysis 228 (2004) 100-113.

cracking products. The production of ring-contraction and ring-opening products from tetralin is greatly enhanced in the presence of Pt due to hydrogenation of tetralin to decalin. In the presence of hydrogen, Pt/HY catalysts as well as physical mixtures of HY and Pt, are much more effective than HY catalysts.

3.1 Introduction

Removal of poly-nuclear aromatics from diesel fuel (e.g. anthracene, naphthalene, tetralin) has become a focus of intense research due to the stringent environmental legislation associate with clean-fuels [2-4]. In addition to their negative environmental impact, poly-nuclear aromatics decrease the cetane number (poor iginition) and diminish the overall quality of diesel. In this case, the couple hydrogenation and selective ring opening (SRO) have been recently proposed [16,57].

Selective ring opening can be accomplished on noble metals (Pt, Pd, Ir, and Rh) by hydrogenolysis [45]. McVicker et al. [16] suggested that the ring opening of C_6-naphthenic compounds requires the ring contraction step resulting from faster ring opening rate of C_5-naphthenic compounds. This ring contraction step can be achieved by an acidic function of catalyst. Therefore, the introduction of acid catalysts is interesting.

As illustrated in Fig. 3.1 for some relevant C_{10} compounds, the cetane number [58] greatly increases when a molecule such as decalin with two naphthenic

rings is converted into paraffin. However, it must be noted that both, the ring contraction and one-ring opening reactions that have been investigated in this work are only intermediate steps in this task. Neither ring-contraction (RC) nor one-ring opening (RO) alone results in an improvement in cetane number. However, these reactions might play an essential role in generating the intermediate one-ring or C_5-ring compounds that can be further converted to high cetane number compounds, such as normal paraffins and some iso-paraffins. This is an important point to emphasize because it may have been ignored in many of the previous investigations dealing with ring opening of decalin.

It is well known that on proton-form zeolites the ring opening of decalin is much faster than that of tetralin [4]. In a practical application, it is conceivable that aromatics such as tetralin or naphthalene would first undergo hydrogenation and subsequently the fully saturated decalin would be the reactive compound for the production of ring-opening products. Therefore, in the present contribution, the reactions of decalin and tetralin were investigated in a fixed bed flow reactor at 2 MPa and 533 K and 600 K, respectively, in the presence of excess hydrogen. We have selected the conditions that one would typically expect if the ring opening is conducted in combination with hydrogenation. These conditions are similar to those previously used by Arribas and Martinez [27] but differ significantly from those used by Corma et al. [4] and Kubicka et al. [26,59]. To systematically study the acid and metal functions, we have prepared a series of HY zeolites with varying degrees of

ion exchange to vary the acid site concentrations and on Pt-containing HY zeolite catalysts.

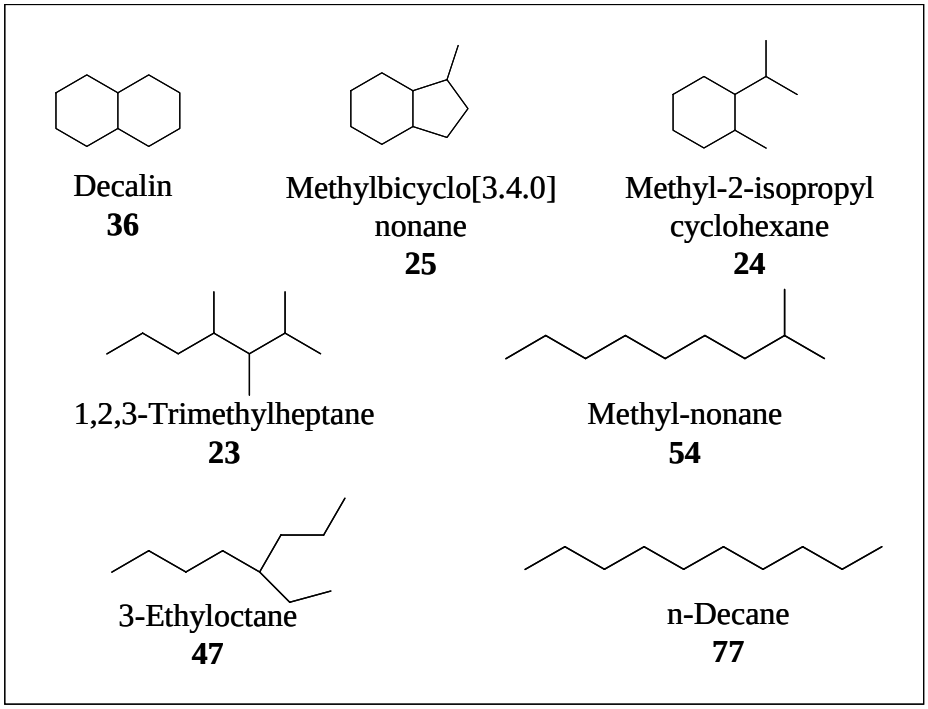

Figure 3.1 Cetane number of decalin and some relevant products.

Decalin has two configurational isomers, *cis* and *trans*. Between the two isomers, *trans*-decalin is more stable because it has no axial substituents. *Cis*-decalin is conformationally more mobile than *trans*, but it is less stable because it has one axial substituent in each ring. From the hydrogenation of naphthalene and tetralin a mixture of *cis*- and *trans*-decalin is obtained. Depending on the catalyst and the reaction conditions, the *trans/cis* ratio may widely vary. Not only different catalysts have different selectivities towards *trans*- or *cis*-decalin, but also the *cis*-to-*trans* isomerization may affect the resulting *trans/cis* ratio [60,61]. A distinctive aspect of the present study is that we have paid special attention to the differences in reactivity for the two decalin isomers and conducted measurements with isomerically pure feeds. If, as we propose here, *cis* and *trans* have on HY catalysts a very different reactivity towards ring opening, a product optimization could be expected if one can maximize the concentration of the isomer that is most reactive towards ring opening. This contribution also includes a set of experiments that has not been done before in the study of tetralin conversion. These experiments compare the product distribution of different physical mixtures and segregated beds of individual Pt and HY catalysts to that of single bed Pt/HY and HY catalysts.

3.2 Experimental

A series of ion-exchanged Y zeolite (HY1, HY2, and HY3) were used as acid catalysts and supports for Pt catalysts in this study. The ring opening reactions of a mixture of decalin (*trans*/*cis*-decalin, 63/37) were carried out in a continuous flow system and the ring opening reactions of pure isomers (cis-decalin, 99% and trans-decalin, 99%) were carried out in a pulse system as described in Section 2.3.1.1 and 2.3.1.2, respectively. In addition, the ring opening reactions of tetralin (98+%) were investigated in the four different physical mixtures of HY3 and Pt/SiO_2 according to Section 2.3.2.

3.3 Results and Discussion

3.3.1 Characterization of Catalysts

Table 3.1 shows the density of acid sites as determined from the integration of the NH_3 TPD and from FTIR of adsorbed pyridine. A clear trend indicates that, as expected, the density of acid sites (both Brønsted and Lewis) increased after each subsequent ion exchange with ammonium chloride. An interesting point to draw attention to is that the impregnation with metals leads to a significant loss in the number of acid sites, not only Brønsted, which may result from direct anchoring on proton sites, but also Lewis.

Table 3.1 Characterization of acidity of fresh catalysts

Sample	Total acidity[a]	Acidity[b] (μmol Py/g)					
	Amount of desorbed NH_3	Brønsted (1545 cm^{-1})			Lewis (1445 cm^{-1})		
	(μmol / g-cat.)	523 K	623 K	673 K	523 K	623 K	673 K
HY1[c]	665	232	222	199	223	209	34
HY2[d]	1487	515	475	394	525	377	212
HY3[e]	1670	628	610	501	581	461	289
Pt/HY[f]	1141	452	398	301	377	313	224

[a] Total acidity measured by TPD of NH_3

[b] Acidity measured by pyridine adsorbed and desorbed at different temperatures

[c,d,e] NaY after 1st, 2nd and 4th ion-exchang with NH_4Cl

[f] Pt supported on HY3 zeolite

The EXAFS analysis of the reduced Pt/HY at 673 K results in a coordination number for Pt-Pt of 7.0, indicating a good dispersion of the metal and an average particle size that would fit in a sphere of about 1.1 nm. This coordination number compares well with other well-dispersed Pt clusters on HY zeolites reported in the literature [62]. However, De Graaf et al. [63] have shown that for a 1 wt % Pt loading, one can only expect to have all of the Pt inside the HY zeolite structure when using ion exchange with tetra-amine precursor and a heating rate as low as 0.2°C/min. In that case, coordination numbers of the order of 5.5 have been obtained. Since the preparation method employed in the present contribution is not optimized we may expect the typical bimodal distribution, with a fraction of small metal clusters inside the HY zeolite structure and a fraction outside forming

relatively large particles. Therefore, the coordination number of 7.0 represents an average between these two types of Pt particles, more than a typical particle size.

3.3.2 Catalytic Activity Measurements

3.3.2.1 Conversion of Decalin over HY and Metal-HY Catalysts

Table 3.2 shows the product distribution obtained on the different catalysts at 2 MPa and 533 K with a decalin feed (*trans/cis* feed ratio: 63/37) after 75 min and 155 min on stream. The initial conversion (not shown) paralleled the trend in acid density (i.e., HY1<HY2<HY3). However, as shown in Table 3.2 the deactivation patterns were significantly different over the different catalysts and as a result, after 75 min on stream, the conversion on the zeolite with the highest acidity (HY3) was already lower than that on HY2. To investigate the effect of deactivation on the product distribution, the flow reactor that we have used in this work is more appropriate than the batch reactor used in recent studies [26] as it allows one to follow the overall conversion and product distribution as a function of time on stream. For example, the rapid deactivation observed on catalyst HY3 is paralleled by a rapid decrease in the yield of C1-C5 products, which are dominant during the first few minutes on stream, but decrease to very low values after 2 hours.

Table 3.2 Product distribution and conversion of decalin over HY zeolites and Pt/HY catalyst. Reaction conditions: Total pressure = 2 MPa, Temperature = 533 K, LSV = 1.89 h^{-1}, and H_2/HC molar ratio = 65

	Feed	**HY1**		**HY2**		**HY3**		**Pt/HY**	
Time on stream (min)		**75**	**155**	**75**	**155**	**75**	**155**	**75**	**155**
Trans -decalin (wt%)	63.0	73.9	73.5	33.3	47.2	54.2	63.8	65.5	66.2
Cis -decalin (wt%)	37.0	15.2	15.7	1.8	3.1	4.9	6.5	5.8	6.4
Conversion* (%)		10.9	10.9	64.9	49.7	40.8	29.8	28.7	27.4
Products		Yield (wt%)							
C1-C5		0.6	0.5	22.2	16.2	10.4	3.5	1.7	1.7
C6-C9		0.2	0.3	9.6	3.8	3.4	1.9	4.3	3.7
C10 Products		10.2	10.0	33.1	29.6	27.1	24.4	22.7	22.0
Alkylcyclonaphthenes, and alkylcyclobenzenes		9.4	9.0	19.1	19.0	19.1	15.1	11.8	11.1
Ring contranction products		0.1	0.2	14.0	10.6	8.0	9.3	10.9	10.9
Tetralin and naphthalene		0.7	0.8	0.0	0.0	0.0	0.0	0.0	0.0

* Conversion based on *trans*-decalin and *cis*-decalin

The addition of Pt to the acidic zeolite HY3 results in the loss of an important fraction of acid sites (see Table 3.1). As a consequence, the lower amount of cracking products and initial overall conversion observed on the Pt/HY compared to the proton-form zeolite HY3 is not unexpected. In addition, it was observed that the presence of Pt greatly enhanced the stability of the catalyst since the fast deactivation of the HY3 catalyst was not observed for the Pt/HY. In parallel to the rapid deactivation of HY3 catalyst a significant drop in the cracking products is observed on this catalyst as a function of time on stream. Moreover, the yields of C10 products of higher interest to this study, RC and RO, are higher for the catalyst of higher acidity, but they decrease as the catalysts deactivate. As a result, the catalyst with intermediate acidity is after a few hours the most effective for C10 product yield. Fig. 3.2 illustrates the variation of overall conversion as a function of time on stream for all the catalysts; clearly, the activity was lower for the two catalysts with lower acidity, HY1 and Pt/HY, but at the same time the deactivation was much less pronounced for these catalysts than for those with higher acidity density.

An interesting change in the *trans/cis*-decalin ratio was observed in the product compared to that in the feed (63/37). In all cases, as shown in Table 3.2, this ratio was observed to increase significantly. The preferential disappearance of *cis*-decalin may be due to two causes, a) *cis*-to-trans isomerization or b) higher reactivity of *cis* that makes it react faster than *trans*. Both effects may be present, although the latter seems to be dominant on these catalysts. The *trans/cis*

ratio was as high when using the Pt/HY catalyst as when using the proton-form of HY zeolites. However, as previously shown [64], the *cis*-to-*trans* isomerization should be more significant in the presence of Pt/HY than on the bare HY zeolites, which indicates that the *cis*-to-*trans* isomerization is not the dominant factor in determining the *trans/cis*-decalin ratio.

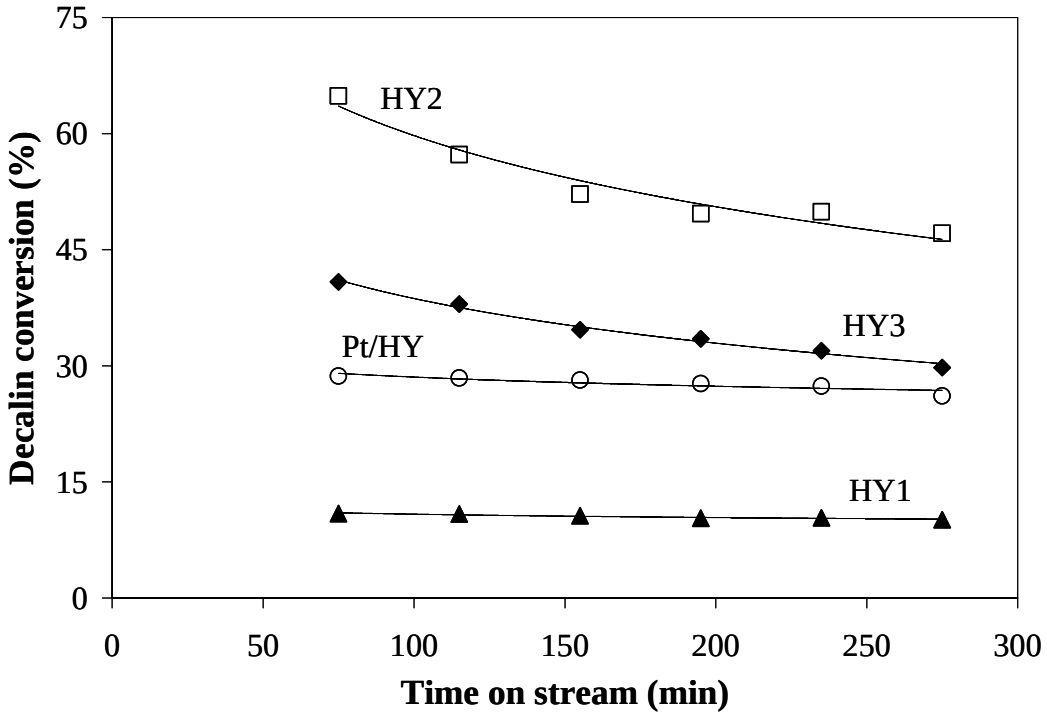

Figure 3.2 Total conversion of decalin on various catalysts. Reaction conditions: Total pressure = 2 MPa, Temperature = 533 K, and H_2/HC molar ratio = 65.

The results of Table 3.2 strongly suggest that on all catalysts most of the conversion occurs on the *cis*-decalin, the reactant that is preferentially consumed. A plausible explanation is that the reactivity of *cis*-decalin for cracking and ring opening on HY is much higher than that of *trans*-decalin. In fact, differences in the reactivity of the two isomers have been observed previously by other authors [65,66]. As demonstrated by Mostad et al. [65] the difference in reactivity between *cis*- and *trans*-decalin is much more obvious for zeolite Y than for amorphous silica-alumina. The preferential reactivity might be related to the greater ability of the *cis* isomer to penetrate the Y zeolite pore (about 0.74 nm) due to its slightly smaller molecular dimensions and, most importantly, its higher conformational mobility. It is also reasonable to expect that the *cis* isomer can generate the surface reaction intermediate more easily than the *trans* isomer. The trans form has more hindered C-H bonds than the *cis* form, this steric difference may account for the lower reactivity. If the reaction intermediate has the positive charge on the tertiary carbon, it will be the same for both isomers. If that is the case, being *trans* more stable than *cis*, the difference in energy with the reaction intermediate (activation energy) would be higher for *trans*-decalin. The reactivity difference manifests again in Fig. 3.3 for the ring opening reaction, which shows the product distribution for the reaction of the 63/37 *trans/cis*-decalin feed as a function of the space time (W/F). At low W/F, the amount of *cis*-decalin dramatically decreases with increasing W/F. Although some of the *cis* conversion may have been isomerization to *trans*, most of the *cis*-decalin consumption is mirrored by the

increase in the amount of C10 ring opening products (RO). Beyond a certain W/F (i.e ~ 0.45 h), increasing the reactor size results in selectivity losses as secondary cracking products begin to be formed in larger quantities. It is also seen that the *trans*-decalin, does not decrease at low W/F, but rather slightly increases due to *cis*-*trans* isomerization and only decreases at very high W/F, when the cracking products begin to appear. From these trends it seems that *cis*-decalin mainly converts into RO products while *trans*-decalin is much less reactive, but when it reacts it does it unselectively to multiple cracking. However, the parallel *cis*-to-*trans* isomerization may mask the contribution of the direct *trans* conversion. Therefore, it is important to use isomerically pure *cis*- and *trans*-decalin feeds to compare the reactivity of the two isomers. Those experiments are shown below in Section 3.2.2.2.

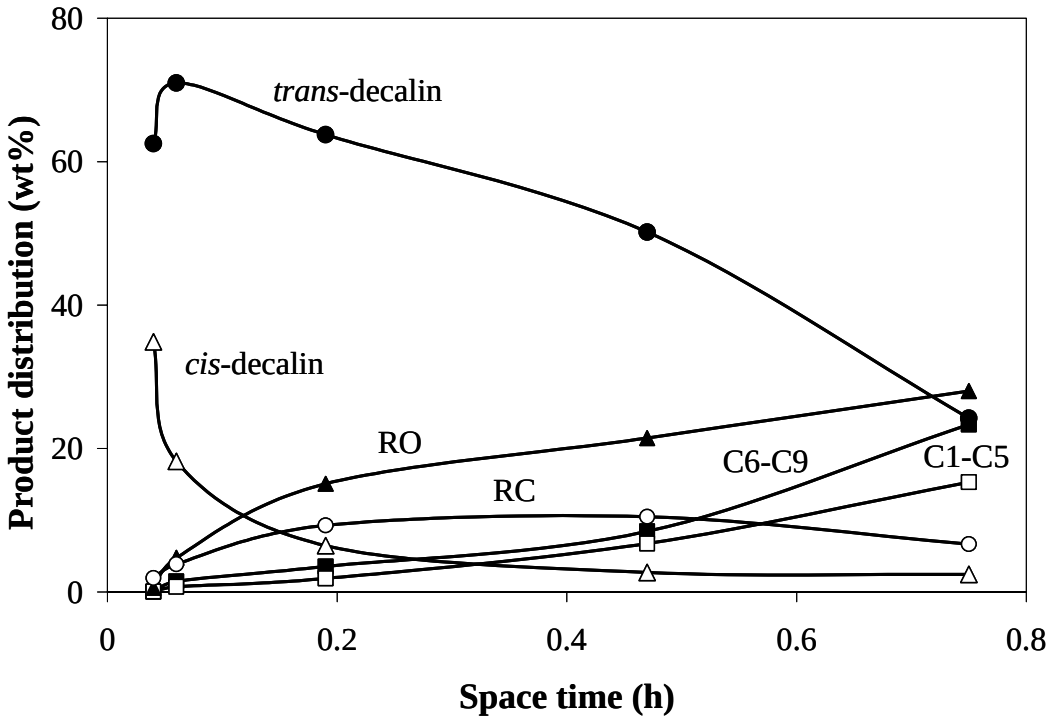

Figure 3.3 Product distribution of decalin ring opening on HY3 at different space velocities. Reaction conditions: Total pressure = 2 MPa, Temperature = 533 K, and H_2/HC molar ratio = 65 after time on stream = 155 min.

To further analyze the evolution of RC and RO with overall conversion, we summarize in Fig. 3.4 a larger number of data points obtained on the three HY catalysts at various W/F and at various times on stream. It can be observed that both the RC and RO products initially increase in concentration as a function of conversion, but at some point the evolution of RC products levels off and finally decrease, while the concentration of RO products keeps increasing. As proposed by Kubicka et al. [26], the reactivity of RC products is much higher than that of RO. products, either due to a higher strain in the five carbon ring or due to a larger number of tertiary carbons in the molecule. Therefore, it is not surprising that as conversion increases, RC products are gradually converted into RO products.

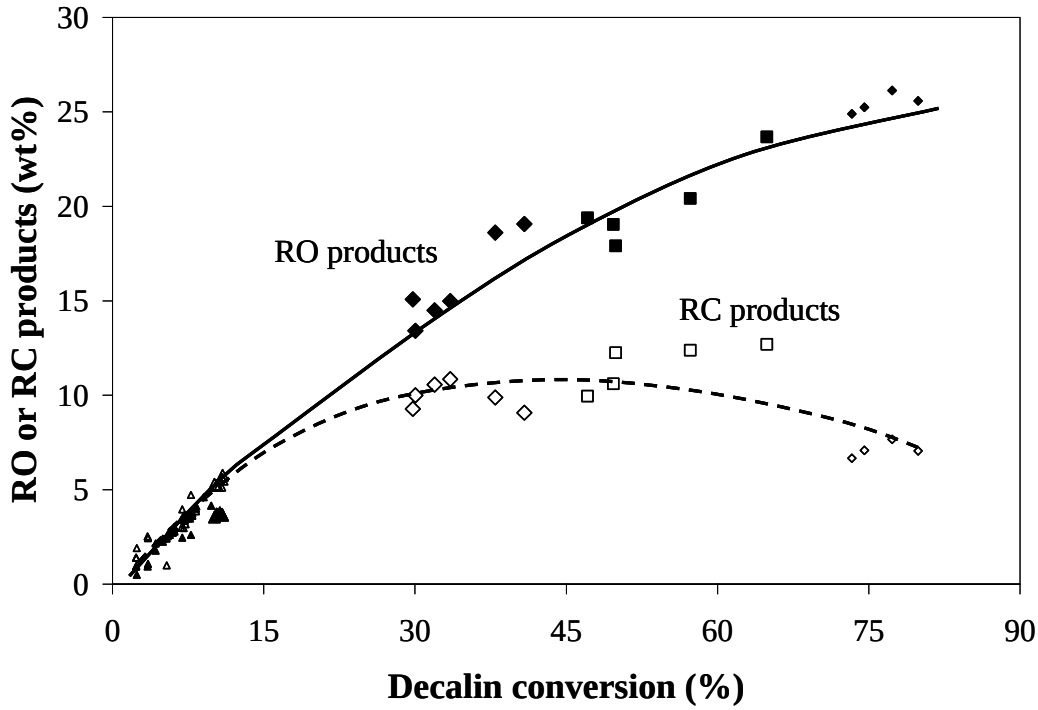

Figure 3.4 Ring opening (RO) and ring contraction (RC) products of decalin ring opening on various catalysts at varying conversions (both by space times and time on stream). Diamonds: HY3; Squares: HY2; triangles: HY1. Reaction conditions: Total pressure = 2 MPa, Temperature = 533 K, and H_2/HC molar ratio = 65.

Fig. 3.5 shows that the evolution of the RC/RO ratio follows the same pattern as a function of conversion for all the HY catalysts, whether conversion has been varied by increasing space-time (W/F) or by catalyst deactivation.

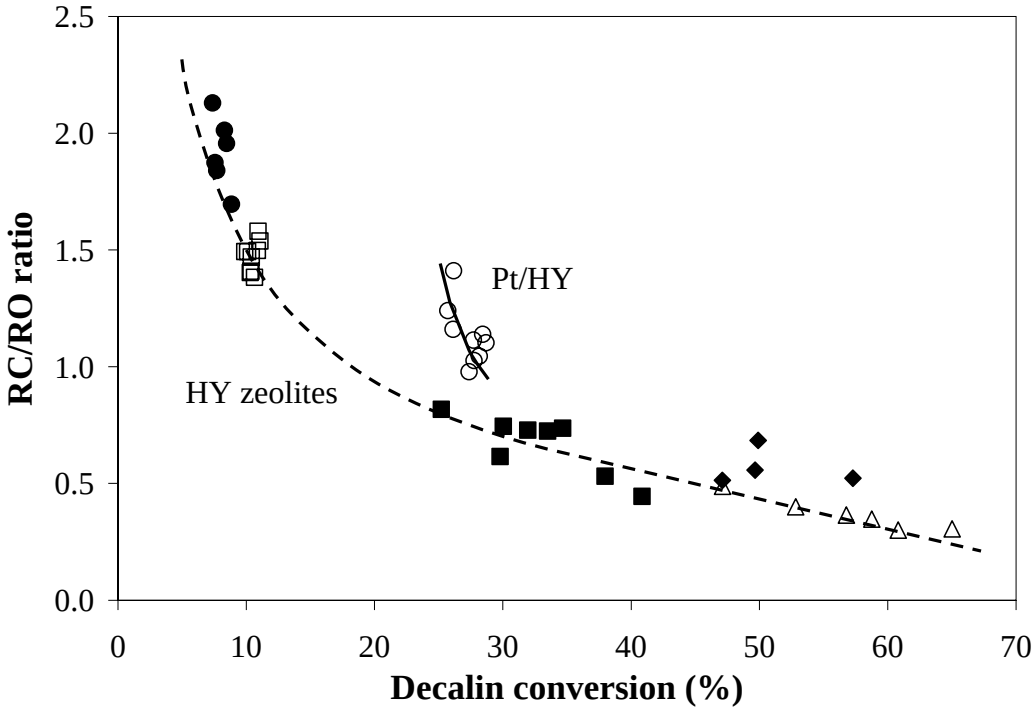

Figure 3.5 RC/RO ratio of decalin ring opening on HY zeolites and Pt/HY at different conversions. Conversions were varied by changing space time and time on stream. Reaction conditions: Total pressure = 2 MPa, Temperature = 533 K, and H_2/HC molar ratio = 65.

An interesting change in product distribution is observed in Fig. 3.4 when Pt is added to the HY zeolite. Although the RC/RO ratio still decreases with overall conversion the absolute value of this RC/RO ratio for any given conversion is higher on the metal containing catalyst than on any of the proton-form zeolites. The metal containing Pt/HY catalyst contains a significantly lower acidity density than the pure HY3 zeolite. This lower acidity density may account for the lower amount of cracking products. However, the high RC/RO ratio indicates that the presence of the metal favors the RC step while inhibiting the RO. A possible explanation of this effect is that a partial dehydrogenation over the metal would accelerate the activation of decalin, but at the same time, an enhanced hydrogen transfer would reduce the lifetime of surface carbenium ions, allowing the desorption of RC products and preventing their further reaction to RO products. An interesting comparison is made below in section 3.2.2.3 with physical mixtures in which the Pt metal is not inside the zeolite. In that case, the RC/RO ratio is as low as for the proton-form zeolite alone, which supports the idea that the change in RC/RO ratio is due to enhanced hydrogen transfer inside the zeolite.

According to the reaction scheme proposed by Corma et al. [4], RO products could be obtained either by direct opening of the decalin molecule via protolytic cracking (PC) or via a secondary cracking of RC products. In Fig. 3.6, we report the evolution of two relevant RO and RC products as a function of conversion on catalyst HY3. It can be seen that while the RC product, 1H-Indene,octahydro-1-methyl appears as a primary product, the RO product

cyclohexane,butyl behaves as a secondary product. It must be noted that cyclohexane,butyl can only be formed by two alternative paths, either as a primary product by direct PC followed by hydride transfer and desorption [4] or as a secondary product from the opening of 1H-Indene,octahydro-1-methyl. The observed trend as a function of conversion and the zero derivative at zero conversion indicate that most of cyclohexane,butyl is formed as a secondary product from the cracking of the 1H-Indene,octahydro-1-methyl, which by contrast, starts decreasing as the cyclohexane,butyl increases. In fact, RC products are generally considered primary products. However, in doing this type of analysis one must take into account the possibility that, by the time the molecule leaves the zeolite, it may have already undergone secondary reactions. For example, the evolution of cyclohexane,1-methyl-4-(1-methylethenyl) looks as if it were a primary product. However, the formation of this RO product obviously requires a complicated skeletal rearrangement that may includes ring contraction, ring opening, and skeletal isomerization or transalkylation. It was observed that even at very low conversions, the yield of the RO product was significant. Therefore, it appears that in this system it is difficult to observe truly primary products, even when running at very low conversions.

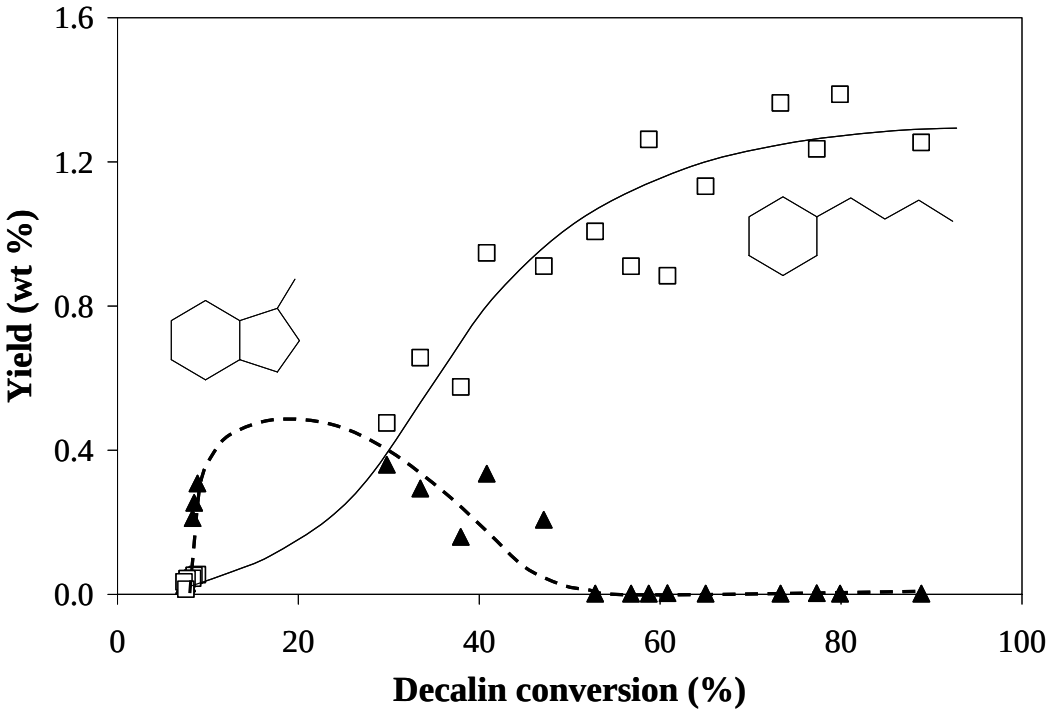

Figure 3.6 Yield of two relevant products as a function of conversion. Solid triangles: 1H-Indene,octahydro-1-methyl; open squares: cyclohexane,butyl.

3.3.2.2 Conversion of Isomerically Pure Cis- and Trans-Decalin

As mentioned, the comparison of the intrinsic activity of the two decalin isomers may be obscured by the *cis*-to-*trans* isomerization reaction that occurs in parallel. Therefore, in order to compare their reactivities we measured the conversion of isomerically pure *trans*- and *cis*-decalin feeds at 533 K and 2 MPa on the HY3 and Pt/HY3 catalysts in the flow reactor. The observed inequalities in activity and selectivity were indeed remarkable for both HY and PtHY catalysts. The overall conversion for the two different pure feeds is compared in Figs. 3.7a and 3.7b, which unambiguously demonstrates that the *cis*-decalin is not only much more reactive than *trans*-decalin, but also more selective to C10 ring opening products. In fact, the dominant products from *trans*-decalin were cracking products (C1-C9), rather than C10 products.

To confirm that the difference between the two isomers is related to the reactivity of the molecules on these particular catalysts, rather than to an indirect effect, such as a different degree of coking and deactivation, we conducted another comparison in a pulse reactor over clean catalysts at low pressures (0.2 MPa). In these experiments, micropulses of pure *trans*-decalin and pure *cis*-decalin were sent over the proton-form of HY3 zeolite. The product distributions for these experiments are shown in Table 3.3. High conversions were observed for pure *cis*-decalin on the HY3 catalyst at 593 K and 630 K, 83 and 92 %, respectively.

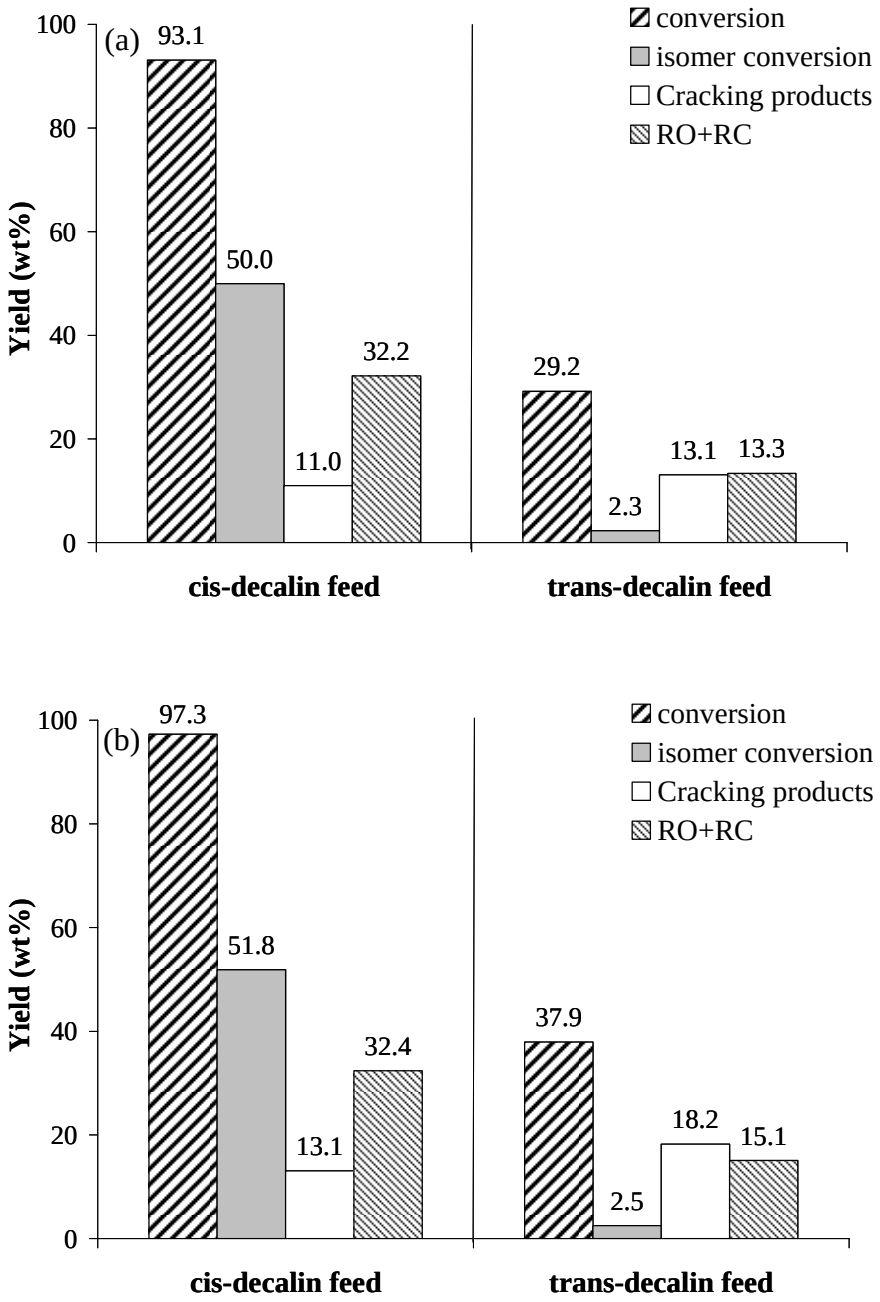

Figure 3.7 Pure *cis*- and *trans*-decalin in flow mode on (a) HY3 and (b) Pt/HY. Reaction conditions: Total pressure = 2 MPa, Temperature = 533 K, LSV = 1.89 h^{-1}, and H_2/HC molar ratio = 65.after time on stream = 155 min.

By contrast, very low conversions, 13 and 27 %, were obtained with *trans*-decalin under the same conditions that is 593 K and 630 K, respectively. At the lower temperature, the overall yield to C10 ring opening from *cis*- decalin was almost 30 times higher than that from the *trans* isomer. As the temperature increased, the selectivity to RO products decreased as secondary cracking became more dominant. Nevertheless, the important conclusion from these studies is that regardless of the presence or absence of metal in the catalyst, or of the pressure at which the reaction takes place, reactive of *cis*-decalin on HY-based catalysts is clearly superior to that of *trans*-decalin.

Table 3.3 Conversion of pure *cis*- and *trans*-decalin in pulse reactor on HY3 zeolite. Total pressure = 0.14 MPa

Feed	***Cis* -decalin**	***Trans* -decalin**	***Cis* -decalin**	***Trans* -decalin**
Temperature (K)	**593**	**593**	**629**	**629**
Trans -decalin (wt%)	8.8	87.5	7.0	73.4
Cis -decalin (wt%)	17.5	0.3	8.5	0.0
Products	Yield (wt%)			
C1-C9	53.7	10.8	62.1	21.3
Ring opening products	11.7	0.6	11.9	1.4
Ring contraction products	7.6	0.7	9.1	3.1
Tetralin	0.4	0.2	1.0	0.8
Naphthalene	0.3	0.0	0.2	0.0

3.3.2.3 Conversion of Tetralin

Due to the presence of the aromatic ring, tetralin is more difficult to convert than decalin. Corma et al. [4] have seen activity differences between tetralin and decalin on HY zeolites, but since their study was conducted at 723 K, the differences were not so dramatic as those seen here at lower temperatures. In fact, while the conversion measurements on decalin were conducted at 533 K, those with tetralin had to be conducted at 600 K to get comparable conversions. As shown in Table 3.4, the most obvious contrast with the decalin study (Table 3.2) is the large increase in activity observed in the presence of a metal. While in the case of decalin conversion, the addition of metal causes a decrease in initial conversion, when tetralin was used, the presence of the metal greatly increased the conversion. In fact, despite the lower acidity density, the overall conversion on the Pt/HY3 catalysts was at the same W/F more than four times that on HY3. Even when subtracting the conversion to hydrogenation products, the conversion is significantly higher than on HY3. The obvious explanation for this increase is the metal catalyzed hydrogenation that converts tetralin into decalin, which is then further converted as seen above. In agreement with our findings, Arribas and Martinez [27] have concluded that the initiation step for the hydrocracking of naphthalenes on Pt/HY is the sequential hydrogenation of naphthalenes to tetralins and decalins on the metal, followed by formation of carbocations on the Brønsted sites of the zeolite, which lead to cracking and RO products.

Table 3.4 Conversion of tetralin over HY zeolites and Pt/HY catalyst. Reaction conditions: Total pressure = 2 MPa, Temperature = 598 K, and H_2/HC molar ratio = 60 after time on stream = 155 min

Catalyst	**HY1**	**HY2**	**HY3**	**Pt/HY**
Tetralin conversion (%)	16.3	16.8	23.9	92.6
Products	Yield (wt%)			
C1-C5	0.0	0.3	1.9	1.4
C6-C9	5.4	4.4	7.6	5.0
C10 products				
Ring opening products	3.0	4.2	5.2	15.0
alkyl-cyclo compounds	0.7	1.4	0.5	14.1
alkylbenzene	2.2	2.8	4.7	0.9
Ring contraction products	1.9	2.6	3.2	19.7
Trans -decalin	1.1	1.7	0.8	44.4
Cis -decalin	0.5	0.5	0.3	6.2
Naphthalene	4.6	3.1	4.8	1.0

This sequence is demonstrated in Fig. 3.8, which shows the product distribution for the reaction the tetralin feed as a function of space-time (W/F) over Pt/HY. This graph clearly establishes that on this catalyst the only primary products from tetralin are *cis*- and *trans*-decalin. Regarding the variation of the *trans/cis*-decalin ratio, it is also seen in Fig. 3.8 that both isomers start with identical slopes, at W/F near zero, but very quickly the slope for the *cis*-decalin yield decreases while the *trans/cis* ratio increases. At this point, the secondary products appear (i.e., cracking, ring contraction, and ring opening).

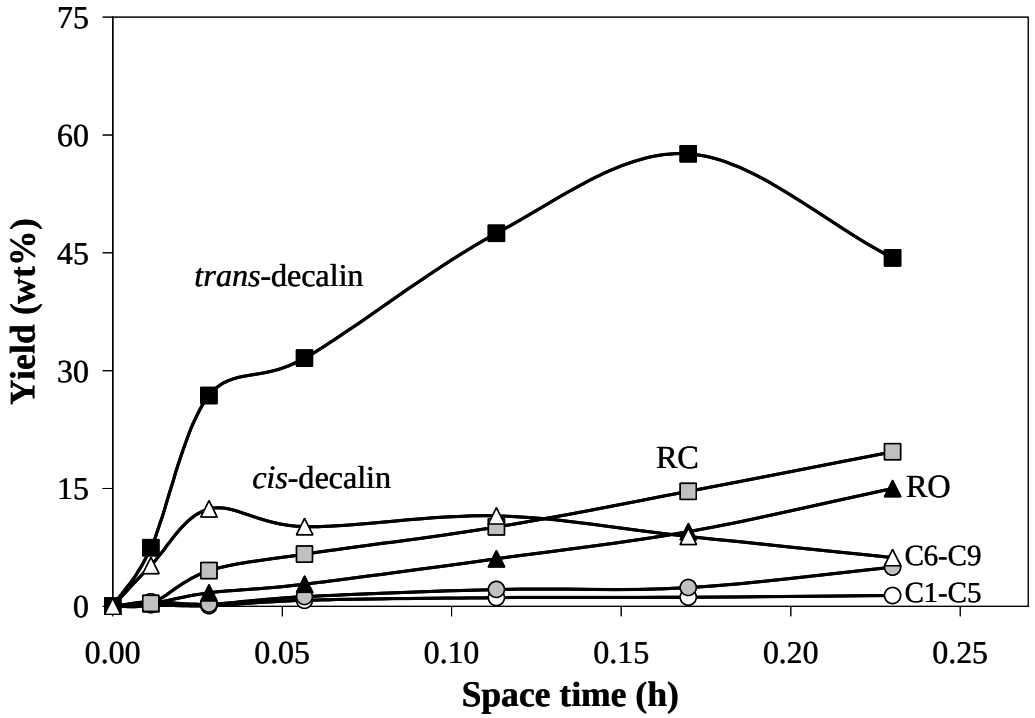

Figure 3.8 Product distribution of tetralin ring opening on Pt/HY. Reaction conditions: Total pressure = 2 MPa, Temperature = 598 K, and H_2/HC molar ratio = 60 after time on stream = 155 min.

The concentration of *trans*-decalin in the reactor keeps increasing with W/F up to high W/F values, at which point, its decrease is accompanied by an increase in light cracking products. The different trends observed for *cis*- and *trans*-decalin can be explained, as discussed above, in terms of the *cis*-to-*trans* isomerization and the higher reactivity of the *cis* isomer.

Another interesting contrast observed in Table 3.4 is that when tetralin is used as a feed instead of decalin the production of naphthalene greatly increases, particularly on the HY zeolites without metals. Corma et al. [4] have ascribed the appearance of naphthalene when reacting tetralin over different zeolites to a hydrogen transfer between tetralin and the adsorbed carbenium ions.

Fig. 3.9 shows the evolution of the RC/RO ratio as a function of conversion for Pt/HY and HY3. On the Pt/HY3 catalyst, different initial conversions were obtained by varying W/F. Clearly, the RC/RO ratio is much higher for the Pt/HY catalyst than for the HY catalysts. At the same time, it is observed that the RC/RO ratio greatly increases as the catalyst deactivates.

As indicated above for the decalin reaction, the high RC/RO ratio indicates that the presence of the metal enhances the RC step more than the RO step. The generation of olefins accelerates the activation of decalin, but at the same time, the hydrogen transfer enhanced by the presence of Pt can reduce the lifetime of the surface intermediates, allowing the desorption of RC products and preventing their subsequent reaction to RO products.

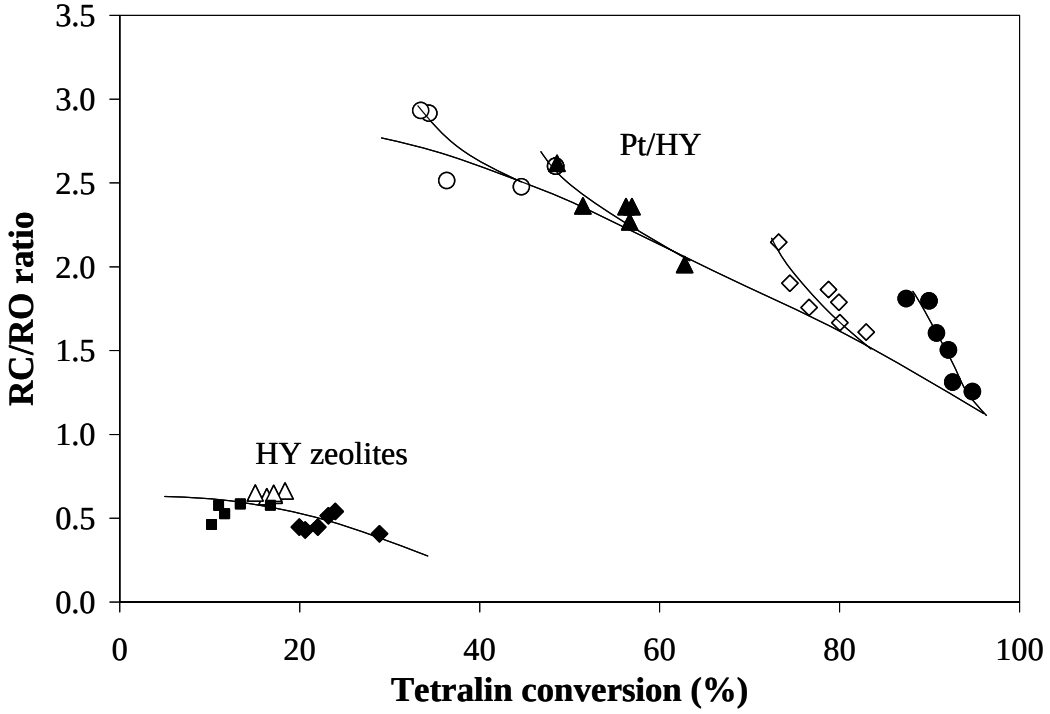

Figure 3.9 RC/RO ratio of tetralin ring opening on HY3 and Pt/HY. Different symbols indicate runs conducted at different space times. Reaction conditions: Total pressure = 2 MPa, Temperature = 598 K, and H_2/HC molar ratio = 60.

3.3.2.4. Tetralin Conversion on Physical Mixtures and Segregated Beds of Pt/SiO_2 and HY Catalysts

To discern the role of the individual functions of the catalyst (metallic and acidic) we devised a series of experiments to react tetralin over physical mixtures of catalysts and sequential catalyst beds. A Pt/SiO_2 sample was used to represent the monofunctional metallic catalyst and the proton-form HY3 zeolite was used as the monofunctional acid catalyst. In one of the sequential bed reactors, the 1 wt. % Pt/SiO_2 catalyst was placed in front of the HY3. In the other, the 1 wt. % Pt/SiO_2 bed was placed after the HY3 bed. In addition, two other samples were prepared by physically mixing the 1 wt. % Pt/SiO_2 and HY3 catalysts in two different Pt/SiO_2:HY ratios, 1:1 and 1:2. The product distributions obtained on the different samples for the reaction of tetralin at 600 K and 2 MPa after 7 h on stream are summarized in Table 3.5.

Table 3.5 Conversion of tetralin on physical mixtures of Pt/SiO_2 and HY3 catalysts. Reaction conditions: Total pressure = 2 MPa, Temperature = 598 K, and H_2/HC molar ratio = 60 after time on stream = 420 min

Catalyst	**HY**	**Pt>>HY**	**HY>>Pt**	**Pt+HY**	**Pt+HY**	**Pt/HY**
Pt/SiO_2:HY ratio	-	-	-	1:1	1:2	-
mmoles of H^{+*}	0.3	0.2	0.2	0.2	0.3	0.2
mmoles of Pt	0.0	0.6	0.6	0.6	0.5	1.0
Tetralin conversion (%)	11.8	97.5	91.3	86.4	98.7	91.4
Products			Yield (wt%)			
C1-C5	ND	ND	ND	ND	ND	ND
C6-C9	0.2	0.6	0.5	0.2	0.5	0.2
C10 products						
Ring opening products	3.1	8.8	3.2	5.1	12.6	12.4
alkylcyclo compounds	0.9	8.7	2.7	4.9	12.4	11.1
alkylbenzenes	2.2	0.1	0.5	0.3	0.2	1.3
Ring contraction products	2.3	4.1	2.5	3.3	7.1	12.7
Trans-decalin	1.1	75.3	70.5	62.0	70.6	55.4
Cis-decalin	0.6	7.1	14.0	14.5	7.8	9.7
Naphthalene	4.6	1.7	0.7	1.2	0.1	1.0

* Based on TPD of NH_3

As mentioned above, the reaction on the HY catalyst alone produces alkyl-benzenes as the major RO products together with naphthalene, which results from the hydrogen transfer from tetralin to the surface carbenium ions. Over this catalyst, the production of decalin is minimal; therefore we can envision a surface carbenium ion which still keeps its original aromatic ring intact. A hydrogen transfer step from tetralin should result in the evolution of alkyl-benzene and

dehydrogenation of tetralin. It is interesting to compare the production of alkyl-benzenes from pure HY catalysts as opposed to alkyl-cyclohexanes that are observed when Pt is present. This important disparity can be due to two possible causes. One of them is that alkyl-benzenes are formed, but later hydrogenated over the metal. The other is that they are not formed, that is, the carbenium ion intermediates do not contain the aromatic ring. The experiments that we have designed are most appropriate to differentiate these alternatives. In the run in which Pt is placed before the HY (Pt >> HY) hydrogenation over Pt can only occur before the generation of the carbenium ions. Therefore, the lack of alkyl-benzenes cannot be due to secondary hydrogenation. Rather, the clear increase in the concentration of decalin resulting from hydrogenation of tetralin on the first bed causes that RO products formed in the subsequent HY bed do not contain aromatic rings. That is, the carbenium ion is formed from decalin and the RO products are alkyl cyclohexanes/enes. When Pt is present, any olefin product from the RO is rapidly hydrogenated under these conditions. Olefins only appear in small quantities at temperatures above 320 K and lower pressures.

By contrast, in the run in which HY precedes the Pt bed (HY >> Pt) we expect that in the first bed alkyl-benzenes are formed, but later, they are effectively hydrogenated to alkyl cyclohexanes over the Pt catalyst. In fact, it is observed that very small amounts of alkyl-benzenes are seen after the Pt bed. Since the reactivity of decalin towards RO on HY is much higher than that of tetralin, the

remarkable increase in the yield of RO products is simply due to the initial hydrogenation of tetralin to decalin in the case of the Pt-first system (Pt >> HY).

Another important question that can be addressed on the basis of this set of experiments is why the disappearance of *cis* is so much faster than that of *trans*, as seen in Figs. 3.3 and 3.8. As mentioned above, this difference is due to two reasons. One is the isomerization of *cis* to *trans*, the other is the higher reactivity of *cis* compared to *trans*. The two effects are clearly apparent in the results presented in Table 3.5. In the first place, it is seen that the production of decalin from tetralin is, at least, two orders of magnitude slower on HY than on Pt. At the same time, the *cis*-to-*trans* conversion is also slower. In agreement with this result, Lai and Song [64] have observed that the *cis*-to-*trans* isomerization over Pt- and Pd-modified zeolites is much faster than over proton-form zeolites. The *trans/cis* ratio obtained on HY is only 1.7. On the metal, the *trans/cis* ratio should increase. We have previously shown [67] that, in the decalin produced by hydrogenation of tetralin on pure Pt catalysts at low conversions, the *trans/cis* ratio is about 1.0 and remains fairly constant up to tetralin conversion levels of 80% and above. At high conversions, the *trans/cis* ratio increases to about 4-6. In the two-bed reactor (HY >> Pt) one expects a low conversion to decalin in the first part (HY) while on the second part of the reactor (Pt/SiO_2) initial hydrogenation produces a 1:1 mixture of *cis* and *trans*, followed by isomerization of *cis*-to-*trans*, as indicated by the observed trans/cis ratio of about 5. By contrast, in the two-bed reactor (Pt >> HY), we expect a ratio of about 5 after the first part (Pt/SiO_2) but little *cis*-to-*trans*

isomerization in the second part (HY). Therefore, the very high *trans/cis* ratio observed, which approaches the equilibrium value of 11, is due to the preferential consumption of *cis* by the RO reaction.

Another interesting comparison is the concentration of RC products obtained over Pt/HY compared to that obtained on the physical mixtures Pt + HY. The catalyst in which Pt is directly supported on the HY zeolite, with an important fraction of metal deposited inside the zeolite porous structure exhibits a very high concentration of RC products. In fact if a bifunctional mechanism of isomerization is involved then the proximity of Pt and acid sites can be responsible for the observed higher isomerization activity. Although, as shown in Fig. 3.9, the RC/RO ratio greatly decreases with conversion, the ratio is 1.03 for the Pt/HY catalyst at a tetralin conversion of 91 %, while it is only 0.65 for the physical mixture Pt + HY (1:1) at a tetralin conversion of 86 %. From the line corresponding to the Pt/HY catalyst in Fig. 8, a RC/RO ratio of about 1.3 should be expected for a conversion of 86 %. We have previously mentioned that the RC/RO ratio is much lower for the proton-zeolites without metal. Here, it is demonstrated that this enhancement is only observed when Pt is inside the zeolite. A possible explanation for this effect is the enhanced hydrogen transfer that occurs inside the zeolite when Pt is present. This hydrogen transfer would reduce the lifetime of the carbenium ion on the surface and, as a result, inhibit the transformation of RC products into RO products.

3.4 Conclusion

The main conclusions of this work can be summarized as follows:

- HY zeolites can be effective catalysts for the ring-contraction and one-ring-opening of decalin, but the density of acid sites needs to be adjusted to an intermediate optimum, high enough to achieve conversion, but not too high that would result in fast deactivation.

- From the conversion of decalin, RO products can be obtained as secondary products via cracking of RC intermediates.

- The low *cis*-to-*trans* ratios obtained in the products are due to both, the *cis*-to-*trans* isomerization, but more importantly, to a much higher reactivity of *cis*-decalin than *trans*-decalin. Also, cis-decalin converts much more selectively to RO products than *trans*-decalin.

- The production of RC and RO products from tetralin is greatly enhanced in the presence of Pt due to hydrogenation of tetralin to decalin. In the presence of hydrogen Pt/HY catalysts as well as physical mixtures of HY and Pt are much more effective than HY catalysts.

ACKNOWLEDGEMENTS

I would like to acknowledge Oklahoma Center for Advancement of Science and Technology (OCAST) and ConocoPhillips for financial support of the ConocoPhillips Catalysis Lab at the University of Oklahoma. Partial support was received from the National Science Foundation under Grant No. EPS-0132534. I also thank the technical support of the personnel at NSLS, Brookhaven National Laboratory, for the X-ray absorption experiments and James Straw for reactor construction. I am thankful the Energy Policy and Planning Office of the Ministry of Energy of the Royal Thai Government for a scholarship.

CHAPTER IV

ENHANCING THE SELECTIVITY OF DECALIN RING CONTRACTION VS. RING OPENING BY TAILORING THE ACID DENSITY AND Pt PARTICLE LOCATION IN Pt/HY CATALYSTS

The combination of deep hydrogenation and selective ring opening is currently become more interest for the improvement of the quality of transport fuels such as cetane number. Both ring contraction and one-ring opening products, which are the major products from the ring opening of two naphthenic compounds, are not high enough cetane number to meet the future requirement. However, they play an important role as the intermediate resulting from faster opening C_5 rings than C_6 rings. Therefore, this work is focused on the catalytic behavior of zeolite Y loaded Pt catalysts and decalin is the probe molecule. This molecule is the final hydrogenation products of tetralin and naphthalene. The main purposes of this work are to investigate the effect of the location of metal (Pt) and the effect of acidity of catalysts to the RC/RO ratios. The results show that the Pt located on the inside of the zeolite structure will increase the ratio of RC/RO resulting from the enhancement of the RC desorption rate. In addition, the RC/RO ratio is directly related to the available Pt around the acid sites, but inversely related to the acidity due to more available acid sites for the consecutive reaction.

4.1 Introduction

As illustrated in Chapter 3, the products, mostly ring contraction (RC) and one-ring opening products from the ring opening reaction of decalin, do not result in an improvement in cetane number as shown in Fig. 4.1. However, both RC and RO compounds are significantly important as the intermediate compounds that can be further converted to high cetane number (pathway A in Fig. 4.2) or high octane number (pathway B in Fig. 4.2).

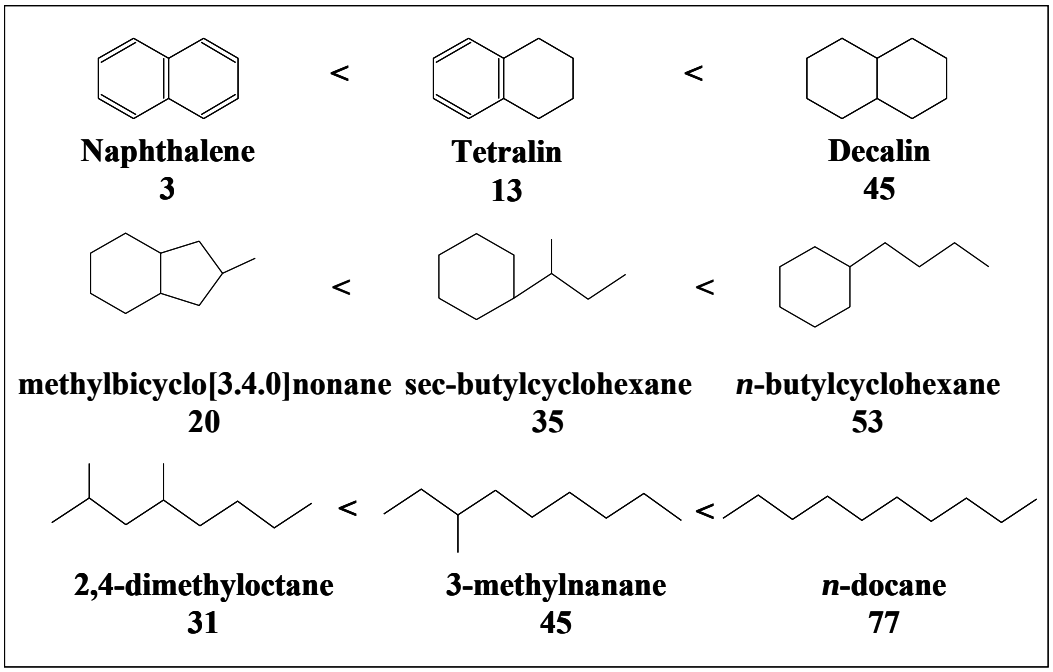

Figure 4.1 Cetane number of some C_{10} compounds.

A strategy for improving cetane number or octane number from aromatics is proposed as shown in Fig. 4.2. In this scheme, an increasing cetane number can be achieved by coupling hydrogenation of aromatics with the opening internal C-C bond of naphthenic rings at the substituted carbon position. Aromatics can undergo deep hydrogenation to saturate naphthenic rings. In order to break the internal C-C bond of bicyclonapthenes with two fused C_6 rings, which are common compounds found in the light cycle oils, a ring contraction step is needed [16]. Under the same condition, the ring opening of five membered-ring napthenes is much faster than that of six membered-rings [16,29]. This step can be successful on acidic catalysts or bifunctional catalysts [31]. From the decalin reaction on zeolites [26] or platinum-modified zeolites [59], ring contraction compounds (bicycloalkanes) are formed at a high selectivity, but ring opening compounds (alkylcycloalkanes) are also produced as secondary products. However, there are not enough products to reach the required cetane number due to the relatively low cetane number of napthenes.

To meet this requirement, the opening of the naphthanic ring with hydrogenolysis of noble metals must be added. Five metals, Pt, Pd, Ir, Ru and Rh, have been found to be able to catalyze in the C_5 cyclization of the alkane reactant to the corresponding paraffins [38,43]. Hydrogenolysis over these metals was considered to be highly sensitive to the nature of feed molecule and catalyst structure such as particle sizes. Two alternative paths for hydrogenolysis of alkylcyclopentanes, including MCP, on Pt metal are the selective path and the non-selective path according to the probability of breaking C-C bonds in the ring [68-72].

Opposite to Pt, rhodium and iridium showed higher selectivity to break the C-C bond of the C_5 ring in secondary-secondary C-C bonds [43].

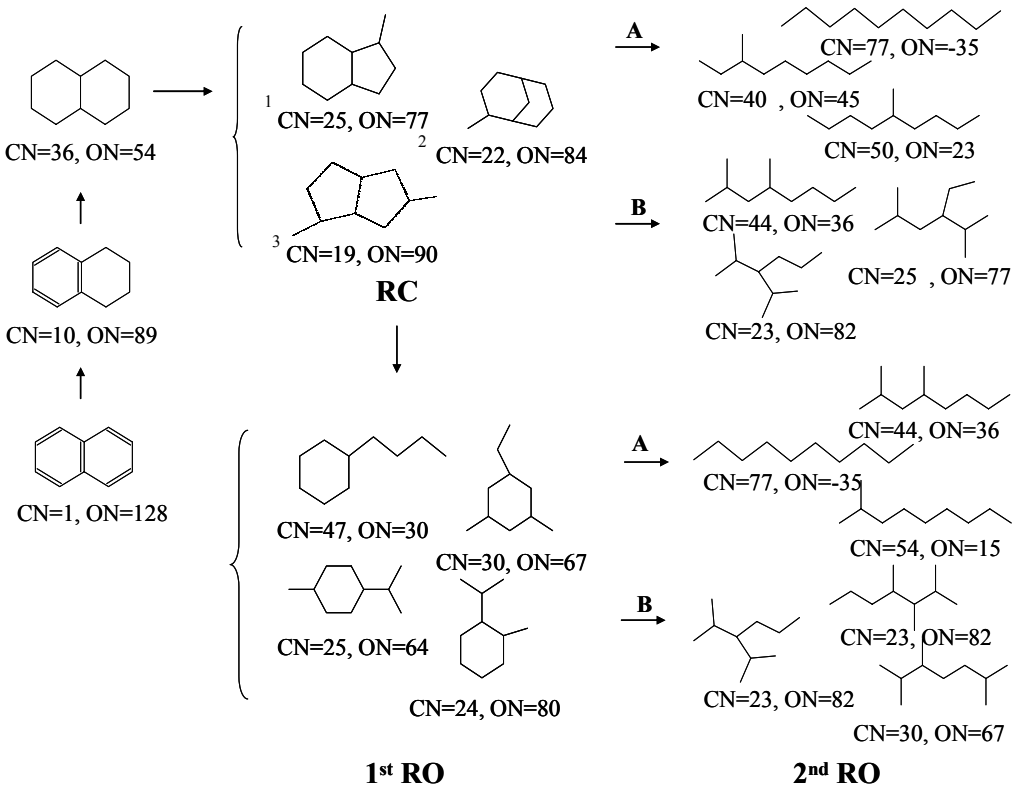

Figure 4.2 A strategy for improving cetane number or octane number from aromatics. [1]9-methylbicyclo[4.3.0]nonane, [2]2-methylbicyclo[3.3.1]nonane, and [3]2,7-bimethylbicyclo[3.3.0]octane[

Weisang and Gault [51] observed that hydrogenolysis of MCP only yields 2-methylpentane and 3-methylpentane. Moreover, van Senden et al. [50] reported that the particle size dependence of the catalytic properties of Ir and its sensitivity to self-poisoning are much less pronounced than with Pt. From particular catalytic properties of these metals, the ring opening products from alkylcycloalkanes might be able to control the degree of branching. Less branching alkanes will be responsible for diesel fuels in terms of a high cetane number. As opposed to less branching alkanes, high branching alkanes have a high octane number, which is suitable for gasoline.

From the proposed strategy, before the hydrogenolysis step can be applied, the ring contraction step is required in order to convert a six-membered ring into a five-membered ring. It is well known that the rate of opening the five membered-rings is much faster than six membered-rings due to high strain in molecules.

The present study investigates the effect of metal and its location, as well as the effect of acidity, on the ratio of ring contraction to ring opening products. Firstly, decalin ring opening with the different preparation methods for Pt supported HY zeolite, as well as a parent Y zeolite, were determined. With different procedures to incorporate Pt, we expect to have Pt metal located (i) at the exterior of the zeolite structure and (ii) at the interior of the zeolite structures. Secondly, the decalin ring opening over different acidity densities of catalysts was evaluated.

4.2 Experimental

A set of different Pt-containing HY catalysts and a proton form (HY) zeolite were tested for the ring opening of decalin. Three different Pt-containing catalysts are PtIE, which prepared by ion-exchange with tetraammineplatinum(II)nitrate solution, PtHY and PtAC, which prepared by incipient wetness impregnation with hexachoroplatinic acid solution and platinum(II)acetylacetonate in acetone, respectively. In addition, a set of faujasite zeolites with different acidic densities (CBV400, CBV720, CBV760, and CBV780) and Pt-containing catalysts (Pt/CBV400, Pt/CBV720, Pt/CBV760, and Pt/CBV780) were also used to study the decalin reaction in this work. The detail of the catalyst preparation methods are described in Section 2.1.2.

Fresh samples were characterizeed by EXAFS spectroscopy at the National Synchrotron Light Source (NSLS) at Brookhaven National Laboratory according to Section 2.2.3. The acidity densities of all samples were determined by TPD of adsorbed ammonia. Metal loadings of calcined catalysts (Pt supported catalysts) were determined using an atomic absorption spectrometer (AAS). In addition, the spent samples were characterized the coke content, which was determined as the carbon content by temperature programmed oxidation. The details of each characterization method were given in Section 2.2.

Catalytic reaction tests were conducted according to Section 2.3.1.1. The analysis of products was described in Section 2.4.1.

4.3 Results and Discussion

4.3.1 Characterization of Catalysts

The main physical properties of Pt supported on an HY zeolite are shown in Table 4.1. Metal dispersions of Pt catalysts were calculated from the curve fitting of the coordination number obtained from the EXAFS. This calculation was based on the properties of platinum crystals of different sizes [73]. This coordination number fits well with other well-dispersed Pt clusters on HY zeolites reported in the literature [62]. The metal dispersion of the PtAc catalyst gives only 83.30%, whereas both PtHY and PtIE catalysts show about 95% in dispersion.

Table 4.1 Characterization of the fresh Pt-containing HY zeolites

Catalyst	Pt content (wt%)	H/Pt	EXAFS			
				N	R (Å)	σ^2 (Å^2)
PtAC	0.48	0.83	Pt-Pt	8.0	2.76	0.0055
PtHY	0.95	0.95	Pt-Pt	6.2	2.76	0.0054
PtIE	0.70	0.95	Pt-Pt	6.2	2.77	0.0059

From the EXAFS analysis of three different Pt catalysts (PtAc, PtHY, and PtIE), the reduced Pt supported on a HY zeolite (PtIE) prepared by an ion-exchange at 673 K results in a coordination number for Pt-Pt of 6.2 indicating well dispersed metal on the surface. In addition to the previous study of Graaf et al. [63], the Pt supported on HY zeolites prepared by ion-exchange give smaller Pt particles than Pt catalysts prepared by the impregnation method. However, the Pt catalyst prepared by ion-exchange with a different heating rate exhibits differences in the coordination number and also the position of Pt on zeolite. In that study, an ion exchange of Pt catalyst with a heating rate of 0.2 K/min have the coordination number of 5.6, and it can be expected to have all Pt particles inside the HY zeolite structure. In addition, an ion exchange of a Pt catalyst with a heating rate of 1 K/min gives a higher coordination number, which is 7.8 and it is expected to be the bimodal distribution. Compared to this study, the coordination number of 6.2 was obtained for the PtIE catalyst, which is expected to have almost all Pt particles inside the zeolite structure. Furthermore, it is found that the coordination number of PtHY catalyst is 6.2 resulting in a large fraction of the Pt particles nearly inside the zeolite. On the other hand, the Pt-Pt coordination number of PtAc was obtained as 8.0. This means that large Pt particles are formed and expected to be at the exterior of the zeolite.

The acid properties of the studied catalysts as determined from the integration of the NH_3 TPD are listed in Table 4.2. A clear trend of the acidic density was observed in case of the zeolites (CBVxxx) with different Si/Al ratios. The density of acid sites increased as Si/Al ratios decreased.

4.3.2 Catalytic Activity Measurements

4.3.2.1 Conversion of Decalins over HY and Metal-HY Catalysts

Figure 4.3 shows the time course of the catalytic activity for decalin conversion in terms of the turnover frequency (TOF). It shows a significant difference in the catalytic activity of decalin conversion between the zeolite impregnated with Pt and a proton form zeolite. An HY catalyst exhibited a dramatic decrease of TOF of decalin with time on stream whereas with the Pt-containing HY catalysts TOF of decalin was substantially increased and almost remained constant over times studied.

Table 4.2 Characterization of acidity of fresh catalysts and coke contents of spent catalysts

Catalyst	Total acidity[a] Amount of desorbed NH_3 (μmol / g-cat.)	Coke[b] (% wt)
HY	1109	10.4
PtAC	983	7.4
PtHY	804	6.7
PtIE	841	0.1
CBV400	518	8.8
CBV720	168	5.1
CBV760	75	2.9
CBV780	22	0.1
Pt/CBV400	470	5.7
Pt/CBV720	124	3.2
Pt/CBV760	77	2.3
Pt/CBV780	19	0.1

[a] Total acidity measured by TPD of NH_3

[b] Coke formation after time on stream = 300 min

Reaction conditions: Total pressure = 2 MPa, temperature = 533 K, LSV = 1.89 h^{-1}, and H_2/HC molar ratio = 65

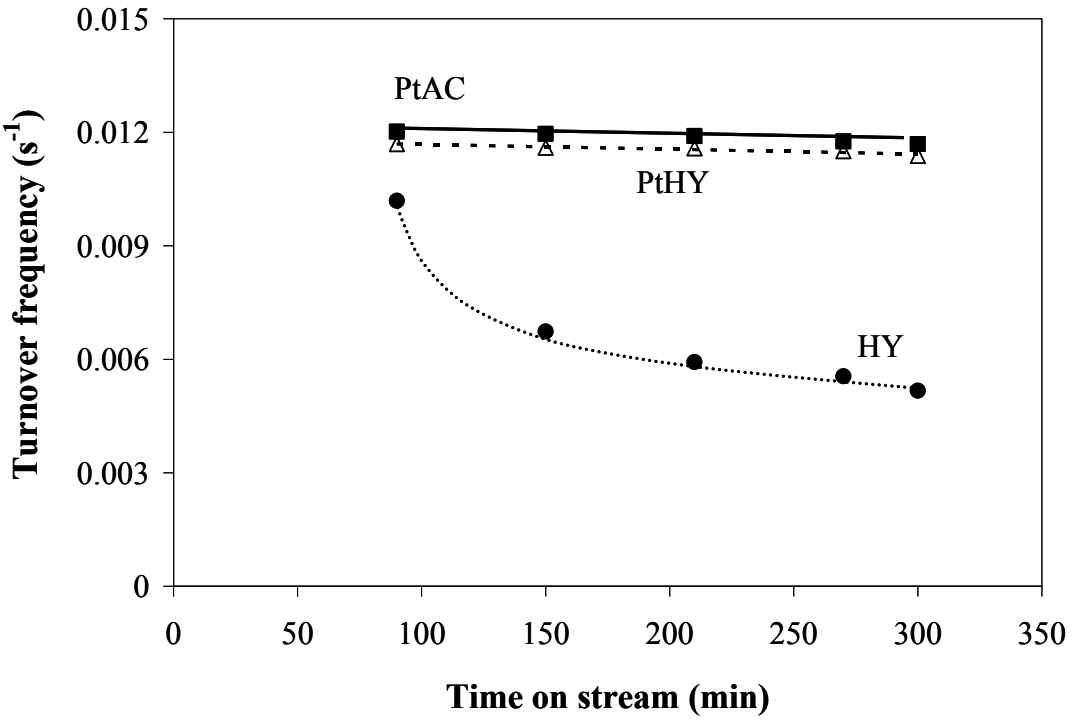

Figure 4.3 Effect of metal supported catalysts on the turnover frequency for decalin ring opening. Reaction conditions: Total pressure = 2 MPa; Temperature = 533 K, H_2/HC molar ratio = 65. The calculated TOF is based on the data obtained from TPD of ammonia.

As observed, an HY catalyst shows the fast deactivation while the impregnated Pt catalysts greatly enhanced the stability of the catalyst. This slow deactivation of metal-containing catalysts may be attributed to a higher hydrogen transfer, which enhances the hydrogenation rate of the adsorbed intermediates. The higher rate of deactivation of a bare HY zeolite can be confirmed by a huge decrease in decalin conversion (from 40% to 20% after 300 min) and a larger amount of coke deposit (see in Table 4.2).

Table 4.3A shows the product distribution over catalysts at 2 MPa and 533 K with a mixture of decalin feed (*trans*/*cis* feed ratio: 63/37) after 90 min and 300 min on stream. We classified these products into several groups so that the catalytic functionality could be treated according to the yields of the grouped products. The products were divided into 4 groups: (i) cracking product (CP: isobutene, etc.) (ii) ring contraction product (RC: methylbicyclo[4.3.0]nonane, etc) (iii) Ring opening product (RO: butylcyclohexane, etc) and (iv) heavy product (HP: tetralin, etc.).

Table 4.3A Conversion of decalin on HY zeolite and Pt/HY catalysts at two times on stream. Reaction conditions: Total pressure = 2 MPa; Temperature = 533 K; LSV = 1.89 h^{-1}; H_2/HC molar ratio = 65

	Feed	**HY**		**PtHY**		**PtAC**	
Time on stream (min)		**90**	**300**	**90**	**300**	**90**	**300**
Trans -decalin (wt%)	63.0	55.5	68.4	55.0	56.3	46.9	48.4
Cis -decalin (wt%)	37.0	4.5	11.3	4.1	3.9	3.6	3.4
Conversion[a] (%)	-	40.0	20.3	40.9	39.8	49.6	48.2
Products				Yield (wt%)			
Cracking products	-	9.6	1.6	8.4	8.6	13.3	12.7
Ring contraction products	-	13.8	10.6	16.5	16.0	15.1	14.9
Ring opening products	-	16.4	7.9	15.9	15.2	21.1	20.6

[a] Conversion based on trans-decalin and cis-decalin.

Table 4.3B shows selectivities of some relevant products in RC and RO groups. As observed, all catalysts displayed high conversions (> 45%). However, the activity measured after 300 min. on stream decreased in the case of HY alone. This indicates a catalyst deactivation taking place over this sample as discussed above.

Table 4.3B Some RC and RO products from the reaction of decalin on HY zeolite and Pt catalysts after 90 min. Reaction conditions: Total pressure = 2 MPa; Temperature = 533 K; LSV = 1.89 h^{-1}; H_2/HC molar ratio = 65

Catalyst	*CN*	*ON*	HY	PtHY	PtAC
			Yield (wt%)		
RC products	-	-	13.8	16.5	15.1
			Selectivity to (%)		
2,7-dimethylbicyclo[3.2.1]octane	*32*	*74*	15	14	14
2,7-dimethylbicyclo[3.3.0]octane	*19*	*90*	19	16	17
2-methylbicyclo[3.3.1]nonane	*22*	*84*	12	11	11
9-methylbicyclo[4.3.0]nonane	*25*	*77*	10	9	9
			Yield (wt%)		
RO products	-	-	16.4	15.9	21.1
			Selectivity to (%)		
n-butylcyclohexane	*47*	*30*	12	12	10
4-methyl-1(1-methylethyl)cyclohexane	*25*	*77*	13	17	13
1,3-dimethyl-5-ethylcyclohexane	*30*	*67*	4	6	4

Fig. 4.4 shows the ratio of RC to RO obtained on the different catalysts as a function of W/F ratio and time on stream. It is clear that from the point of view of fuel upgrading, the aim would be to produce a high amount of RC and less amount of RO on bifunctional catalysts, because it is hard to control the position of the breaking C-C bond of C_5 ring. As the previous study shows [74], a typical bimodal distribution of Pt supported on HY3 enhanced in the RC/RO ratio results from the enhancement of the RC step and the suppression of the RO step by a faster hydrogen transfer. Thus, in this study the effect of locations of Pt metal on zeolite are evaluated on the decalin ring opening.

As it is seen in Fig. 4.4, at the same conversion a RC/RO ratio increased in the following order: PtHY (metal being inside the zeolite) > HY (a proton-form zeolite) ≈ PtAc (metal being outside the zeolite). Indeed, this ratio does not significantly differ over HY and PtAc. However, its value over PtHY is a lot higher than that over HY or PtAc catalysts. This enhancement can be expected to be found only over a Pt metal being inside the zeolite if isomerization occurs via a bifunctional mechanism. An interaction between Brönsted acid sites and Pt located inside the zeolite [75,76] plays an important role. Accordingly, decalin was dehydrogenated to form an olefin on Pt metal. Then, it was protonated by the Brönsted acid site which produces a carbenium ion. This intermediate can be formed the RC products via the isomerization and further react to give the RO products via a β-scission or a cracking reaction. However, the proper combination of the metallic and acidic functions mainly takes into account the efficiency of bifunctional catalysts in hydrocarbon transformations [77,78].

In case of platinum particles located inside the zeolite pores, the high efficiency for hydrogen transfer results in fast desorption of RC intermediates. On the other hand, if platinum particles are located only on the outside of zeolite structure, it would not show the interaction between metal and acid sites because of the long distance between them.

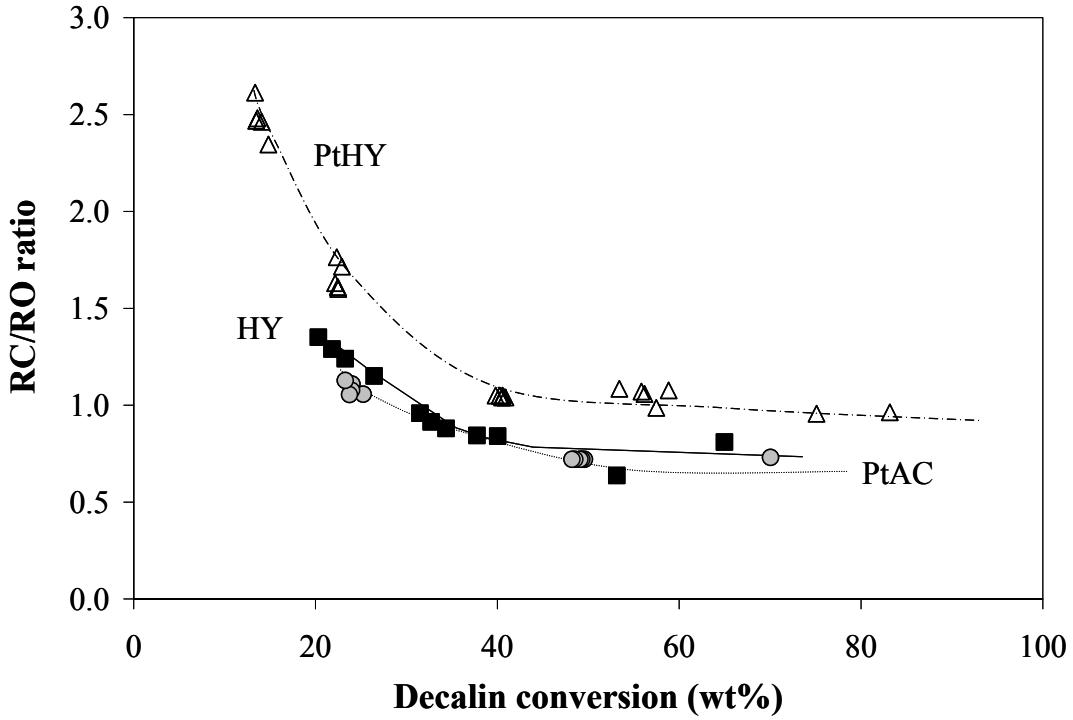

Figure 4.4 RC/RO ratio of decalin ring opening on the HY zeolite and metal (Pt) supported on HY zeolites at different conversions. Conversions were varied by changing space time and time on stream. Reaction conditions: Total pressure = 2 MPa; Temperature = 533 K; H_2/HC molar ratio = 65.

In addition, Arribas et al. [33] studied the effect of metal sites on the hydrogenation and ring opening of tetralin over bifunctional Pt(Ir)/USY catalysts. Their results show that the concentration of Pt loading on USY zeolite can affect the yield of isomer (RC) products. As compared two different Pt catalysts having the Pt metals inside the zeolite pores, the Pt catalyst (PtHY) with higher the Pt/H^+ ratio provide larger amount of the ratio of RC/RO that the Pt catalyst (PtIE) with lower the Pt/H^+ ratio when the comparison is done at the same conversion level (~ 60%) as shown in Table 4.4.

Table 4.4 The RC/RO ratio of two different Pt catalysts (PtHY and PtIE) with almost the same conversion level. Reaction conditions: Total pressure = 2 MPa; Temperature = 533 K; H_2/HC molar ratio = 65

Catalysts	Conversion	Pt/H+	RC/RO
PtHY	60.00	0.06	1.08
PtIE	63.25	0.04	0.89

4.3.2.2 Conversion of Decalin over a Series of Proton-Form Zeolites.

The product distribution of the decalin ring opening reaction over a series of proto-form zeolites at 2 MPa and 535 K are summarized in Table 4.5A and 4.5B for two times on stream: 90 and 300 min.

Table 4.5A Conversion of decalin on various HY zeolites with different acid densities at two times on stream. Reaction conditions: Total pressure = 2 MPa; Temperature = 533 K; LSV = 1.89 h^{-1}; H_2/HC molar ratio = 65

	Feed	**CBV400**		**CBV720**		**CBV760**		**CBV780**	
Time on stream (min)		**90**	**300**	**90**	**300**	**90**	**300**	**90**	**300**
Trans -decalin (wt%)	63.0	56.7	70.6	69.5	71.4	68.2	68.8	70.4	67.3
Cis -decalin (wt%)	37.0	5.4	10.1	7.2	14.8	9.0	14.9	20.5	26.4
Conversion[a] (%)	-	38.0	19.3	23.3	13.8	22.9	16.4	9.1	6.3
Products					Yield (wt%)				
Cracking products	-	7.2	1.4	2.3	0.6	2.2	0.9	0.4	0.3
Ring contraction products	-	13.4	10.0	11.8	9.0	11.1	10.0	5.9	4.5
Ring opening products	-	17.1	7.7	9.0	4.1	9.6	5.3	2.8	1.5
Dehydrogenation products	-	0.3	0.2	0.1	0.1	0.0	0.2	0.0	0.0

[a] Conversion based on trans-decalin and cis-decalin.

Table 4.5B Some RC and RO products from the reaction of decalin on various Y zeolites after 90 min. Reaction conditions: Total pressure = 2 MPa; Temperature = 533 K; LSV = 1.89 h^{-1}; H_2/HC molar ratio = 65

Catalyst	*CN*	*ON*	CBV400	CBV720	CBV760	CBV780
			Yield (wt%)			
RC products	-	-	13.4	11.8	11.1	5.9
			Selectivity to (%)			
2,7-dimethylbicyclo[3.2.1]octane	*32*	*74*	16	15	15	8
2,7-dimethylbicyclo[3.3.0]octane	*19*	*90*	21	21	13	11
2-methylbicyclo[3.3.1]nonane	*22*	*84*	14	16	16	24
9-methylbicyclo[4.3.0]nonane	*25*	*77*	11	12	11	23
			Yield (wt%)			
RO products	-	-	17.1	9.0	9.6	2.8
			Selectivity to (%)			
n-butylcyclohexane	*47*	*30*	11	17	16	21
4-methyl-1(1-methylethyl)cyclohexane	*25*	*77*	13	17	15	13
1,3-dimethyl-5-ethylcyclohexane	*30*	*67*	5	5	4	5

The change of decalin conversion over the bare zeolites with time on stream (TOS) at 535 K is shown in Fig. 4.5. The initial conversion of decalin follows the same trend as the acidity of catalysts. A catalyst having a large amount of the acidity presents a higher reactivity during the ring opening of decalin than a catalyst having a small amount of the acidity. This follows the sequence: CBV400 > CBV720 > CBV760 > CBV780. However, after 150 min on stream the decalin conversion of CBV720, which possessed a higher Brönsted acid site, is lower than that of CBV760. This is due to the faster rate of deactivation on CBV720 compared at the same time on stream. From the TPO results shown in Table 4.2, the

coke deposit on a CBV720 catalyst was about 1.7 times higher than on a CBV760 catalyst.

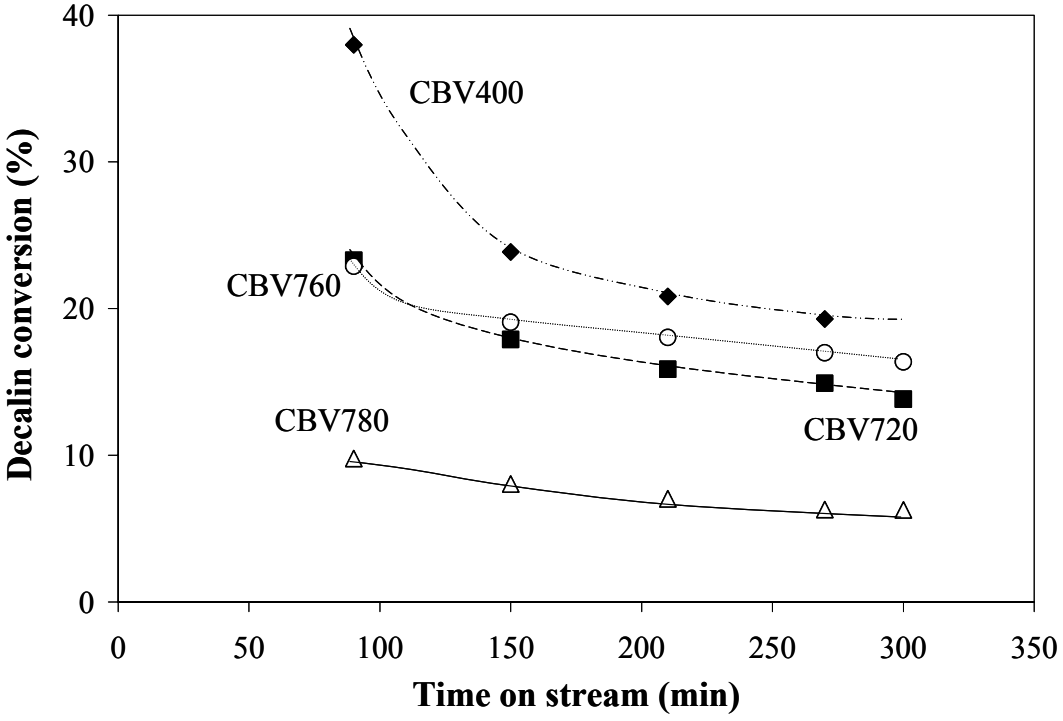

Figure 4.5. Total conversion of decalin on various catalysts. Reaction conditions: Total pressure = 2 MPa; Temperature = 533 K; LSV = 1.89 h^{-1}; H_2/HC molar ratio = 65.

As shown in Fig. 4.5 the decalin conversion rate is low for catalysts having the highest acidity to lowest acidity. Moreover, the higher acidity catalysts have a fast deactivation and the rate of deactivation decreases with the time on stream. As noted, on the highest acidity catalyst (CBV400) the decalin conversion was reduced from ~38.0 wt% at 90 min on stream to ~19.3 wt% at 300 min on stream. Compared to the lowest acidity catalyst (CBV780) the decalin conversion was decreased from ~9.8 wt% to ~6.3 wt% after 300 min on stream. According to the formation of coke on the spent catalysts, it is not surprising that the increase in acidity results in more coke formation deposited on catalysts.

An interesting effect to point out here is the influence of the Brönsted acid sites on the RC/RO ratio. Fig. 4.6 illustrates the effect of the Brönsted acid sites on the RC/RO ratio at three different acidities compared at nearly the same decalin conversion (15.2 wt% - 16.5 wt%).

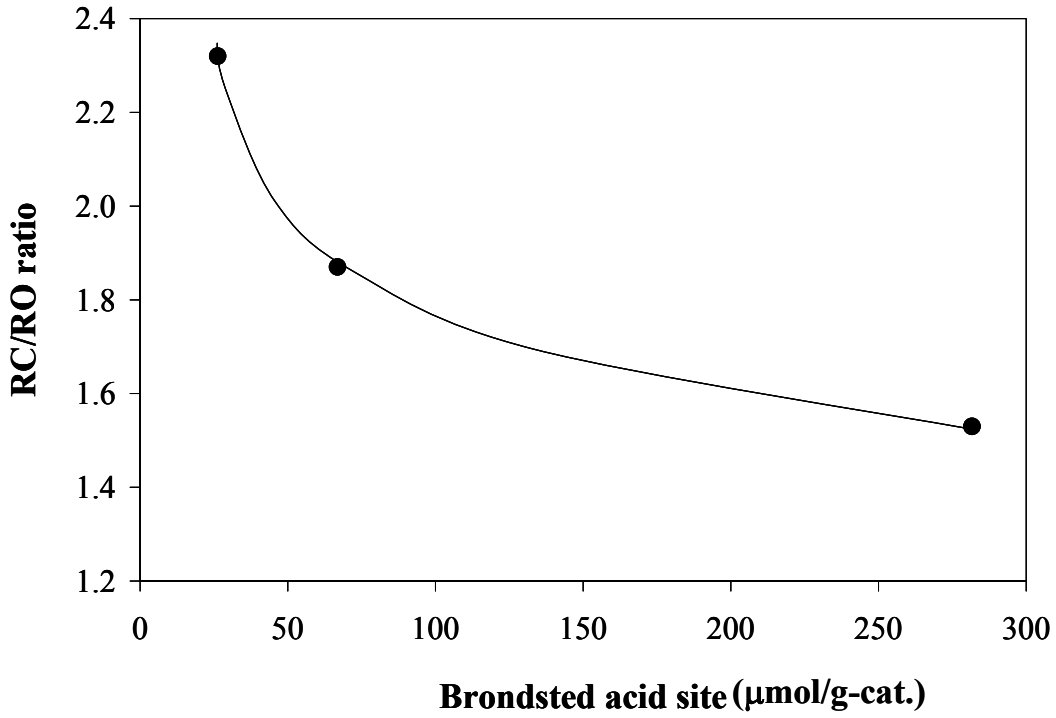

Figure 4.6 Effect of Brønsted acid site over proton-form zeolites on RC/RO ratio at the same conversion. Reaction conditions: Total pressure = 2 MPa; Temperature = 533 K; LSV = 1.89 h^{-1}; H_2/HC molar ratio = 65 and the space velocity adjusted to keep conversion = 15%-16%.

It appears that the RC/RO ratio increases when the acidity density of catalysts decreases. Regarding the recent works [4,26,65] the ring opening mechanism of naphthenic ring compounds on acidic sites of catalysts is proposed. After the intermediate carbenium ion occurs, it can produce either RC or RO products, which depends on the environment of the surface. In the case of RC products, the carbenium ion can pass through isomerization via the protonated cyclopropane ring involing a hydride transfer, then desorbs from the surface. Unlike the formation of RC products, the RO products are formed since the carbenium ion undergoes a β-scission followed by the saturation of the charge. The decrease in the RC/RO ratio over the high Brönsted acid sites could be explained by having more sites available for the consecutive reaction.

4.3.2.3 Influence of Metal on the Stereoisomer of Decalin

In order to elucidate the effect of metal on the ring opening of decalin, the Pt metal was introduced on the entire set of the proton-form zeolites. Tables 4.6A and 4.6B present the product distribution of the decalin ring opening reaction over Pt supported zeolites (Pt/CBVxxx) at 2 MPa and 535 K. It turns out to be more obvious that the metal not only slows down the deactivation rate (the coke content as in Table 4.2), but also accelerates isomerization as explained. At this point it is worthwhile to compare the *trans/cis* decalin ratio because of different reactivity between these two isomers. *Cis*-decalin shows a higher reactivity for this reaction than *trans*-decalin [66].

Table 4.6A Conversion of decalin on various HY zeolites with different acid densities at two times on stream. Reaction conditions: Total pressure = 2 MPa; Temperature = 533 K; LSV = 1.89 h^{-1}; H_2/HC molar ratio = 65

	Feed	**Pt/CBV400**		**Pt/CBV720**		**Pt/CBV760**		**Pt/CBV780**	
Time on stream (min)		**90**	**300**	**90**	**300**	**90**	**300**	**90**	**300**
Trans -decalin (wt%)	63.0	72.8	74.9	76.0	76.8	84.4	85.3	86.7	87.1
Cis -decalin (wt%)	37.0	5.2	7.0	4.5	6.0	5.8	7.1	6.8	6.9
Conversion[a] (%)	-	22.0	18.2	19.5	17.2	9.8	7.6	6.5	6.0
Products		Yield (wt%)							
Cracking products	-	3.5	2.0	2.8	1.8	0.7	0.3	0.3	0.3
Ring contraction products	-	9.9	10.0	9.2	9.6	6.2	5.2	4.3	4.1
Ring opening products	-	8.6	6.1	7.4	5.7	2.9	2.1	1.9	1.6
Dehydrogenation products	-	0.0	0.1	0.0	0.1	0.0	0.0	0.0	0.0

The ratio of *trans*-decalin to *cis*-decalin was studied as a function of conversion over the metal-containing zeolites and the parent zeolites as shown in Fig. 4.7. The observed *trans/cis* decalin ratios over the additional Pt catalysts (Pt/CBVxxx) are higher than those over the parent catalysts. Although the *trans/cis* decalin ratio is thermodynamically favored, and it is about 12 under this reaction condition, the experimental values of *trans/cis* decalin ratio are around the thermodynamic value of the Pt supporting catalysts. Compared to the proton-form catalysts, the observed *trans/cis* decalin ratios are between ~2 to ~8 only.

Table 4.6B Some RC and RO products from the reaction of decalin on different Pt supported Y zeolites after 90 min. Reaction conditions: Total pressure = 2 MPa; Temperature = 533 K; LSV = 1.89 h^{-1}; H_2/HC molar ratio = 65

Catalyst	*CN*	*ON*	Pt/CBV400	Pt/CBV720	Pt/CBV760	Pt/CBV780
				Yield (wt%)		
RC products			9.9	9.2	6.2	4.3
				Selectivity to (%)		
2,7-dimethylbicyclo[3.2.1]octane	*32*	*74*	16	16	16	16
2,7-dimethylbicyclo[3.3.0]octane	*19*	*90*	19	18	17	18
2-methylbicyclo[3.3.1]nonane	*22*	*84*	12	14	13	14
9-methylbicyclo[4.3.0]nonane	*25*	*77*	9	10	10	10
				Yield (wt%)		
RO products			8.6	7.4	2.9	1.9
				Selectivity to (%)		
n-butylcyclohexane	*47*	*30*	13	14	18	17
4-methyl-1(1-methylethyl)cyclohexane	*25*	*77*	20	22	34	33
1,3-dimethyl-5-ethylcyclohexane	*30*	*67*	7	7	9	9

Correspondingly, Kubička et al. [59] found that the isomerization rate increases over the impregnated Pt catalysts. It could be explained that the addition of Pt on the zeolite enhances the *cis* to *trans* isomerization. This result agrees with the previous studies [26,64,65]. Mostad et al. [65] studied the stereoisomerization of pure decalin isomers (*trans*- and *cis*-decalin) on HY zeolite and found that *cis*-decalin shows a higher stereoisomerization than *trans*-decalin. Furthermore, Lai et al. [64] have seen that the *cis* to *trans* isomerization is more significant in the presence of Pt metal supported zeolites than on the bare zeolites. The isomerization of *cis*-decalin to *trans*-decalin should be followed by three different pathways. Lai et al. [64] proposed the stereoisomerization of decalin by

dehydrogenation/hydrogenation mechanism. *Cis*-decalin is first dehydrogenated to 1, 9-octalin or 9, 10-octalin and followed by hydrogenation to yield *trans*-decalin.

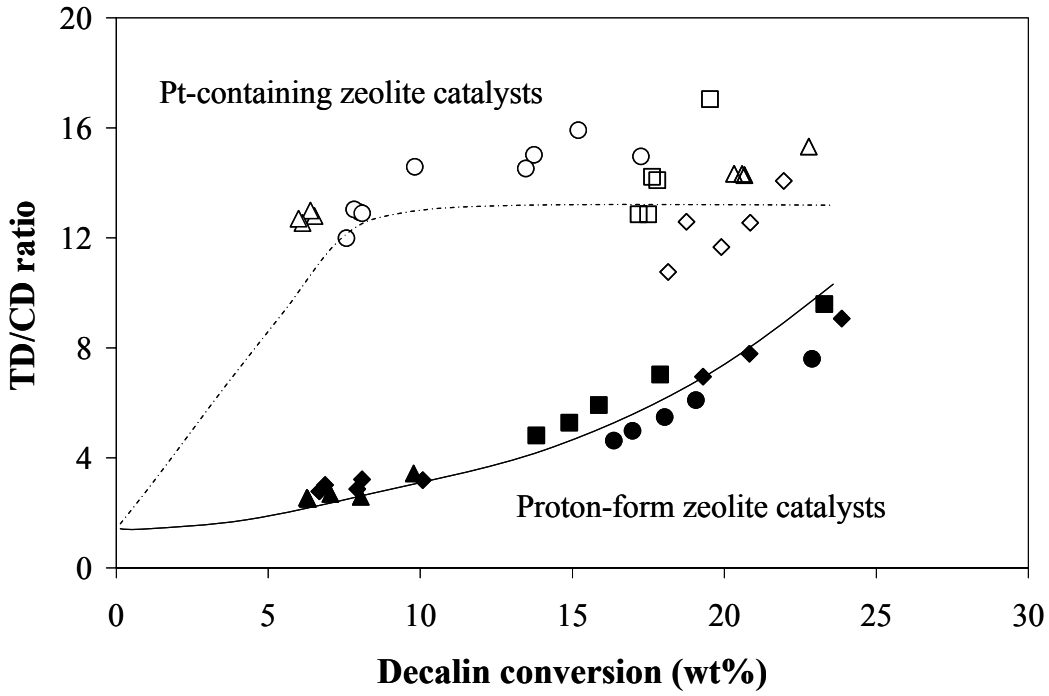

Figure 4.7 Comparison between the Pt supported on zeolites and the bare zeolites on the *trans/cis*-decalin ratio on various conversions. Reaction conditions: Total pressure = 2 MPa; Temperature = 533 K; LSV = 1.89 h^{-1}; H_2/HC molar ratio = 65.

Kubička et al. [26] said that the decalin stereoisomerization on the proton-form zeolite should occur by a protonation of tertiary carbon to form a pentacarbocation following the donation of a proton and finally to form the other isomer. The last mechanism involves carbenium ion, which proceeded either by protolytic dehydrogenation [79-82] or by hydride abstraction [81,83].

4.3 Conclusion

The main conclusions of this work are summarized below:

- The location of Pt metal on the zeolite influences the RC/RO ratio. The Pt located on the inside of the zeolite structure will enhance the RC desorption rate. The RC/RO ratio is also related to the available Pt around the acid sites.
- For the proton-form catalysts, the RC/RO ratio is inversely proportional to the number of Brönsted acid sites. The high acidity of catalysts will have more sites available for a consecutive reaction.
- The decalin stereoisomerization is greatly enhanced over the metal supported zeolites when compared to the parent zeolites.

Acknowledgments

We would like to acknowledge Oklahoma Center for Advancement of Science and Technology (OCAST) and ConocoPhillips for financial support of the ConocoPhillips Catalysis Lab at the University of Oklahoma.

CHAPTER V

RING CONTRACTION AND SELECTIVE RING OPENING OF NAPHTHENIC MOLECULES FOR OCTANE NUMBER IMPROVEMENT[1]

Different catalytic strategies have been evaluated to maximize the production of non-aromatic compounds with high octane number, starting from naphthenic molecules, typically obtained from the saturation of aromatics. The research octane number (RON), the motor octane number (MON), and the specific volume of the product mixtures were evaluated in each case. The product distribution of acidic and Pt-containing zeolite was investigated in the temperature range 533-563 K in the presence of hydrogen at a total pressure of 2 MPa. It was found that skeletal isomerization (ring-contraction) was the primary reaction in both HY and Pt/HY catalysts. The presence of Pt was found to enhance the stability of the catalyst, but also greatly altered the distribution of RC products, enhancing 1,1-dimethylcyclopentane. This enhancement can be explained in terms of a higher rate of hydride transfer. Evaluation of the octane numbers of the product indicated that mixture of RC products results in rather high RON, but had little effect or even negative effect on MON and specific volume. To improve MON and specific volume an Ir/SiO_2 catalyst with high hydrogenolysis activity was added to realize the

---

[1] Submitted to Journal of Catalysis.

ring opening (RO). The combination of RC and RO was tested on physical mixtures and segregated beds of Pt/HY and Ir/SiO_2 catalysts in order to optimize the production of the iso-alkanes with highest octane number. It was found that with segregated catalyst beds, a better control of the selective breaking of C-C bonds of RC isomers can be achieved, which optimizes octane number and volume.

5.1. Introduction

Hydrogenation of aromatics into alkyl-cyclohexanes (naphthenes) would result in significant losses of octane number [86-88] and hydrocracking would lead to losses in molecular weight with consequent losses, in gasoline yield [89,90]. An interesting aspect to investigate is the conversion of naphthenes into non-aromatic compounds with the same number of carbon atoms as the original molecule, but with higher octane number. Octane number provides an indication of the ability of a gasoline to resist knocking as it burns in the engine. There are two test methods to measure the octane number of a gasoline. These methods use different engine conditions, mainly the intake temperature and the engine speed. The Research Octane Number (RON) method represents engine operations typical of mild driving, without consistent heavy loads on the engine, while the Motor Octane Number (MON) method represents severe, sustained high speed, high load driving. The pump octane number is the average between the two methods (RON+MON)/2. For most gasoline fuels, RON is higher than MON. The difference between the two (RON –

MON) is called Sensitivity. Modern fuels are expected to have low sensitivities. Therefore, refiners are concerned about keeping both high RON and high MON.

The conversion of naphthenic molecules has been extensively investigated on metal, acidic, and bifunctional (metal/acid) catalysts for many years. Several reactions are known to occur, such as isomerization (including ring contraction), ring opening, dehydrogenation, and cracking, depending mainly on the reaction conditions, the feed, and the catalysts used [74]. Methylcyclohexane (MCH) is an interesting probe molecule that can undergo all of the reactions mentioned above and can be used as a model feed. Therefore, it is interesting to compare the octane number of each of different products that can result in each reaction that MCH can undergo and determine which catalyst or combination of catalysts and reaction conditions can be used to maximize octane numbers (both RON and MON).

As illustrated in Fig. 5.1, a direct ring opening (RO) of the C_6-ring is not desirable because all of the resulting RO products have low octane number. By contrast, some ring contraction (RC) products (dimethylcyclopentanes DMCPs) and some secondary ring opening products of the DMCPs (see Fig. 5.2) have relatively high octane number and would be a desirable product in gasoline.

In general, the RC products have higher RON, while the RO products trend to have higher MON. In this contribution, we analyze different catalysts and catalyst bed configurations to maximize those products of high octane number. We have quantified the effectiveness of different reaction strategies to maximize RON, MON, and gasoline volume.

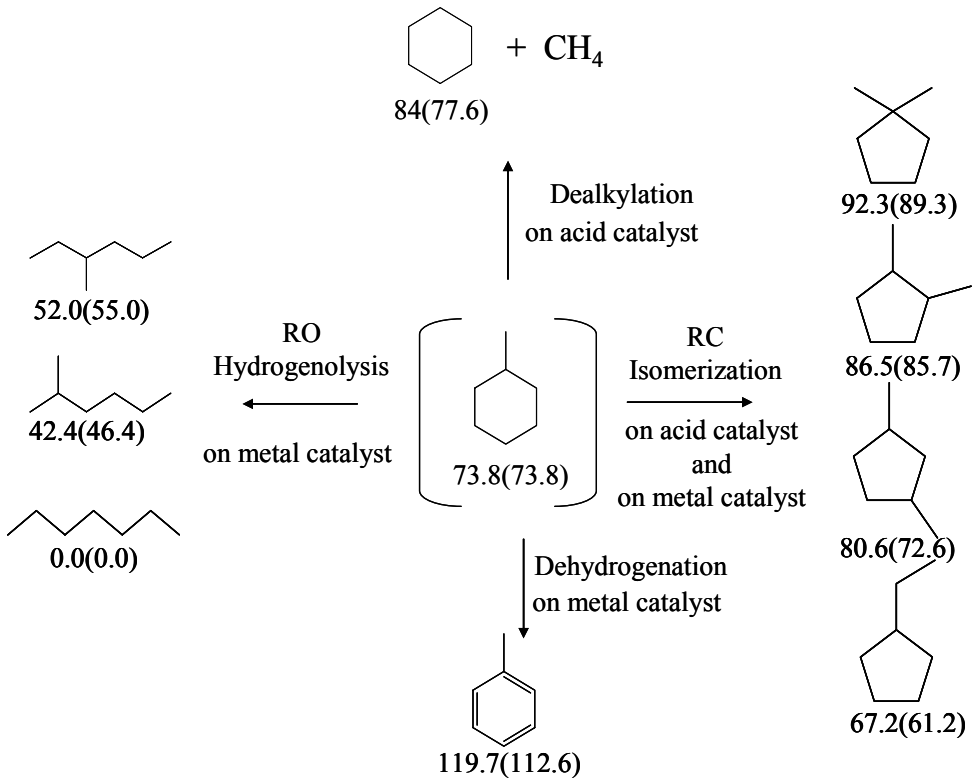

Figure 5.1 Possible products from methylcyclohexane and their research octane number (RON) and their motor octane number (MON).

Previous researchers have studied the reaction paths and the role of catalyst structure on product distribution for MCH reaction. For example, Mignard et. al. [91] have studied the conversion of MCH on Pt/USY catalysts. They found that MCH is first isomerized via ring-contraction (RC) into ethylcyclohexane (ECP) and dimethylcyclopentanes (DMCPs) and then transformed into C_7 iso-alkanes and cracking ($<C_7$) products, respectively, as the reaction temperature increases. In that study the individual RC products were lamped, but as shown in Fig. 5.1, different RC products have very different ON. The intermediate RC step has been made evident in several other studies on acidic catalysts, both zeolitic and non-zeolitic [92]. In some cases, the RC reaction has been proposed to occur by a bifunctional path, involving dehydrogenation on metals. For example, Belatel et al. [93] investigated the MCH reaction on Pt-Ir/sulfated zirconia catalysts and showed that no isomerization was found to take place in the absence of metals.

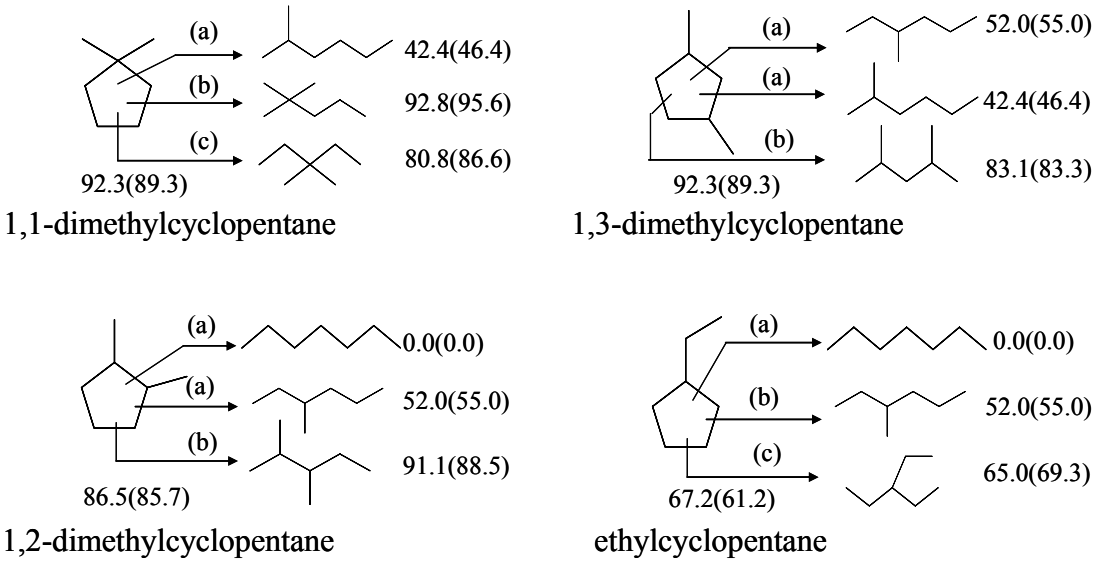

Figure 5.2 Hydrogenolysis products on metal catalysts from ring opening reactions of C_7 ring contraction compounds and their corresponding research octane number (RON) and motor octane number (MON).

On zeolitic catalysts, the structure of the zeolite can be used to greatly modify the product distribution. The role of shape selectivity in determining the product distribution of isomerization of naphthenic rings was pointed out by Weitkamp et. al. [94] in their work on Pt/HZSM-5 catalysts. They found that on these small-pore catalysts, no 1,1- or 1,2-dimehtylcyclopentane were formed while cis/trans-1,3-dimethylcyclopentane appeared even at very low conversions. These results are very relevant to understand some of the findings of the present investigation and will be further discussed.

The role of metals is not only the dehydrogenation/hydrogenation steps. It may also participate in ring opening of naphthenic molecules. The principal path for ring opening on catalysts with only the metal function is hydrogenolysis. In this reaction, the cleavage of a C-C bond of alkylcycloalkanes depends on the nature of the catalyst, the type of ring, and the presence of alkyl substituents. Gault [43] identified three different paths for ring opening via hydrogenolysis. The most common pathway involves a dicarbene intermediate with cleavage at the unsubstituted secondary-secondary C-C bond.

In the other two reaction paths the cleavage occurs at substituted C-C bonds through π-adsorbed olefin and metallocyclobutane intermediates, respectively. The product distribution from the hydrogenolytic ring opening over metals (i.e. Pt, Ir, Rh and Ru) is strongly dependent on the nature of reactants and catalyst structure, which in turn can be modified by parameters such as particle size or metal-support interactions. For example, the products obtained from ring opening of methylcyclopentane on high loading, low dispersion Pt/Al_2O_3 catalysts were mostly 2-methylpentane (2-MP) and 3-methylpentane (3-MP) with no n-hexane (n-Hx). The first two products result from a dicarbene intermediate, the third one requires cleavage of a substituted C-C bond. By contrast, significant amounts of n-Hx were found in the products when the catalyst was a highly dispersed, low loading Pt/Al_2O_3. In contrast to Pt, the behavior of Ir was found to be much less sensitive to catalyst particle size [16,50,51]. Mc Vicker et al. [16] have investigated that the ring opening of alkylcyclohexanes on iridium (Ir) metal is mainly via a dicarbene

mechanism. Also, Weisang and Gault [51] observed that hydrogenolysis of MCP on Ir only yields 2-methylpentane and 3-methylpentane. More recently, our group has found that the dicarbene path is dominant when Ir is supported on silica. However, when the support is alumina, the contribution of products arising from the cleavage of substituted C-C bonds becomes important [95].

In the present contribution, experiments were conducted on acidic and bifunctional catalysts (HY and Pt/HY zeolites, respectively) as well as on the metal catalysts of high hydrogenolysis activity (Ir/SiO_2). We have chosen Ir/SiO_2 because, as shown before [51], this catalyst preferentially opens C-C bonds via dicarbene intermediates involving secondary-secondary carbons. As shown in Fig. 5.2, this type of cleavage results in higher ON. Also, to study the combination of RC and RO reactions, several experiments were conducted on consecutive catalyst beds of Pt/HY and Ir/SiO_2 at different reaction temperatures.

5.2 Experimental

The HY and the Pt/HY catalysts were were used to investigate the methylcyclohexane reaction (MCH, Aldrich, >99%) at temperature of 533-563 K, total pressure of 2 MPa under H_2 flow. In addition, the Ir/SiO_2 catalyst was studied the hydrogenolytic activity at the same reaction conditions. All reactions were carried out in the system as shown in Section 2.3.1.1. In addition to the runs on individual catalysts, a set of experiments was conducted with physical mixtures of Pt/HY and Ir/SiO_2 catalysts. In two of these experiments, the two catalysts were segregated in separate beds with the Pt/HY catalyst placed in the front end and the Ir/SiO_2 catalyst in the back. In the system identified as Pt/HY > Ir/SiO_2, both catalysts were kept at the same temperature. By contrast, in the system identified as Pt/HY >> Ir/SiO_2, the Pt/HY catalyst was kept at 20 K higher temperature than the Ir/SiO_2 catalyst. In the third experiment, the Pt/HY and Ir/SiO_2 catalysts were well mixed in a weight ratio of 2:1, respectively. The schematic diagram of these three different catalytic bed configurations is shown in Section 2.3.3. In all runs, the products were analyzed online in a HP5890 gas chromatograph with FID detector.

The methods for catalytic preparation and characterization of catalysts are described in Section 2.1. and 2.2.

5. 3 Results and Discussion

5.3.1 Characterization of Catalysts

The acidic properties of the HY zeolite, Pt/HY and Ir/SiO_2 catalysts are summarized in Table 5.1. It is clear that the bare HY zeolite contains a larger amount of Brönsted and Lewis acid sites than that impregnated with Pt. As previously observed, [59] the impregnation with Pt results in a loss of acid sites (150-300 μmol/g) that significantly exceeds the number of moles of metal incorporated (50 μmol/g). However, it does not modify the fraction of strong and weak sites as illustrated by a rather uniform decrease in the amount of pyridine adsorbed at different temperatures.

Table 5.1 Acidity of HY and Pt/HY catalysts.

Sample	Total acidity[a]	Acidity[b] (μmole Py/g-cat.)					
	Amount of desorbed NH_3	Brønsted (1545 cm^{-1})			Lewis (1445 cm^{-1})		
	(μmole/g-cat.)	523 K	623 K	673 K	523 K	623 K	673 K
HY	1109	352	328	324	666	523	76
Pt/HY	795	311	295	273	551	512	140

[a] Total acidity measured by TPD of NH_3

[b] Acidity measured by pyridine adsorbed and desorbed at different temperatures

The H_2 uptakes of H/Pt = 2.0 and H/Ir = 2.3 for the Pt/HY and Ir/SiO_2 catalysts, respectively, indicate a high metal dispersion in both cases (Table 5.2). H/M ratios higher than one have been previously reported [96]. In the case of Ir catalysts, an H/Ir stoichiometry greater than 2.6 has been measured for small Ir particles corresponding to metal dispersions higher than 0.9 while a stoichiometry of about 2 was measured for particles corresponding to a dispersion of about 0.5 [97,98].

Table 5.2 Hydrogen chemisorption of Pt/HY and Ir/SiO_2 catalysts

Sample	**Metal loading (wt%)**	**H/M experiments**	
		V(H_2) (cm^3/g-cat.)	**H/M**
Pt/HY	1.0	1.2	2.0
Ir/SiO_2	1.0	1.4	2.3

Representative TEM images for Pt/HY and Ir/SiO_2 catalysts are shown in Fig. 5.3. The images reveal that the metal particles in both catalysts were uniformly dispersed on the supports with a fraction of the particles ranging in the size 5-10 nm and another fraction below 1 nm, in agreement with the high hydrogen uptakes.

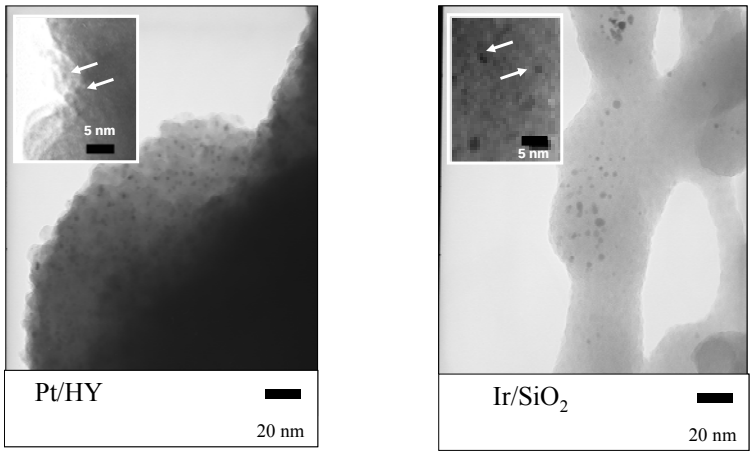

Figure 5.3 TEM images of the Pt/HY and Ir/SiO_2 samples. The length of the bar is 20 nm in the micrographs and 5 nm in the insets.

5.3.2 Catalytic Activity Measurements

5.3.2.1 Conversion of Methylcyclohexane over HY and Pt/HY Catalysts

The product distribution and level of MCH conversion obtained over an acidic HY catalyst and a bifunctional Pt/HY catalyst are compared in Table 5.3 for two different times on stream, 1 and 6 h. Significant differences in initial activity, rate of deactivation, and product distribution are observed between the two catalysts. The higher initial activity of the HY catalyst can be attributed to the higher density of acid sites present on the bare HY zeolite. A drastic decay in activity as a function of time on stream was observed for the HY catalyst (51.3%

conversion after 1 h, 32.3% after 6 h). The fast deactivation was accompanied by a pronounced decrease in the concentration of cracking products (<C7), which went from 13.5 wt% during the first hour on stream to 2.3 wt% after 6 h. In contrast, almost no deactivation was evident on the Pt/HY catalyst, for which the total conversion remained practically constant (~29%) over the time of the study. This slow deactivation may be attributed to a higher rate of hydrogen transfer accelerated by the presence of Pt.

A significant difference between HY and Pt/HY catalysts was also observed in the product distribution. Similar to the reaction of most naphthenes [74], in the conversion of MCH the ring contraction is the primary reaction; subsequently the RC products are consumed by consecutive reactions that first produce RO products and then cracking products (< C7). A clear demonstration of this sequence of reactions is obtained by plotting the evolution of products as a function of conversion, as discussed below.

Table 5.3 Product distributions of methylcyclohexane reaction on acid catalysts and metal catalyst at two times on stream.

Catalysts		**HY**		**Pt/HY**	
Space time; W/F (h)		0.49		0.47	
Time on stream (h)		1	6	1	6
Conversion (%)		51.3	32.3	29.9	29.2
MCH (wt%)		48.7	67.7	70.1	70.8
RC/RO ratio		10.1	38.2	40.9	46.6
Products		Selectivity to (%)			
Cracking Products		26.3	7.2	0.3	0.2
RC products	(RON)	Selectivity to (%)			
1,1-DMCP	(92.3)	2.6	1.3	13.3	13.1
cis -1,3-DMCP	(79.2)	16.7	24.8	16.0	15.9
trans -1,3-DMCP	(80.6)	16.2	23.3	15.8	15.6
trans -1,2-DMCP	(86.5)	20.7	25.2	26.0	26.0
ECP	(67.2)	10.0	15.7	26.2	27.0
RO products	(RON)	Selectivity to (%)			
3,3-DMP	(80.8)	-	-	-	-
2,2-DMP	(92.8)	-	-	0.2	0.1
2,4-DMP	(83.1)	5.7	2.1	0.6	0.5
2,3-DMP	(91.1)	0.2	-	0.2	0.2
n -heptane	(0.0)	-	-	0.7	0.6
2-MH	(42.4)	0.6	0.2	0.7	0.6
3-MH	(52.0)	-	-	-	-
3-EP	(65.0)	-	-	-	-
Heavy products		1.0	-	-	-

On the HY catalyst, while equilibrium is not reached, the distribution of RC products are more or less in line with their thermodynamic stability; that is, *trans*-1,2 dimethylcyclopentane (*trans*-1,2 DMCP) is the most abundant product, followed by *cis*- and *trans*-1,3 DMCP. These three products have relatively high octane number. These three products have relatively high octane number. Unfortunately, together with these products, ethylcyclopentane (ECP), which has a very low octane number, is produced in large concentrations. As shown in Fig. 5.2, opening the ECP ring would not enhance the octane number either, since every RO product from ECP has an octane number that is even lower than that of ECP. Interestingly, some RO products are observed on the HY catalyst, and the most abundant product is 2,4-dimethylpentane (2,4-DMP), which is obtained by β-scission of 1,3-dimethylcyclopentane (1,3-DMCP). One may have expected a comparable amount of 2,3-DMP, which could produced by an analogous β-scission of 1,2-DMCP and has a high octane number. However, this product is only produced in small quantities.

The product distribution obtained on the Pt/HY catalyst was significantly different from that on the HY catalyst. The most obvious difference was the drastic decrease in cracking products, which can be ascribed to the enhanced hydrogen transfer by the presence of Pt. At the same time, the distribution of DMCP products is significantly altered. It is seen that, at a given conversion the yield of 1,1-DMCP and ECP is greatly enhanced when Pt is present.

5.3.2.2 Evolution of Product Distribution with Conversion

The yields of the different products obtained over HY and Pt/HY as a function of total conversion are compared in Figs. 5.4a and 5.4b. It is observed, that at low conversions, only the RC products are found on both catalysts, while as the conversion increases, RO and cracking products start to appear. This trend clearly shows that the RC isomerization of MCH to ECP and DMCPs is a primary reaction. The secondary ring opening products consist mostly of 2,4-DMP, 2-MH, and *n*-heptane, but they further react yielding cracking products, a trend that is particularly apparent on the HY catalyst.

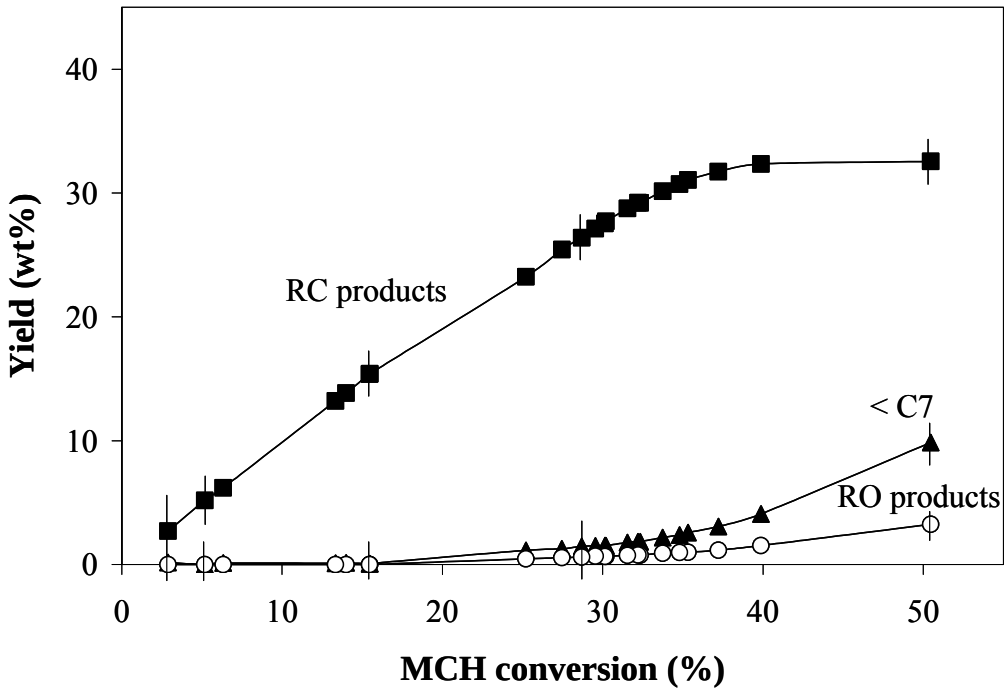

Figure 5.4a Product distribution of methylcyclohexane reaction over HY as a function of conversion. Conversions were varied by changing space time. Reaction conditions: Total pressure = 2 MPa; Temperature = 533 K; H_2/MCH molar ratio = 40.

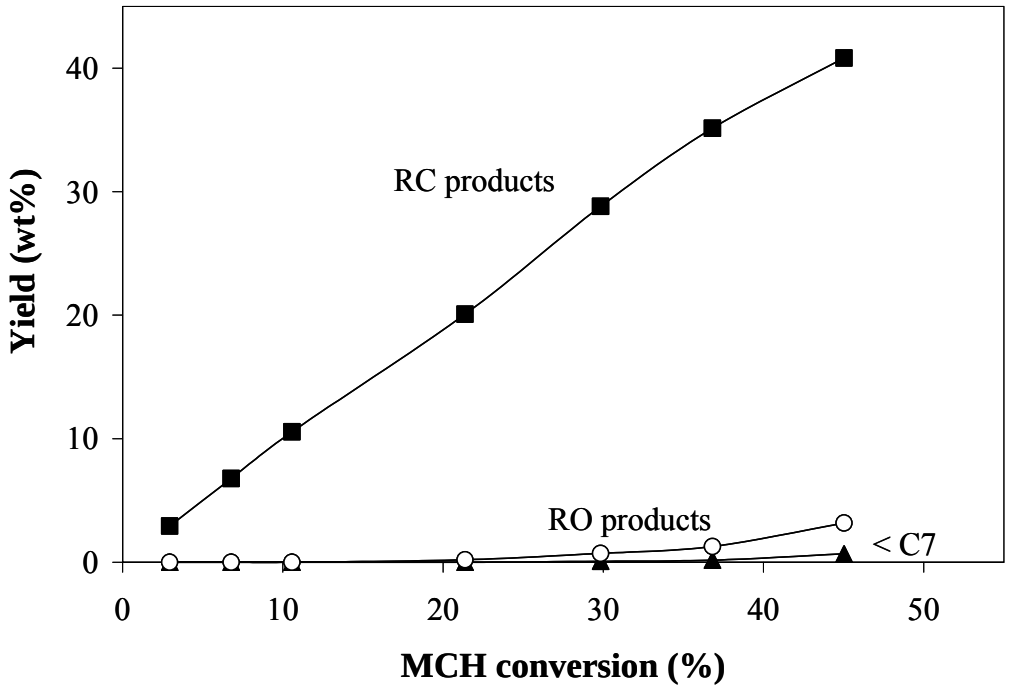

Figure 5.4b Product distribution of methylcyclohexane reaction over Pt/HY as a function of conversion. Conversions were varied by changing space time. Reaction conditions: Total pressure = 2 MPa; Temperature = 533 K; H_2/MCH molar ratio = 40.

Fig. 5.5 shows some differences in the distribution of the RC products for HY and Pt/HY catalysts. It can be seen that the selectivity to the low octane-number, monobranched isomer (ECP) decreases with conversion, while that to the dibranched isomers (DMCPs) increases. This is a favorable selectivity change because it should result in an increase in octane number. This trend may be explained considering that at low conversions ECP is easily formed via an internal alkyl shifts, called type-A isomerization in previous studies [82]. The increase in the selectivity to the thermodynamically favored DMCP isomers observed at higher space times may be due to a stepwise isomerization [91] as that observed in the isomerization of ethylcyclohexane on Pt/HZSM-5 [99], which produces propylcyclopentane as a main primary product, followed by formation of dibranched isomers as secondary products. In contrast to this proposed sequence, Calemma et.al. [100] have shown that both ECP and DMCPs are primary products from the MCH reaction over Pt/H-mordenite. In fact, the extrapolation to zero conversion in Fig. 5.5 indicates that it is possible that some DMCPs are produced as primary products at low space times and low conversions. However, they are also formed by secondary reaction at higher conversions.

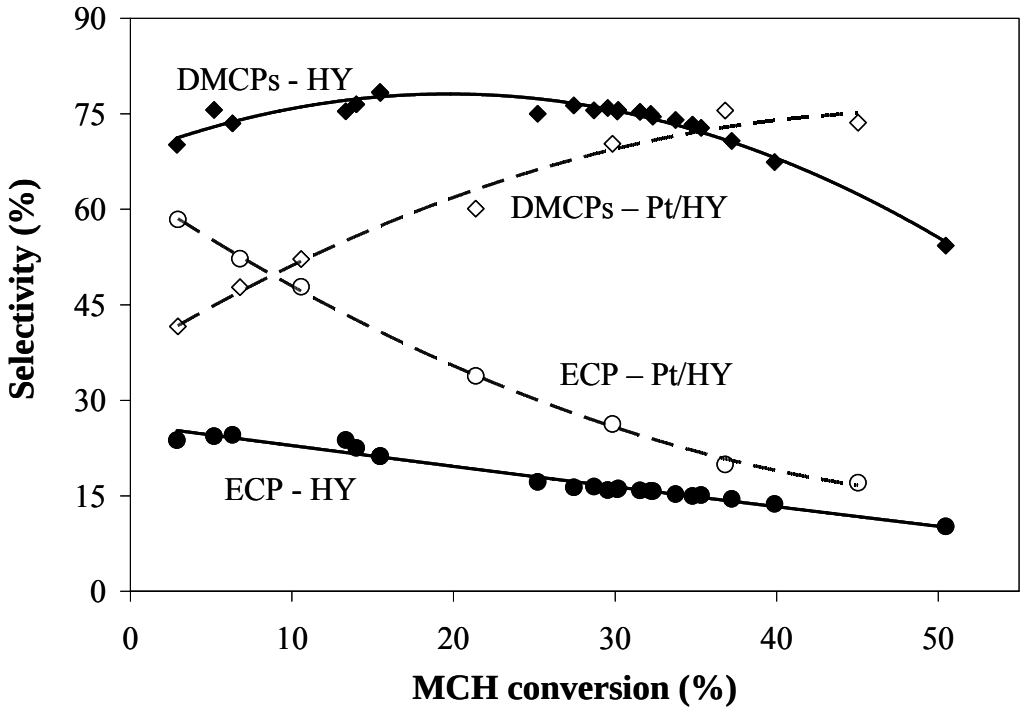

Figure 5.5 Isomerized RC products of methylcyclohexane reaction over HY (solid symbols) and Pt/HY (open symbols) at varying conversion. Conversions were varied by space time and time on stream. Reaction conditions: Total pressure = 2 MPa; Temperature = 533 K; H_2/MCH molar ratio = 40.

More detailed information on the distribution of RC products over HY and Pt/HY catalysts at two different total MCH conversions (~16% and ~30%) are shown in Figs. 5.6a and 5.6b. These figures clearly illustrate the characteristic differences between HY and Pt/HY; that is, for a given conversion, the selectivities to ECP and 1,1-DMCP are lower on HY than on Pt/HY while the selectivity to 1,3-DMCP is higher. The difference is particularly important for the selectivity towards the most desirable isomer 1,1-DMCP (high octane number), which is significant for Pt/HY but very low on HY at both conversion levels.

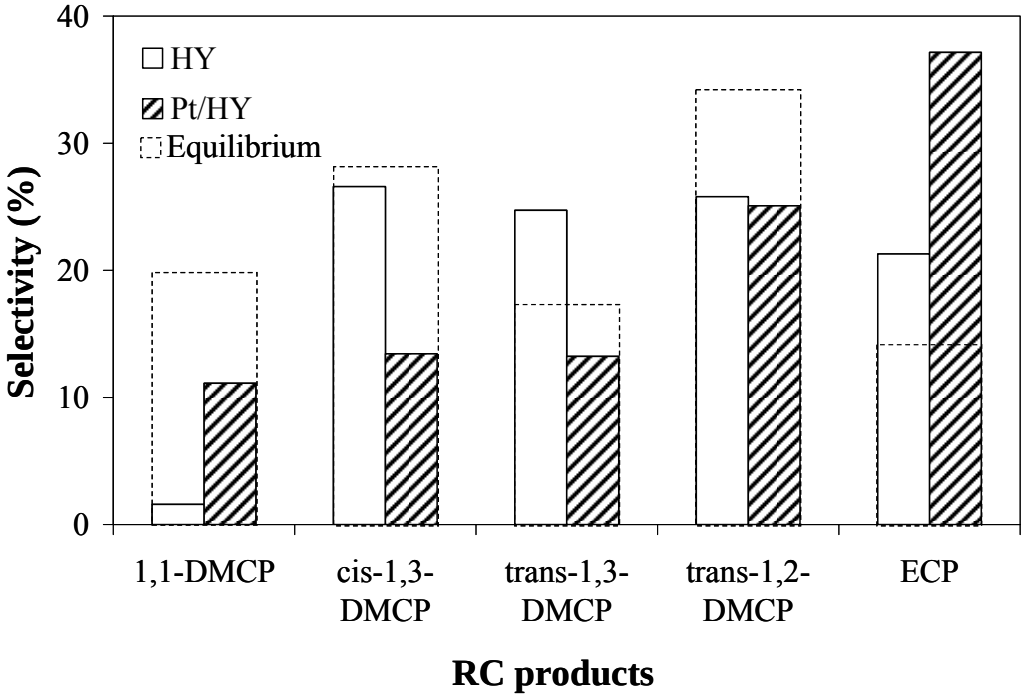

Figure 5.6a Selectivities of isomerized RC products on HY and Pt/HY at the same conversion (~16%). Simulated RC composition at thermodynamic equilibrium was calculated by using SimSci PRO/II PROVISION. Reaction conditions: Total pressure = 2 MPa; Temperature = 533 K; H_2/MCH molar ratio = 40.

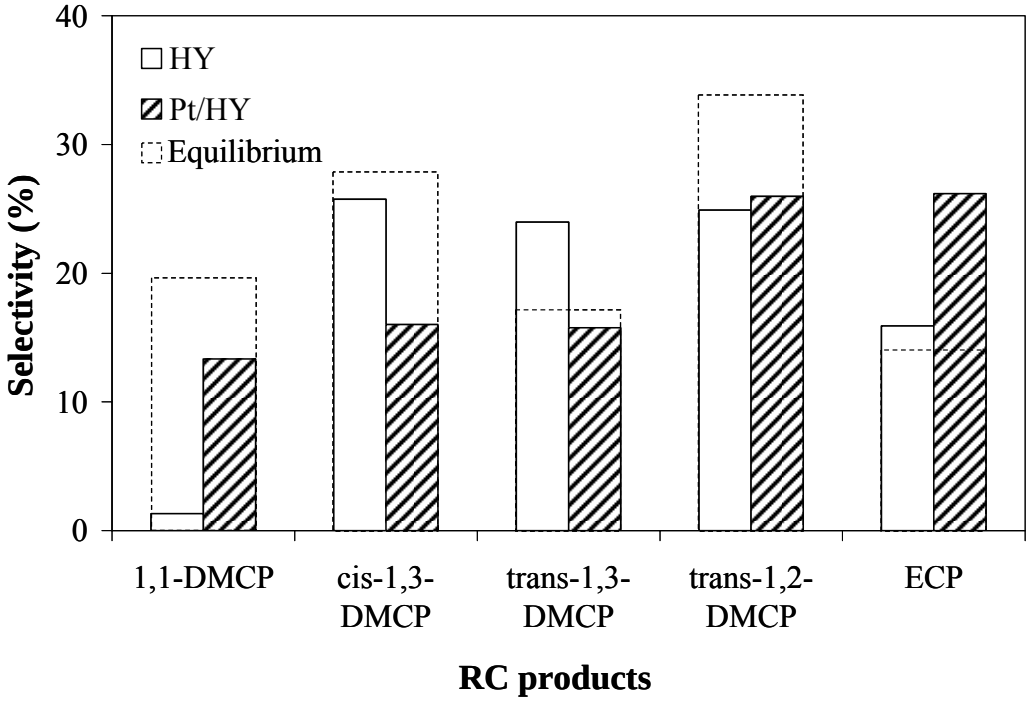

Figure 5.6b Selectivities of isomerized RC products on HY and Pt/HY at the same conversion (~30%). Simulated RC composition at thermodynamic equilibrium was calculated by using SimSci PRO/II PROVISION. Reaction conditions: Total pressure = 2 MPa; Temperature = 533 K; H_2/MCH molar ratio = 40.

The enhanced selectivity to ECP on the Pt/HY, particularly at low conversions, can be ascribed to both, a lower acidity density [92] and an enhanced rate of hydrogen transfer in this catalyst compared to HY [101]. The capacity of Pt for activating hydrogen and accelerating the hydride transfer step has been well documented in the literature [102-104]. An enhanced rate of hydride transfer accelerates the rate of desorption and thus reduces the residence time of intermediates on the surface. Since ECP is the product resulting from the C6-ring surface carbocation that is the easiest to form (intermediate A in Fig. 5.7), shortening the residence time of this surface intermediate will increase the concentration of ECP in the products. By contrast, on the HY catalyst, the carbocation has more time on the surface to isomerize and, as a result, the 1,3-DMCP and 1,2-DMCP are formed via the least favored intermediates B, C, and D.

Similarly, the enhanced selectivity to 1,1-DMCP on Pt/HY can be ascribed to enhanced hydride transfer. However, in this case the fate of the C_5-ring carbocations needs to be addressed. Once the RC step occurs on the surface and the corresponding C_5-ring carbocation is formed, the RC product can only be obtained by a hydride transfer step (see Fig. 5.8). On the HY catalyst, this step is bimolecular and involves electroneutral RH molecules (e.g. MCH).

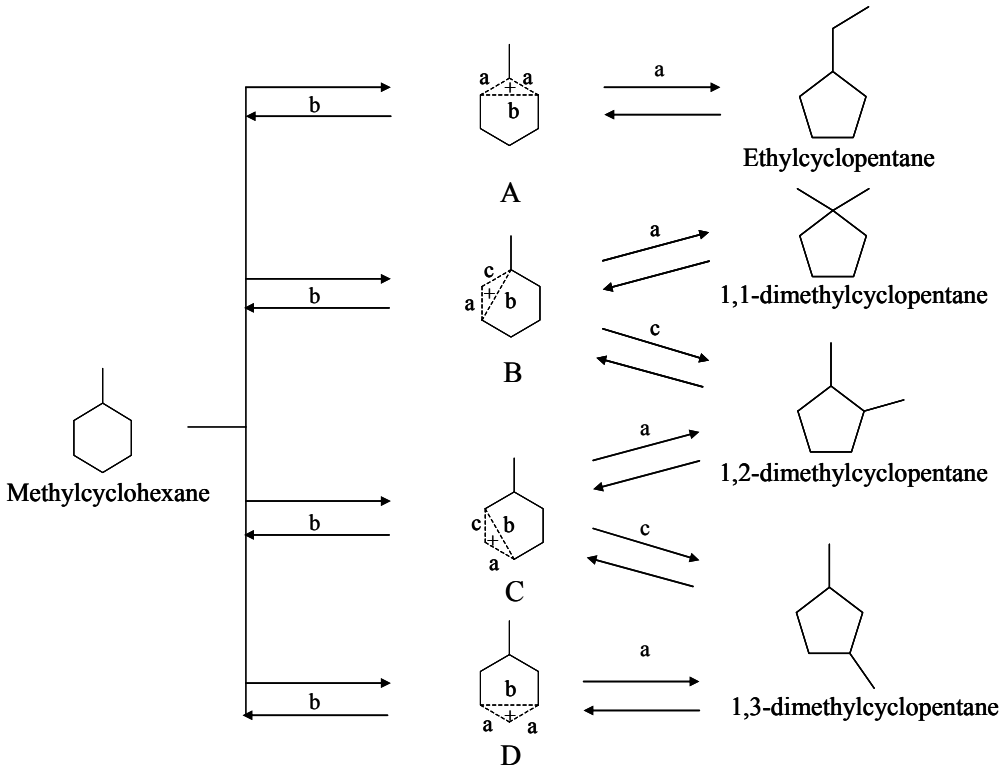

Figure 5.7 Carbocation chemistry for the ring contraction reactions.

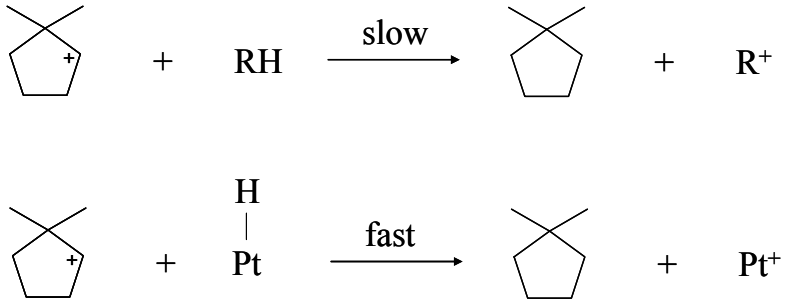

Figure 5.8 Hydride transfer paths involving C_5-ring carbocation intermediates.

As shown in Fig. 5.8, the production of 1,1-DMCP involves a 2,2-dimethylcyclopent-1-yl cation, (i.e., the positive charge in a secondary C). With such a bulky intermediate, the hydride transfer from an electroneutral RH molecule is sterically unfavorable and one can expect this step to be slow. As a result, the production of 1,1-DMCP is very low on an HY catalyst. However, in the presence of Pt the hydride transfer is enhanced and as a result significant amounts of 1,1 DMCP can be obtained. A similar situation was reported by Santiesteban et al. [105] in the isomerization of *n*-hexane on highly acidic WO_x/ZrO_2-based catalysts. These authors found that the 2,2-dimethylbutane isomer was not formed in the absence of Pt, but it was produced in significant amounts when Pt was added to the catalyst. They suggested that the presence of Pt gives rise to a high concentration of atomic hydrogen on the surface, enough to overcome the high kinetic barrier associated with the intermolecular hydride transfer to the sterically-hindered intermediate (i.e., 2,2-dimethyl-3-butyl cation).

The effect of reaction temperature on product distribution is summarized in Table 5.4 for two different space times (0.6 and 0.8 h). The isomerization products (RC) (primary products) decrease with increasing space time; while the ring opening and cracking products (secondary products) increase. The effect of temperature is further illustrated in Fig. 5.9 for a constant W/F = 0.5 h. Below 533 K, the only observed products are RC products, while RO and cracking products only appear at high temperatures. At the lower temperature end, ECP is the dominant product, while at 593 K the equilibrium product distribution is obtained.

Table 5.4 Product distribution of methylcyclohexane reaction over Pt/HY catalyst at different temperatures.

Catalyst		**Pt/HY W/F = 0.6 h**				**Pt/HY W/F = 0.8 h**			**Equilibrium**	
Temperature (K)		**513**	**533**	**553**	**573**	**533**	**553**	**593**	**533**	**553**
Conversion (%)		13.2	31.6	48.4	58.9	38.2	50.9	70.3	49.5	54.3
MCH (wt%)		86.8	68.4	51.6	41.1	61.8	49.1	29.7	50.5	46.6
Products		Yield (wt%)				Yield (wt%)			Yield (wt%)	
Cracking Products	(RON)	0.4	0.5	0.8	2.3	0.4	1.4	13.5	-	-
1,1-DMCP	(92.3)	1.2	4.3	7.2	9.0	5.5	7.5	9.4	8.0	8.4
cis -1,3-DMCP	(79.2)	1.3	5.2	9.4	11.1	6.9	9.7	9.4	11.7	12.5
trans -1,3-DMCP	(80.6)	1.2	5.1	9.3	11.1	6.8	9.6	9.7	7.0	7.7
cis -1,2-DMCP	(85.7)	-	-	-	-	-	-	-	2.6	3.0
trans -1,2-DMCP	(86.5)	3.1	8.3	12.9	14.5	10.1	13.2	12.2	14.2	15.1
ECP	(67.2)	5.9	7.7	7.2	6.7	7.5	7.3	6.1	5.9	6.7
3,3-DMP	(80.8)	-	-	0.1	0.2	-	0.1	0.5	-	-
2,2-DMP	(92.8)	-	-	0.1	0.3	0.1	0.2	0.7	-	-
2,4-DMP	(83.1)	-	0.1	0.4	1.0	0.3	0.6	2.6	-	-
2,3-DMP	(91.1)	-	-	0.1	0.4	0.1	0.2	1.0	-	-
n -heptane	(0.0)	0.1	0.1	0.3	0.7	0.2	0.4	1.8	-	-
2-MH	(42.4)	-	0.1	0.4	1.3	0.3	0.7	2.9	-	-
3-MH	(52.0)	-	-	-	-	-	-	-	-	-
3-EP	(65.0)	-	-	-	-	-	-	-	-	-

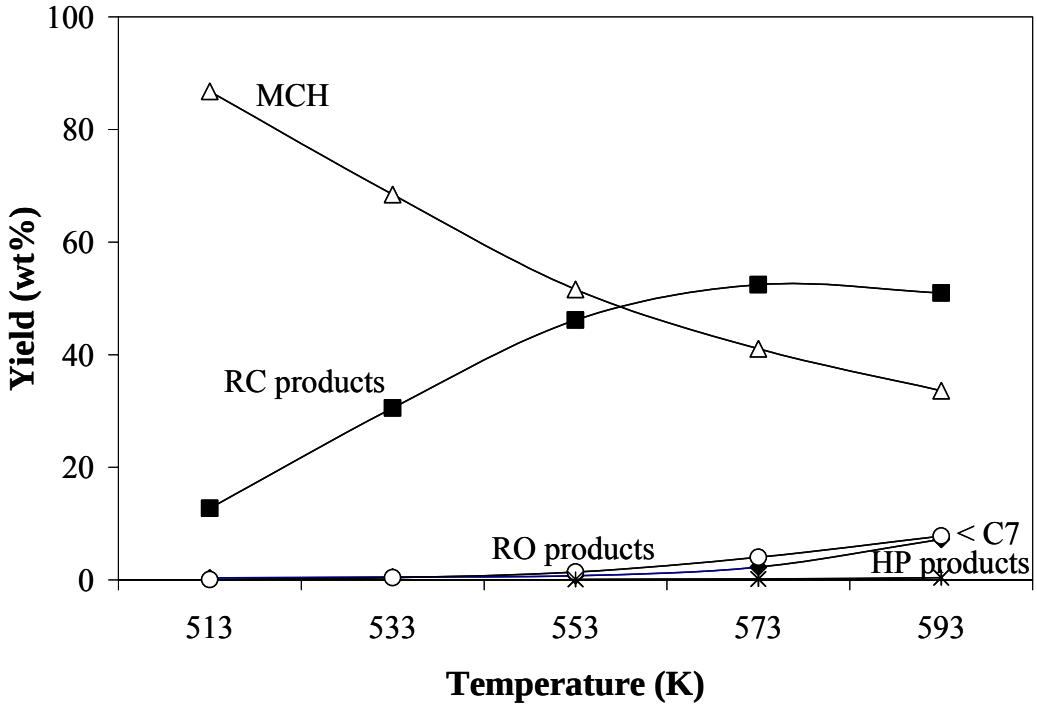

Figure 5.9a Product distributions of methylcyclohexane reaction over Pt/HY catalyst at different reaction temperatures. Reaction conditions: Total pressure = 2 MPa; W/F = 0.6 h; H_2/MCH molar ratio = 40.

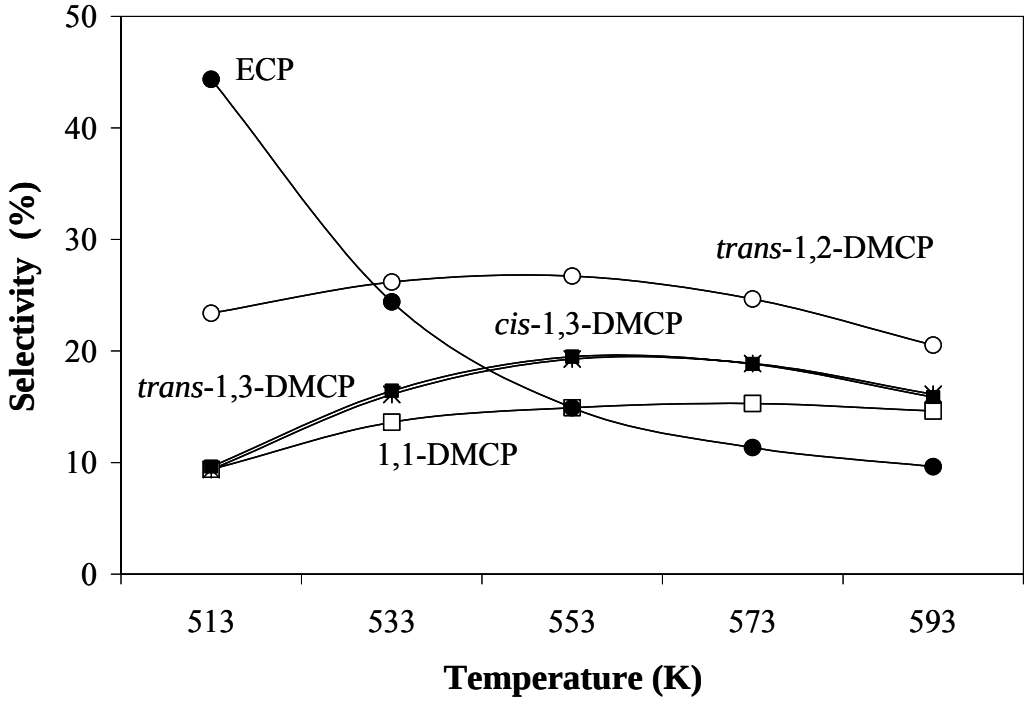

Figure 5.9b Selectivities to ring contraction products of methylcyclohexane reaction over Pt/HY catalyst at different reaction temperatures. Reaction conditions: Total pressure = 2 MPa; W/F = 0.6 h; H_2/MCH molar ratio = 40.

Among the RC isomers, only ECP has an octane number (both RON and MON) lower than the feed, but as shown above, ECP is the dominant product only at low conversions. One can evaluate the variation of octane number as a function of conversion in the product mixture. However, it is well known that the RON and MON of a hydrocarbon mixture is not the direct linear combination of the individual contributions, but rather they vary in a non-linear form.

Ghosh et al. [106] have recently recommended the use of a model for the prediction of RON and MON in gasoline blends. They have confirmed that equation (1) shown below can accurately predict RON and MON, within 1 number. This model takes into account the interactions among the different hydrocarbon classes (paraffins, olefins, aromatics, etc.) in a gasoline blend that are responsible for the non-linear behavior of octane numbers. The advantage of this equation is that it does not use blending numbers, but rather the individual ON of the pure components, that are readily available [107,108]. The equation used is:

$$ON = \frac{\sum_{PONA} \upsilon_i \beta_i ON_i + I_P \sum_{P} \upsilon_i \beta_i ON_i}{\sum_{PONA} \upsilon_i \beta_i + I_P \left(\sum_{P} \upsilon_i \beta_i - \sum_{P} \upsilon_i \right)} \qquad (1)$$

$$I_i = \left[\left(\frac{k_{PN}^{(a)} \upsilon_N + k_{PO}^{(a)} \upsilon_O}{1 + k_{PN}^{(b)} \upsilon_N + k_{PO}^{(b)} \upsilon_O} \right) \right] \qquad \text{for i} \in \text{P} \qquad (2)$$

Otherwise = 0

where υ_i is the volume fraction of molecule *i* in the sample; ON_i represents the pure component octane number for each molecule *i* in the sample; β_i and $k_{xx}^{(x)}$ are the adjustable parameters and the interaction parameters, experimentally obtained by Ghosh et al. [106].

Following this ON prediction method, we calculated octane numbers (both RON and MON) for the product mixtures obtained in this work. The results for the products obtained over the HY and Pt/HY catalysts, as well as the equilibrium composition for MCH and all the RC products are presented in Figs. 5.10a and 5.10b, for RON and MON, respectively. It is observed that the RON of the product mixture on both HY and Pt/HY catalysts increase as a function of MCH conversion. However, at the higher end of MCH conversion (i.e. high reaction temperatures), RON sharply decreases due to the contribution of the reactions mentioned above that produce low RON molecules. When only RC is considered in the calculation of equilibrium the increase in RON is higher. However, an interesting point to address is that only RON increases as the MCH conversion increases; by contrast MON does not increase, but rather it decreases as MCH is converted into RC isomers.

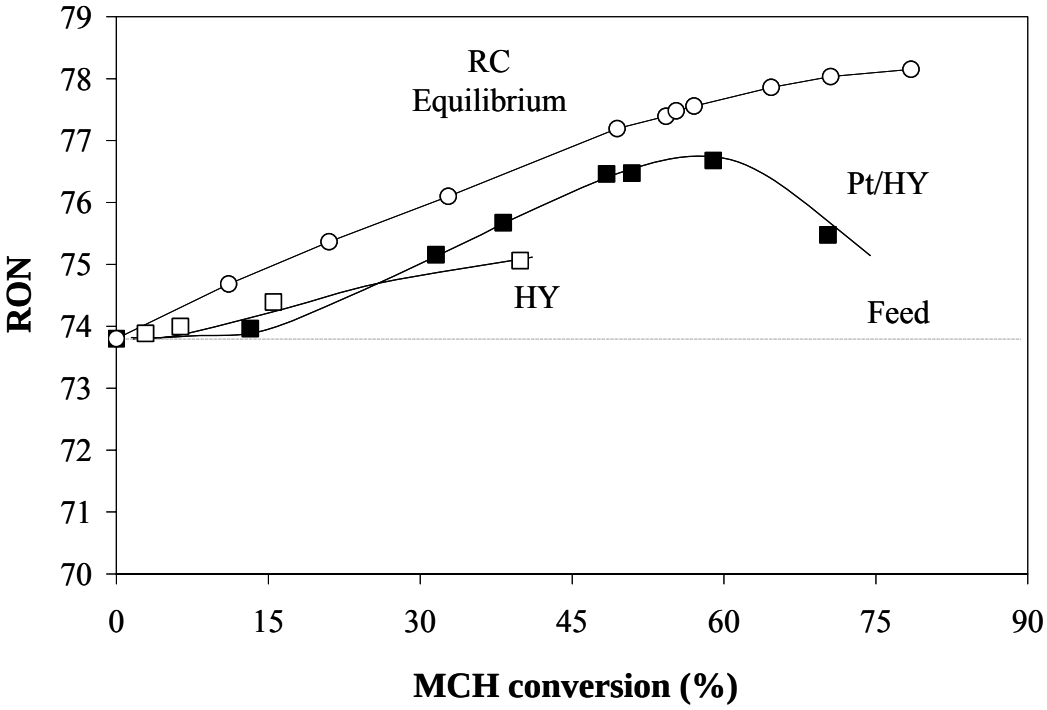

Figure 5.10a Reseach octane number (RON) of the product mixture as a function of methylcyclohexane conversion, calculated by the method of Ref. [106]. Conversion was varied by changing W/F and temperature as shown in Table 5.4. Simulated RC composition at thermodynamic equilibrium was calculated by using SimSci PRO/II PROVISION. Total pressure = 2 MPa; H_2/MCH molar ratio = 40.

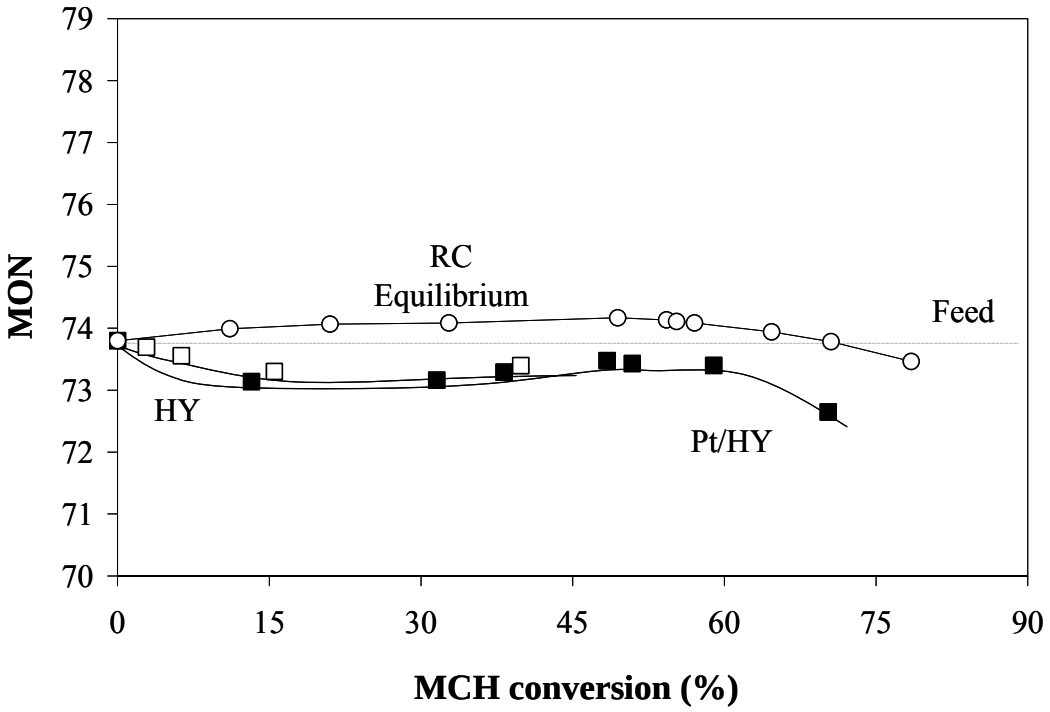

Figure 5.10b Motor octane number (MON) of the product mixture as a function of methylcyclohexane conversion, calculated by the method of Ref. [106]. Conversion was varied by changing W/F and temperature as shown in Table 5.4. Simulated RC composition at thermodynamic equilibrium was calculated by using SimSci PRO/II PROVISION. Total pressure = 2 MPa; H2/MCH molar ratio = 40.

When analyzing the RON and particularly the MON of some of the RO products in Fig. 5.2, one can see that selective C-C bond cleavage might lead to isoparaffins of high octane number. We have attempted to investigate different catalysts and catalytic bed configurations that might result in octane numbers higher than those obtained by ring contraction alone. As previously proposed by McVicker et al. [16], Iridium is a promising catalytic material for selective ring opening. As described below, we have investigated using Ir/SiO_2 catalysts in combination with Pt/HY.

5.3.2.3 Conversion of Methylcyclohexane over Ir/SiO_2 Catalyst

Figs. 5.11a and 5.11b show the different products obtained when MCH is reacted over the Ir/SiO_2 catalyst at different temperatures. It is clear that, on this catalyst, the only reaction observed under these conditions is the direct ring opening of the C6-ring of MCH into C_7-alkanes (i.e., 2-MH, 3-MH, and *n*-heptane). In contrast to the other two catalysts, no RC products were observed on Ir/SiO_2, clearly showing that the RC is catalyzed by acids [92,93]. Monofunctional isomerization has been previously observed on Ir catalysts, but under the conditions of this study, hydrogenolysis is dominant. As first reported by Gault et al. [43] iridium has the tendency of breaking secondary-secondary C-C bonds via dicarbene intermediates while the C-C bond rupture in the vicinity of the tertiary carbon is strongly hindered. This is indeed the behavior observed in this case for the Ir/SiO_2 catalyst. We have previously shown that when the support is alumina, the

contribution of products arising from the tertiary-secondary C-C bond cleavage may be greatly increased [95].

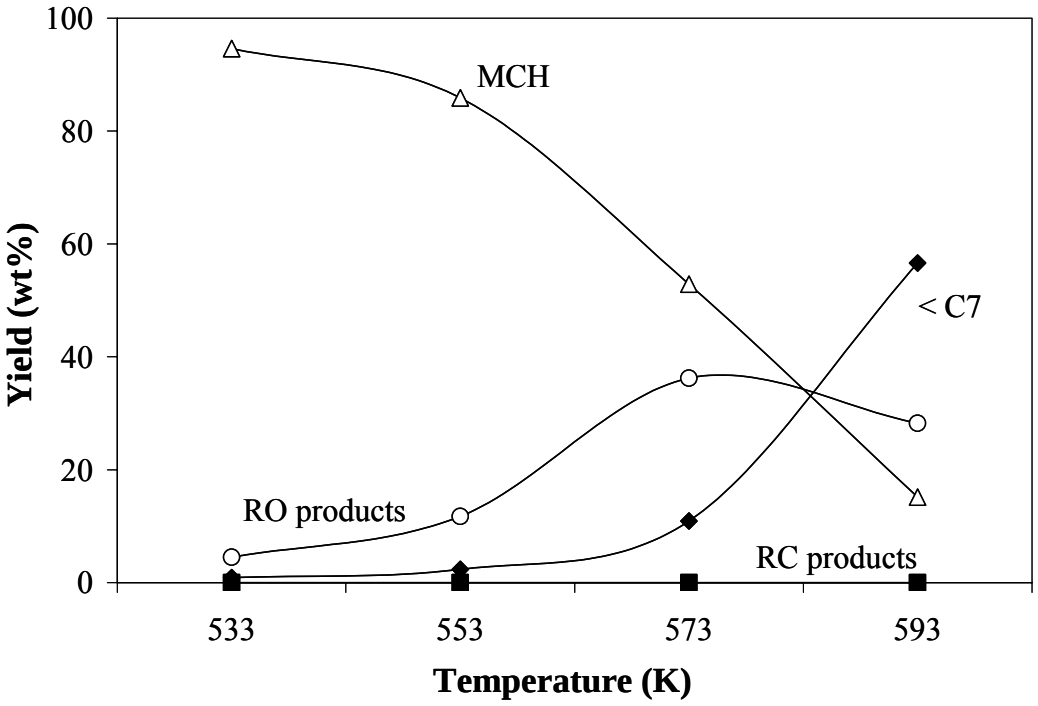

Figure 5.11a Product distributions of methylcyclohexane reaction over Ir/SiO_2 at different reaction temperatures. Reaction conditions: Total pressure = 2 MPa; W/F = 0.3 h; H_2/MCH molar ratio = 40.

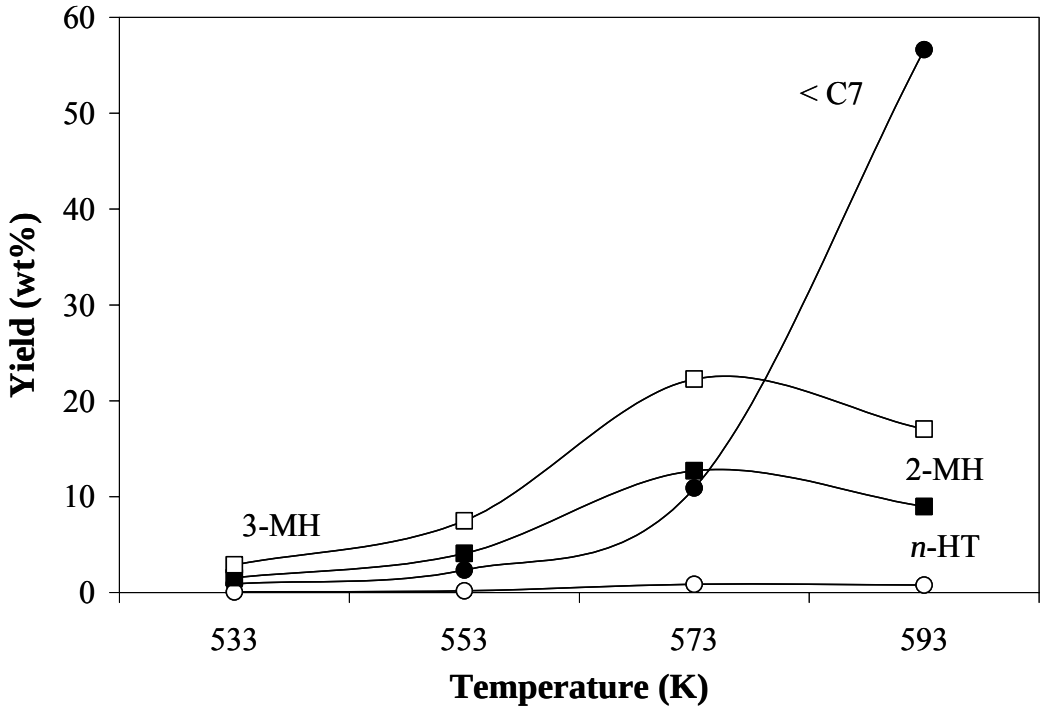

Figure 5.11b The distribution of ring opening and cracking products of methylcyclohexane reaction over Ir/SiO_2 at different reaction temperatures. Reaction conditions: Total pressure = 2 MPa; W/F = 0.3 h; H_2/MCH molar ratio = 40.

In general, as shown in Fig. 5.1, ring opening at a tertiary-secondary C-C bond produces molecules of lower octane number. Indeed, in this case, the resulting C7 alkane is *n*-heptane with RON = MON =0. In fact, all three products obtained from direct opening of MCH have RON/MON lower than the feed. Therefore, in order to be effective, the iridium catalyst must be used in combination with an acidic catalyst that produces RC compounds, which as shown in Fig. 5.2 may lead to higher octane numbers if opened at the right C-C bond.

5.3.2.4 Conversion of Methylcyclohexane on Physical Mixtures and Segregated Beds of Pt/HY and Ir/SiO_2 Catalysts

As shown in Fig. 5.2, only a few of the RO products have higher RON than the RC products. However, two aspects of RO products may be desirable in comparison to RC products. In the first place, while the MON of C5 naphthenic molecules is lower than the corresponding RON, the opposite is true for the isoparaffins. That is, the MONs of RC products are generally higher than the corresponding RONs. Second, the density of isoparaffins is generally lower than that of the corresponding naphthene. As a result, there is a volume gain for refiners when the rings are opened. That is, even when there is no gain in octane number, RO may represent a significant gain in volume.

As illustrated in Figure 5.12, the following set experiments were conducted to investigate the combination of RC and RO for a given MCH feed:

(a) a homogeneous physical mixture of Pt/HY and Ir/SiO_2 designated as ($Pt/HY+Ir/SiO_2$); in this case, the temperature of the two catalysts is the same during reaction; (b) a two-bed configuration, where the front bed is Pt/HY and the back bed is Ir/SiO_2 ; in this configuration, designated as ($Pt/HY => Ir/SiO_2$), the temperature of the two catalyst beds is kept the same; and (c) a two-bed configuration, in which the front bed is Pt/HY and the back bed is Ir/SiO_2, designated as ($Pt/HY = => Ir/SiO_2$); the two beds are separated by quartz wood and glass beads and there is temperature difference of 20 K, with the front bed at a higher temperature. In all three configurations the total amount of each of the catalyst was kept constant.

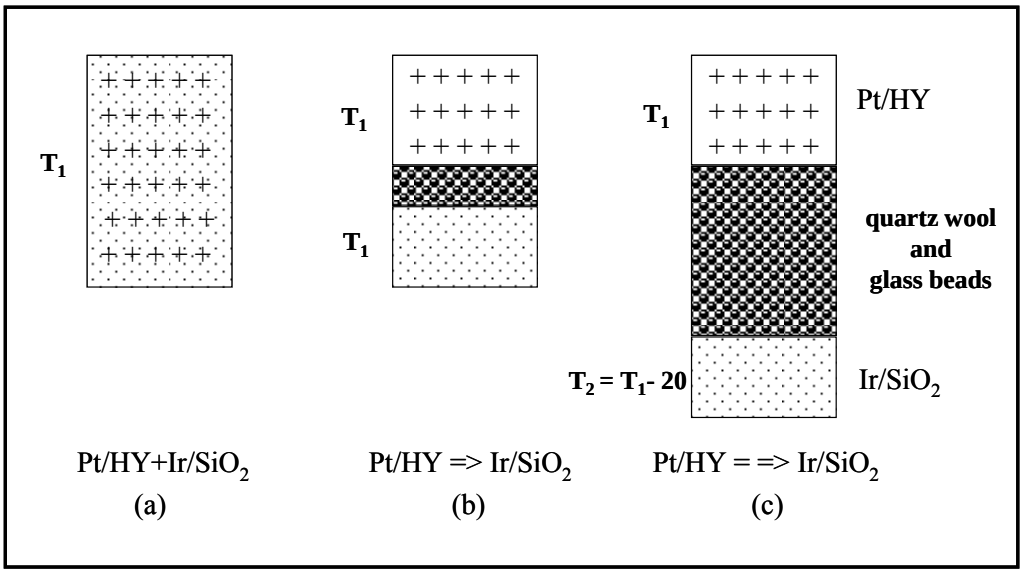

Figure 5.12 Schematic reaction system configurations.

The results obtained with the three different system configurations are summarized in Table 5.5. It can be observed that the total MCH conversion increases with temperature much more rapidly for the physical mixture, case (a) Pt/HY+Ir/SiO_2, than for the sequential bed configurations. In the physical mixture, a significant amount of C_6-member ring opening takes place, which as mentioned above it is not desirable because it produces compounds of low octane numbers. By contrast, in case (b) (Pt/HY => Ir/SiO_2), a large fraction of MCH is converted to RC products before reaching the Ir/SiO_2 bed. In this case, the opening of C_5-member ring compounds is fast and readily occurs at lower temperatures. As a result, this configuration yields a larger fraction of DMP products, which result from the opening of C_5-member rings. This is a desirable outcome since DMP products have relatively high octane numbers. However, on this configuration, working at low temperatures results in low MCH conversions, while working at higher temperatures initiates the opening of C_6-member rings, i.e., direct RO of MCH, which produces compounds of low octane numbers. In addition, high reaction temperatures (e.g. 573 K) generate a large fraction of cracking products.

Table 5.5 Product distribution of methylcyclohexane reaction at different reaction system configurations. (see Fig. 5.12)

Catalysts		Pt/HY + Ir/SiO_2			Pt/HY =>Ir/SiO_2			Pt/HY ==> Ir/SiO_2		
Temperature (K)		513	533	553	533	553	573	533/513	553/533	573/553
Conversion (%)		30.1	65.5	90.3	52.6	68.7	92.7	45.8	60.6	67.1
MCH (wt%)		69.9	34.5	9.7	47.4	31.3	7.3	54.2	39.4	25.4
RC products (wt%)		12.5	12.2	3.1	15.2	4.3	0.4	34.3	20.3	7.3
RO products (wt%)		17.0	49.1	76.7	35.0	59.0	66.1	10.6	37.0	54.9
RC/RO ratio		0.7	0.2	0.0	0.4	0.1	0.0	3.2	0.5	0.1
Products		Yield (wt%)			Yield (wt%)			Yield (wt%)		
Cracking products	(RON)	0.5	3.9	9.8	2.2	5.2	25.7	0.9	3.1	11.8
1,1-DMCP	(92.3)	0.0	0.0	0.0	0.0	0.0	0.0	7.4	0.0	0.0
cis -1,3-DMCP	(79.2)	1.9	2.3	0.9	3.8	1.8	0.2	6.7	5.4	1.6
trans -1,3-DMCP	(80.6)	2.5	3.4	0.0	5.5	0.0	0.0	7.6	7.2	3.8
trans -1,2-DMCP	(86.5)	3.6	3.5	1.3	4.5	1.9	0.2	8.7	6.0	1.6
ECP	(67.2)	4.5	3.1	1.0	1.5	0.5	0.0	3.9	1.6	0.3
3,3-DMP	(80.8)	0.7	3.4	5.7	0.9	1.5	2.3	0.4	1.1	1.7
2,2-DMP	(92.8)	1.7	6.0	9.1	3.2	5.2	5.7	1.4	3.5	5.2
2,4-DMP	(83.1)	1.9	6.3	8.9	9.7	16.5	14.5	3.5	10.0	15.7
2,3-DMP	(91.1)	2.0	6.7	10.6	9.2	14.5	12.6	4.0	9.9	14.1
n -heptane	(0.0)	0.4	1.4	3.8	0.9	1.2	2.5	0.4	1.1	2.3
2-MH	(42.4)	2.6	10.1	16.7	2.2	4.5	10.1	0.8	2.3	5.1
3-MH	(52.0)	7.7	15.1	19.5	8.8	11.7	16.5	0.0	9.2	10.8
3-EP	(65.0)	0.0	0.0	2.4	0.0	4.0	1.9	0.0	0.0	0.0

Finally, in the reactor configuration with well-separated catalysts, case (c), we can avoid breaking the C-C bond of MCH by keeping the second bed at a lower temperature. In this way, the C-C bond cleavage of the C_5-member rings, with a lower activation energy [39,109], is less affected by the temperature reduction than the opening of the C_6-member rings. At the lowest temperatures investigated (533 K), case (c) presented the favorable situation of

reaching a significant conversion of the RC products, while leaving the C_6-member ring almost unreacted. As the temperature increases, the direct opening of the C_6-member ring starts to occur on both reactor configurations, which generates the low-octane alkane products (*n*-heptane, 2-MH, 3-MH, and 3-EP). As a result, a desirable combination of the two reactors is one in which a high RC conversion is reached while avoiding the start of RO on the Pt/HY bed, followed by low temperature RO on the Ir/SiO_2 to effect the selective RO of the C_5-member rings, without opening the C_6-member rings.

If we evaluate the ratio of products with higher octane number than the feed to those with lower octane number than the feed, we see that this ratio decreases as the temperature increases. This trend is due to the higher activation energy on Ir/SiO_2 of those reactions that generate products of low ON. They are the direct opening of MCH and the cleavage of the RC products at the substituted C-C bonds (see Fig. 5.2). It has been demonstrated in previous studies that the breaking of substituted C-C bond has higher activation energy than that of unsubstituted C-C bond via a dicarbene mechanism [51,110]. The effect of the different strategies on the resulting RON and MON can be compared in a more quantitative way by using the method developed by Ghosh et al. [106] and described above. As shown in Figs. 5.9a and 5.9b the RON and MON of the mixture for case (a) decreases as a function of conversion due to the direct opening of MCH, which as mentioned above generates alkanes of low RON and MON. By contrast, the RON and MON increases with conversion in cases (b) and (c) until it reaches a maximum and starts decreasing

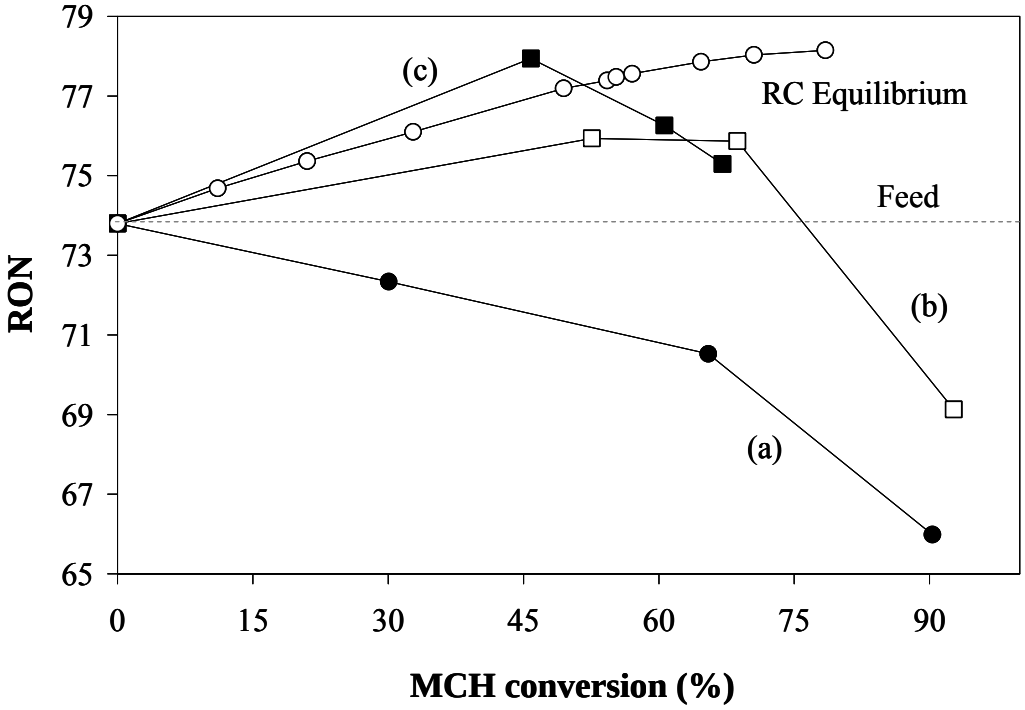

Figure 5.13a RON of the product mixture as a function of methylcyclohexane conversion, calculated by the method of Ref. [109]. For the product distribution obtained on the three Pt/HY + Ir/SiO_2 catalyst bed configurations illustrated in Fig. 5.12. Conversion was varied by changing temperature as shown in Table 5.5. Simulated RC composition at thermodynamic equilibrium was calculated by using SimSci PRO/II PROVISION. Total pressure = 2 MPa; H_2/MCH molar ratio = 40.

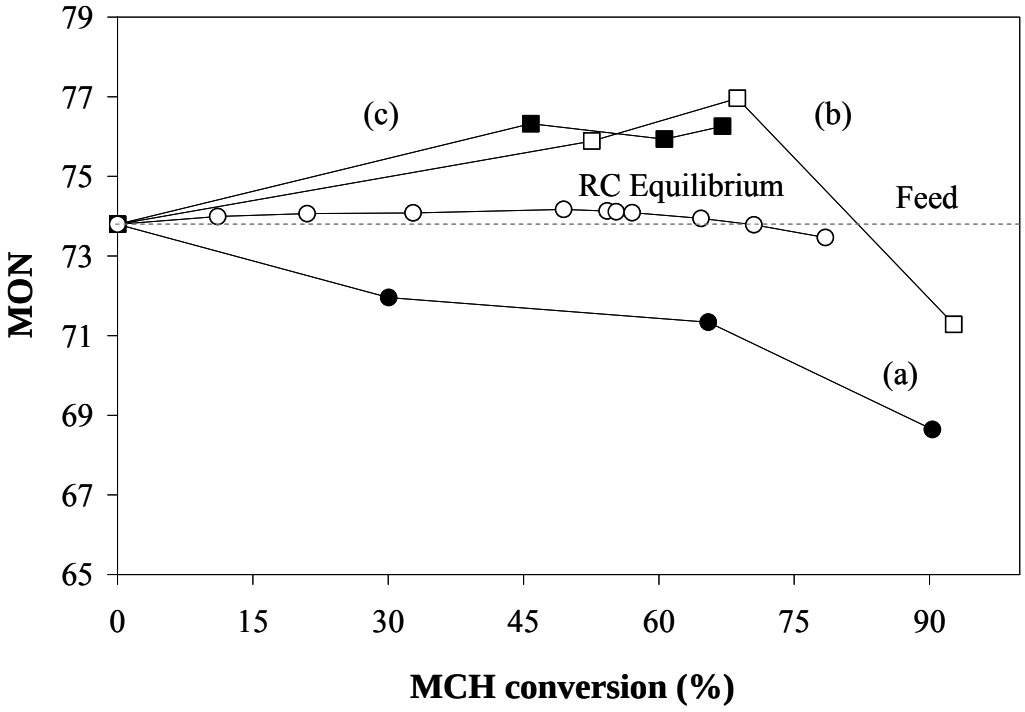

Figure 5.13b MON of the product mixture as a function of methylcyclohexane conversion, calculated by the method of Ref. [109]. For the product distribution obtained on the three Pt/HY + Ir/SiO_2 catalyst bed configurations illustrated in Fig. 5.12. Conversion was varied by changing temperature as shown in Table 5.5. Simulated RC composition at thermodynamic equilibrium was calculated by using SimSci PRO/II PROVISION. Total pressure = 2 MPa; H_2/MCH molar ratio = 40.

at high conversions (high temperatures), due to the contribution of direct MCH ring opening and cleavage of substituted C-C bonds, both producing low-RON/MON molecules.

Figs. 5.14a and 5.14b summarize the resulting RON, MON, and specific volume of the product mixtures for the different catalyst bed configurations. As mentioned, the most desirable outcome would be a product with RON/MON, as well as specific volume, higher than those of the feed. The results of the combined Pt/HY and Ir/SiO_2 with different extents of (RC+RO) reactions are compared to those of the Pt/HY and HY on which mostly RC occurs. Also, the values for an equilibrium mixture considering only RC products are included for comparison. The equilibrium has been calculated in the temperature range 373-773 K, which corresponds to a range of equilibrium conversions of 0-80. It can be observed that with RC alone, a significant increase in RON can be obtained reaching a maximum of 78. However, neither MON or specific volume are seen to increase much when no RO takes place. A significant gain in all three parameters can be obtained for the two configurations involving sequential beds at intermediate MCH conversion levels (i.e. 50-70%). Under these conditions, RON, MON, and specific volume are significantly higher than those of the feed. While RO does not impart a great enhancement in RON, it does benefit MON and specific volume.

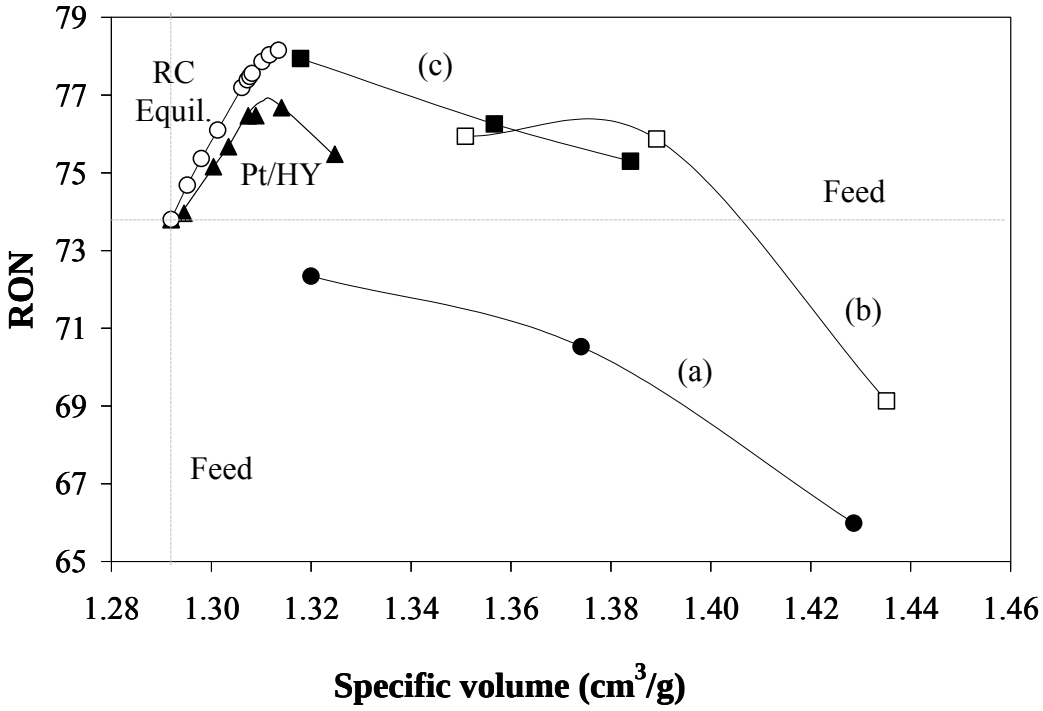

Figure 5.14a RON of the product mixture as a function of the corresponding specific volume. The volume was increased by increasing the MCH conversion through RC and by combination of (RC+RO), see Table 5.5. Specific volume and Simulated RC composition at thermodynamic equilibrium were calculated by using SimSci PRO/II PROVISION. Curves (a), (b), and (c) represent the three Pt/HY + Ir/SiO2 catalyst bed configurations illustrated in Fig. 5.12.

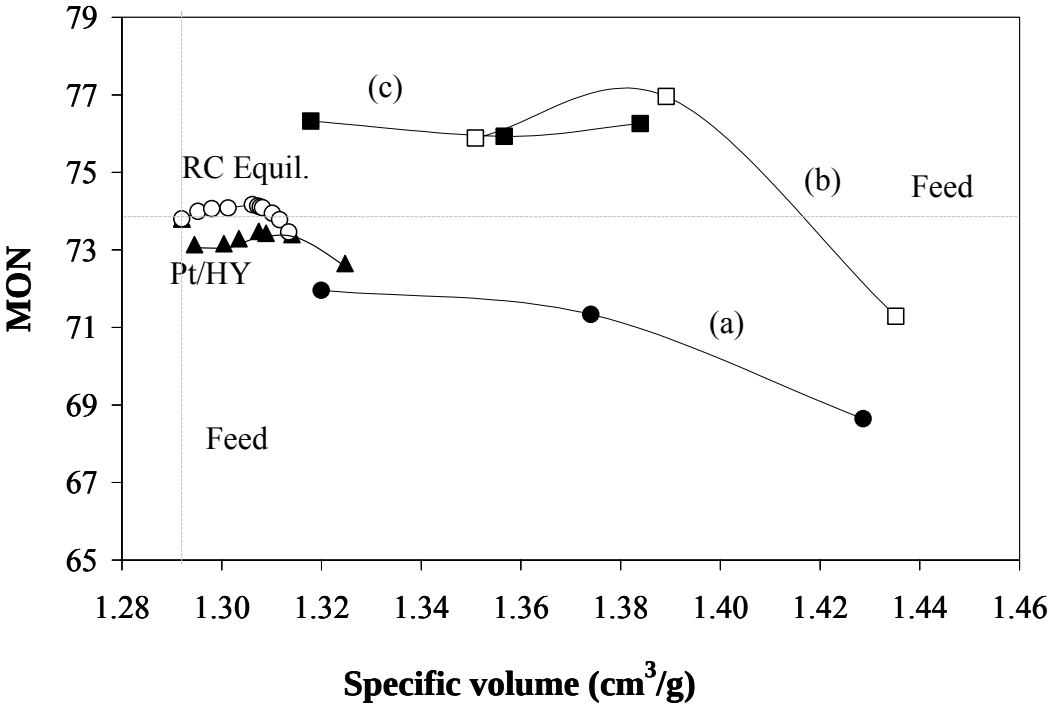

Figure 5.14b MON of the product mixture as a function of the corresponding specific volume. The volume was increased by increasing the MCH conversion through RC and by combination of (RC+RO), see Table 5.5. Specific volume and Simulated RC composition at thermodynamic equilibrium were calculated by using SimSci PRO/II PROVISION. Curves (a), (b), and (c) represent the three Pt/HY + Ir/SiO2 catalyst bed configurations illustrated in Fig. 5.12.

5.4. Conclusions

The main conclusion of this work can be summarized as follows:

- HY and Pt/HY zeolite catalysts are effective catalyst for the ring contraction of naphthenic molecules. The presence of Pt not only improves the catalyst stability but also modifies the product distribution. For example, the presence of Pt enhances the concentration of 1,1-DMCP in the products, a compound with a high octane number. At high MCH conversions, the distribution of ring contraction (RC) isomers reaches thermodynamic equilibrium.

- Ring contraction has a positive effect in RON, but little effect on specific volume and a negative effect on MON of the product mixture.

- Small contributions of acid-catalyzed ring opening are observed only temperatures above 573 K.

- Hydrogenolysis of alkylcycloalkanes (alkylcyclopentane and alkylcyclohexane) over Ir/SiO_2 produces a selective ring opening. The dominant ring opening on Ir occurs via a dicarbene intermediate with preferential cleavage of secondary-secondary C-C bonds. At low temperatures (i.e. below 533 K) the RO products are mostly formed by opening of C_5-member ring molecules via dicarbene interemediates. At higher temperatures, C_6-member ring molecules and cleavage of substituted C-C bonds become important, generating molecules of lower octane number.

- A proposed approach to simultaneously maximize RON, MON and specific volume of feeds containing naphthenic rings is the sequential use of a bifunctional catalyst (Pt/HY), that produces RC, followed by a metallic catalyst (Ir/SiO_2) that produces the RO by opening of C_5-member ring molecules

Acknowledgments

We would like to acknowledge Oklahoma Center for Advancement of Science and Technology (OCAST) and ConocoPhillips for financial support of the ConocoPhillips Catalysis Lab at the University of Oklahoma.

CHAPTER VI

HYDROISOMERIZATION OF METHYLCYCLOHEXANE ON MFI, BEA, FAU ZEOLITES WITH AND WITHOUT Pt METAL

The activity of acidic and Pt containing zeolite catalysts was investigated in the reaction of MCH at 533-563 K in the presence of hydrogen. The catalysts activity was correlated to their acidity. Skeletal isomerization is a dominant reaction on these catalysts due to a low reaction temperature, high pressure and the high ratio of hydrogen/feed. Skeletal isomerization seems to occur with several parallel and consecutive pathways resulting in different product distribution. Among the RC isomers, monobranched isomer (ECP) seems to occur easier than dibranched isomers (DMCPs) due to the formation of a tertiary carbenium ion. The presence of Pt is found to enhance the RC products to equilibrium, except for the medium pore zeolite support, due to the difficulty of the transportation of bulky RC isomers. In addition, the effect of the shape selectivity is dominant on the formation of the most bulky isomers. Moreover, a series of faujasite zeolites, the CBV series (cbv400 and cbv720), and Pt supported zeolites were investigated in order to study the effect of acid density. It has been found that acid density seems to be a less important parameter in the product distribution than the acidic strength. The acid density has a strong influence on activity, but it has a minor or no influence on selectivity.

6.1 Introduction

Hydroisomerization of hydrocarbon leads to the improvement of gasoline quality in several characteristics of interest, such as density, boiling point, and octane number. The hydroisomerization of *n*-alkanes (e.g. *n*-heptane) to iso-alkanes has been a subject of interest for years resulting from the octane number aspect. The octane number of multibranched hydrocarbons is higher than that of monobranched or nonbranched hydrocarbons. Therefore, multibranched hydrocarbons are more favored. The hydroisomerization mechanisms of alkanes over acidic catalysts at a low reaction temperature are proposed via both monomolecular and bimolecular mechanisms. For the monomolecular mechanism, the reaction proceeds through a protonated cyclopropane (PCP) intermediate after the formation of a carbenium ion. For bimolecular mechanism, the reaction proceeds through the formation of a bimolecular intermediate between carbenium ion and an alkene, which is formed during the reaction [133].

Recently, the hydroisomerization of alicyclic compounds (e.g., methylcyclohexane) attracts interests of researchers because of high demand for clean fuels [1,84]. The isomerization of alicyclic hydrocarbon compounds at a low reaction temperature occurs through the monomolecular mechanism. The isomerization reaction can proceed over monofunctional or bifunctional catalysts [73,111-114]. A strong acidic zeolite, with or without metal seems to be a potential catalyst for both isomerization of aliphatic [115-117] and alicyclic hydrocarbons

[91,118,119]. On acidic catalysts, the isomerization involves the formation and rearrangement of carbocation and hydride transfer. In addition to these processes, the hydrogenation and dehydrogenation step occurs on bifunctional catalysts.

The composition of the products from skeletal isomerization of hydrocarbon is principally dependent on the shape selectivity and the acidity of catalysts [120] as well as the hydride transfer step [103]. However, the effects of these factors on isomerization are mostly available for alkanes but not naphthenes. As shown in our previous study (Fig. 6.1) [121], in order to obtain high branched alkanes from the reaction of methylcyclohexane (MCH), the skeletal isomerization of MCH to dimethylcyclopentanes (ring contraction products) over bifunctional catalyst (Pt/HY) is highly recommended before breaking the internal C-C bond of the cyclic compounds over the metal catalyst (Ir/SiO_2). Therefore, the advantage of isomerization of naphthenes is attractive for compensating for the decrease in the octane number of gasoline due to the decrease in aromatic content. Moreover, the mixture of RC isomers and RO products increase in the specific volume resulting from their lower density.

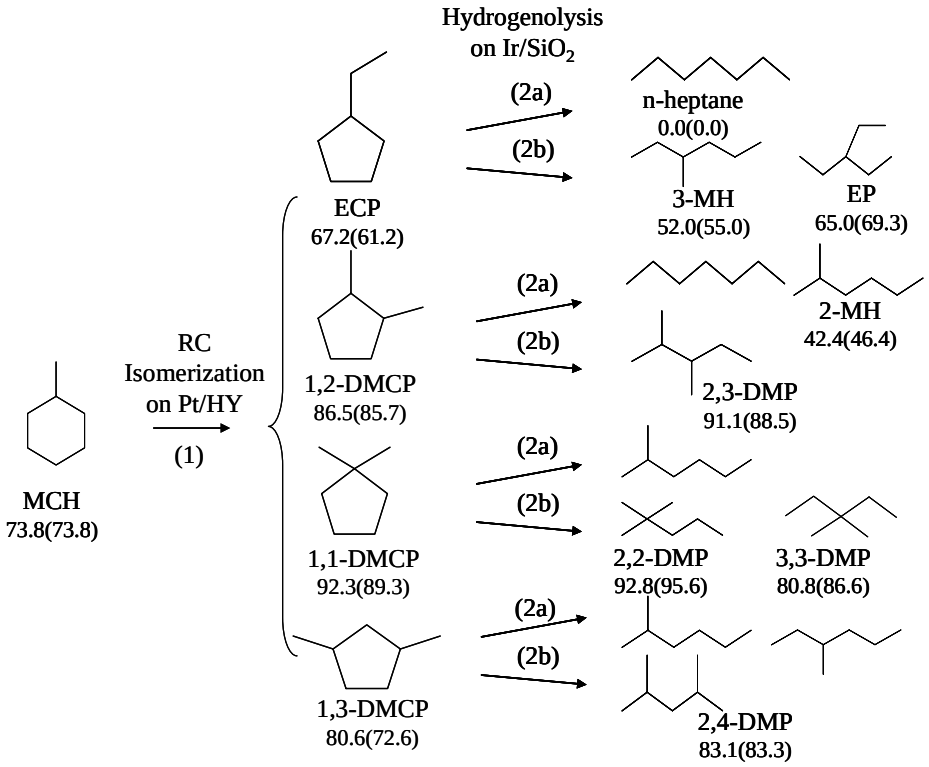

Figure 6.1 A proposed reaction scheme for the hydroconversion of methylcyclohexane and their research (RON) and motor (MON) octane numbers. (2a): the opening C-C bond at substituted C position, and (2b): the opening C-C bond at secondary-secondary C-C bonds.

The isomerization of methylcyclohexane over Pt/HY catalysts was found to be in the equilibrium of C_7 naphthenes (RC) without ring opening and cracking at a low reaction temperature and high pressure [122]. Unlike the Pt/HY catalysts, the product distribution of C_7 isomers (RC) over HY zeolite was not in equilibrium, especially 1,1-dimethylcyclopentane [121]. This behavior was also found on the isomerization of hexane [105,123]. The 2,2-dimethylbutane isomer was not found on $FeO_y/WO_x/ZrO_2$, but it was found on Pt/ $FeO_y/WO_x/ZrO_2$ [108]. This reveals that the hydride transfer plays an important role in the hydrocarbon isomerization. Valyon et al [123] investigated the hydride transfer effect and found that the addition of adamantine, known as a hydride transfer species, increases the isomerization of *n*-heptane over the H-zeolites but not over the Pt containing zeolites.

It is well known that the acidity of catalysts affects the product distribution of the hydroconversion of MCH. The isomerization of MCH to yield dimethylcylopentanes (DMCPs) and ethylcyclopentane (ECP) takes place on different acidic sites (different acidic strength) [124]. The formation of DMCPs is supposed to occur on stronger acid sites than that of ECP due to the ease of the formation of a tertiary carbenium ion of ECP. Unlike the acidic strength, the acid density seems to have a strong effect only on activity and little to no effect on selectivity. However, the shape selectivity appears to have also a strong influence on the product selectivity.

Therefore, in this paper, the catalytic properties in the hydroisomerization of MCH in the presence of hydrogen over acidic and bifuctional zeolite catalysts were

studied in order to elucidate the effect of shape selectivity and the acidic strength of catalysts on the selectivity of RC isomers. MCH was considered a suitable reactant for the catalytic tests, since it comes from the hydrogenation of toluene. Additionally, the effects of acid density are investigated. To emphasize this effect, we chose the same type of zeolite (CBV series) but varied the Si/Al ratios to study.

6.2 Experimental

Commercially available a NaY (Si/Al=5.3), H-MFI (Si/Al = 90), and H-BEA (Si/Al = 2.5-50) obtained from UOP as well as the CBV faujasite zeolites (CBV400, Si/Al = 2.5; CBV720, Si/Al = 30) obtained from Zeolyst International were used as the catalyst and the support materials. The NaY zeolite was transformed to proton form zeolite (H-FAU) by an ion-exchange with ammonium chloride solution. The detail of this procedure was described in Section 2.1.1. In addition to the proton form zeolites, Pt-containing catalysts were prepared by incipient wetness impregnation of the proton form zeolites (FAU, BEA, MFI, CBV400, and CBV720 zeolites) with a 1.0 wt% Pt as described in Section 2.1.2.

Fresh samples were characterized the acidity and the dispersion of metal in term of CO/M, followed by temperature programmed desorption (TPD) of ammonia and CO chemisorption, respectively, according to Section 2.2.

6.3 Results and Discussion

6.3.1 Characterization of Catalysts

Table 6.1 summerizes the characterization of catalysts investigated, including the density of acid sites, which was determined from the integration of the NH3 TPD and the CO uptake (determined from the sequential pulse of CO chemisorption in a dynamic adsorption method and from the standard volumetric method). A clear trend was observed for the acidity of different proton form zeolites, which results from a different Si/Al ratio as follows: BEA > FAU > MFI. As previously observed [74], the impregnation of FAU zeolites with Pt results in a loss of acid sites resulting from the interactions between platinum crystallites and acid sites.

The CO uptakes of the Pt-containing zeolites are also shown in Table 6.1. The CO/Pt ratios obtained from the dynamic adsorption method are in the order of Pt/BEA, Pt/FAU, and Pt/MFI. The measurements carried out under a static condition were relatively low. This suggests that most of the metal sites present a weak interaction with the adsorbate.

Table 6.1 Characterization of fresh catalysts

Sample	H/M experiment		Total acidity
	CO/Pt[a]	CO/Pt[b]	Amount of desorbed NH_3 ($\mu mol/g_{cat}$)
MFI	-	-	680
BEA	-	-	1617
HY	-	-	1109
Pt/MFI	0.2	0.4	630
Pt/BEA	0.2	0.7	1021
Pt/HY	0.4	0.6	795

[a] CO/Pt determined from the standard volumetric method

[b] CO/Pt determined from the dynamic adsorption method

The profiles of temperature-programmed desorption of adsorbed ammonia over various fresh catalysts are shown in Fig. 6.2. Different desorption peaks were observed on the TPD profiles at different temperature ranges. Peaks shown at low and high temperatures can be attributed to ammonia desorbed from weak and strong acid sites, respectively [125-129]. The desorption peak at 470 K represents the very weak acid sites, which are due to an octahedral Al ion formed by dealumination [127]. The desorption peak at about 650 K represents the acid site formed by Al in the zeolite lattice structure. In addition, the peak found at a higher temperature of about 800 K is assigned to strong acid sites, which result from the interaction between Al ions in framework and octahedral Al ions [130,131]. Each

temperature at the peak maximum corresponds to zeolite types, which depend on structure, and the peak area corresponds to the Si/Al molar ratio. The acid strength of zeolites is ordered, MOR > MFI > BEA > FAU, and the strength of acidity is independent of the number of acid density [131]. Among proton form zeolites, the acid strengths are in the order of MFI, BEA and FAU zeolites, while the number of acid sites is in the order of BEA, FAU and MFI zeolites corresponding with the Si/Al molar ratios of each zeolite. These results are in agreement with the total acidity (Table 6.1). In addition, the TPD profiles of ammonia for Pt-containing catalysts gave the same order as proton form zeolites, which mean the impregnation of metal does not change the properties of the parent zeolites.

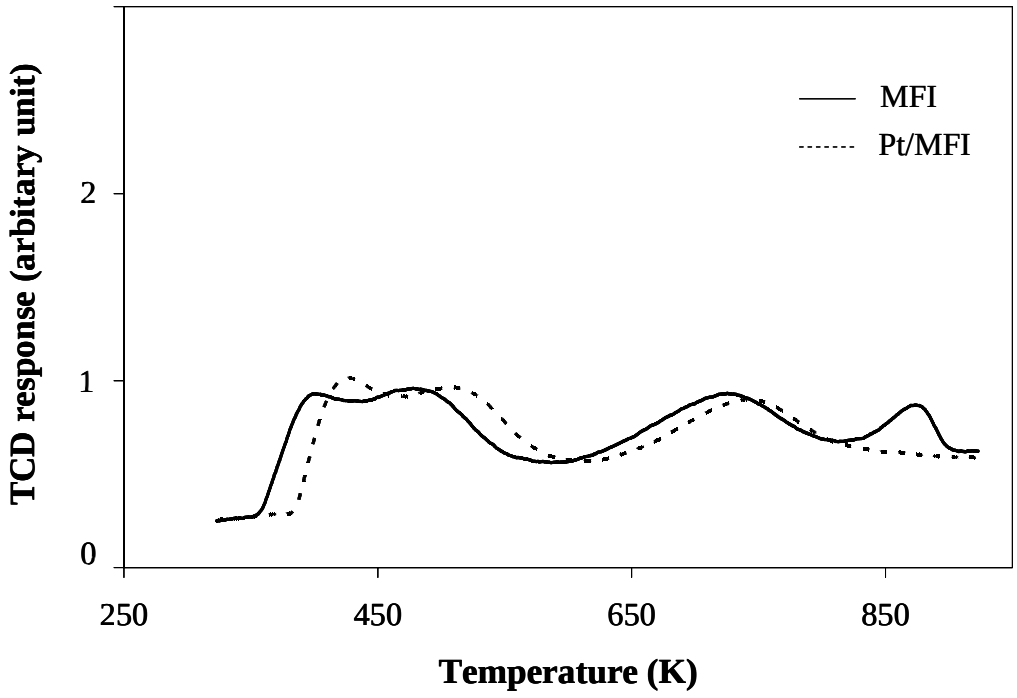

Figure 6.2a TPD profiles of ammonia for MFI and Pt/MFI catalysts.

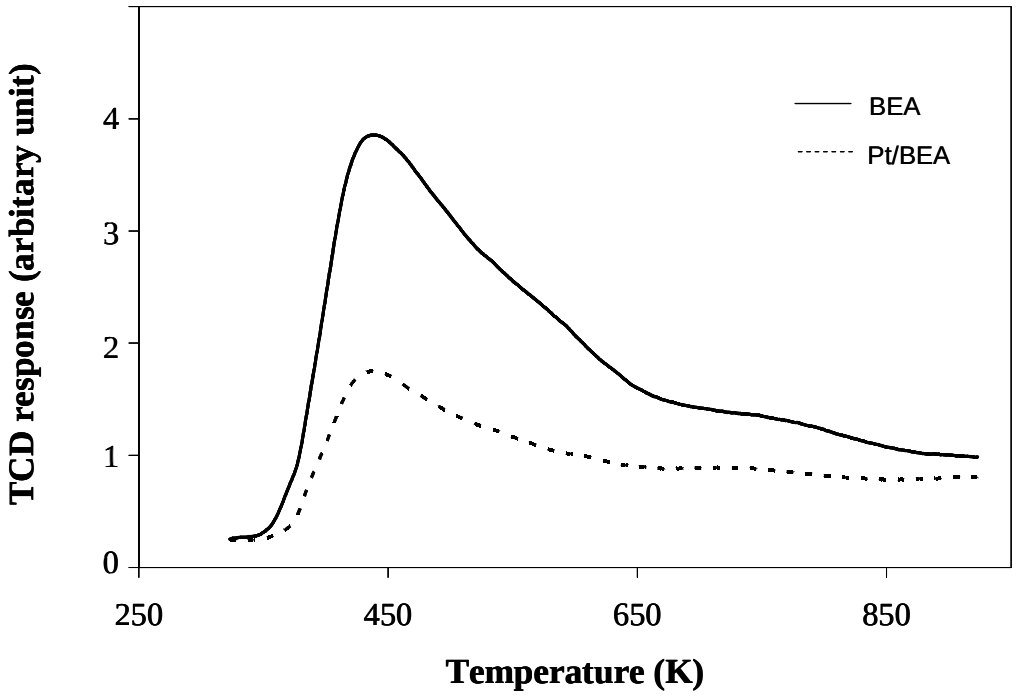

Figure 6.2b TPD profiles of ammonia for BEA and Pt/BEA catalysts.

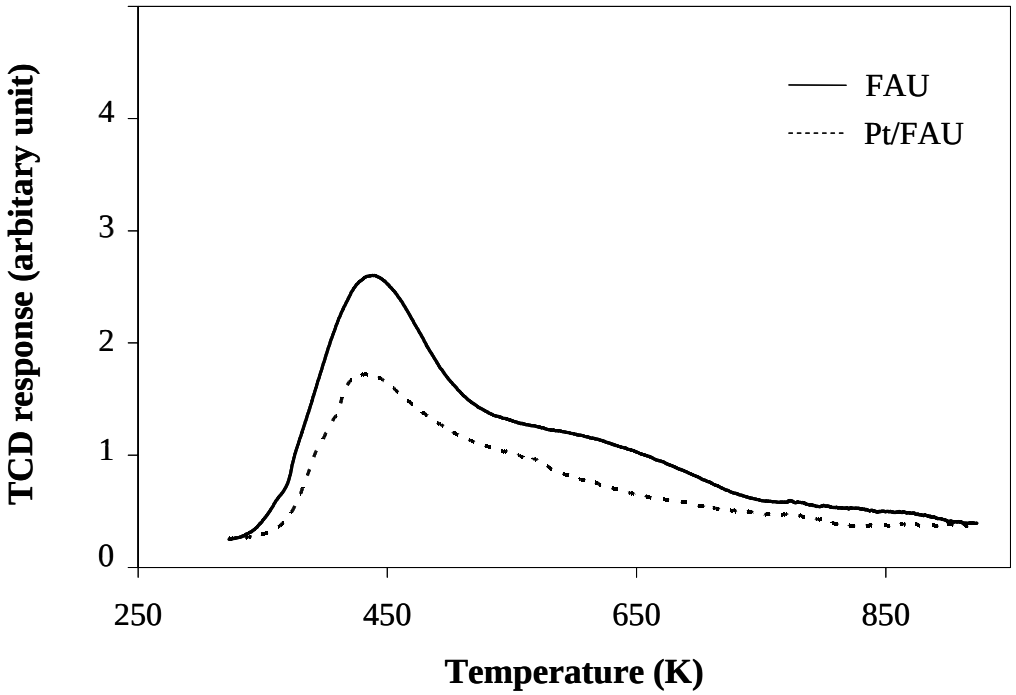

Figure 6.2c TPD profiles of ammonia for FAU and Pt/FAU catalysts.

6.3.2. Catalytic Activity Measurements

The reaction of MCH led to a mixture of products derived from isomerization and ring opening reactions with a trace dehydrogenation reaction. In order to evaluate the products, they were classified into 4 families. The first is monobranched (ethylcyclopentane; ECP) and dibranched (dimethylcyclopentanes; DMCPs) cycloalkanes, denoted as ring-contraction products (RC). The second is monobranched (e.g. *n*-heptane) and multibranched (e.g. 2,4-dimethylpentane) alkanes with 7 carbon atoms in a molecule, noted as ring opening products (RO). The third is known as cracking products (CR) and is both aliphatic and alicyclic compounds with less than 7 carbon atoms in a molecule. The last is dehydrogenation products, which are called heavy products (DH). However, these groups (CR, RO, and HP) were found in only a trace amount due to the mild reaction conditions (i.e. high pressure and low temperature) and the high molar ratio of H_2/feed.

6.3.2.1 Influence of the Acidic Strength and Pore Structure of Zeolites on the MCH Reaction.

The total MCH conversion at the same space time (W/F ratio) was used as the comparison of the activity of different proton form zeolites (Table 6.2). The catalytic activity decreases in the following order: BEA > FAU >> MFI. This follows the trend of decreasing the acid density, which was determined by TPD of NH_3. To illustrate the effect of the deactivation on the catalytic activity of the

MCH reaction, the product distributions obtained after 1 and 4 h on stream are reported in Table 6.2. It can be seen that for all zeolites, the MCH conversion decreases, while time on stream increases. The FAU and BEA zeolites showed a higher deactivation than the MFI zeolite. This can be seen by the huge decrease of selectivity to CR after 1 and 4 h (51.9% to 36.6% for BEA zeolite and 26.3% to 7.0% for FAU zeolite). However, the low MCH conversion was found on MFI zeolite may be due to a fast deactivation from coke deposited inside the narrow channels and pores. Câmara et al. [134] showed the importance of the pore structure of three different zeolites (BEA, FAU and MFI) in the deactivation process by developing a three-dimension model to the coke formation. They found the complete blockage of the structure of large pore sizes is more difficult to occur than that of small pore sizes.

Table 6.2 The catalytic conversion of MCH over various zeolites for TOS of 1 and 4 h. Reaction conditions: Total pressure = 2 MPa; Temperature = 533 K; H_2/MCH molar ratio = 40

Catalyst		**MFI**		**BEA**		**FAU**	
Time on stream (h)		1	4	1	4	1	4
Total conversion (%)		7.8	5.1	71.5	58.5	51.3	34.1
RC/RO ratio		30.1	18.5	3.3	4.5	10.4	31.3
MCH (wt%)		92.2	94.9	28.5	41.5	48.7	65.9
Products		Selectivity to (%)					
Cracking Products		41.6	32.7	51.9	36.6	26.3	7.0
RC products	(RON)	Selectivity to (%)					
1,1-DMCP	(92.3)	1.9	2.4	4.0	3.4	2.6	1.4
Cis -1,3-DMCP	(79.2)	18.0	20.5	10.8	16.8	16.7	24.4
Trans -1,3-DMCP	(80.6)	12.8	13.9	10.6	15.3	16.2	23.1
Trans -1,2-DMCP	(86.5)	11.4	11.2	7.2	5.8	20.7	25.9
ECP	(67.2)	12.5	15.7	3.6	5.7	10.0	15.3
RO products		Selectivity to (%)					
2,2,3-TMB	(100.0)	-	-	-	-	-	-
3,3-DMP	(80.8)	-	-	-	-	-	-
2,2-DMP	(92.8)	-	-	-	-	-	-
2,4-DMP	(83.1)	1.9	2.1	10.5	9.8	5.6	2.6
2,3-DMP	(91.1)	-	-	-	-	0.2	-
n -heptane	(0.0)	-	-	-	-	-	-
2-MH	(42.4)	-	1.3	0.6	0.6	0.6	0.2
3-MH	(52.0)	-	-	-	-	-	-
3-EP	(65.0)	-	-	-	-	-	-
Heavy products		-	-	0.9	6.0	1.0	-

As discussed in the previous paper [121], the product distribution as a function of the MCH conversion over HY zeolite reveals that RC products are formed as the primary products. RO and CR products are consecutive to the formation of RC products. Clearly, they are secondary products of the reaction. At this point, it is interesting to evaluate the effect of the strength of acid sites and the pore structure on the secondary reaction. Fig. 6.3 represents the ratio of RO and CR products to RC products ((RO+CR)/RC) at the MCH conversion of ~3%. These ratios decrease in the following order: MFI > BEA > FAU. This corresponds to the acid strength, pore size and geometry of zeolites. That is, the stronger the acid strength, the higher the RO and CR products. This ratio is more pronounced on MFI due to the high restricted structure of the narrow channel intersections [132]. On the large pore zeolites (BEA and FAU), the ease of the product diffusion suppresses secondary reactions. Lacombe et al. [135] studied the cracking reaction of *n*-heptane and methylcyclohexane on different zeolites (e.g. NU-88, Beta, EU-1, ZSM-5, and ZSM-22). They found that the cracking products appear in parallel with isomers on zeolites (i.e., EU-1) with a high restricted structure, while the cracking products are secondary products on the large pore zeolites (i.e., Beta).

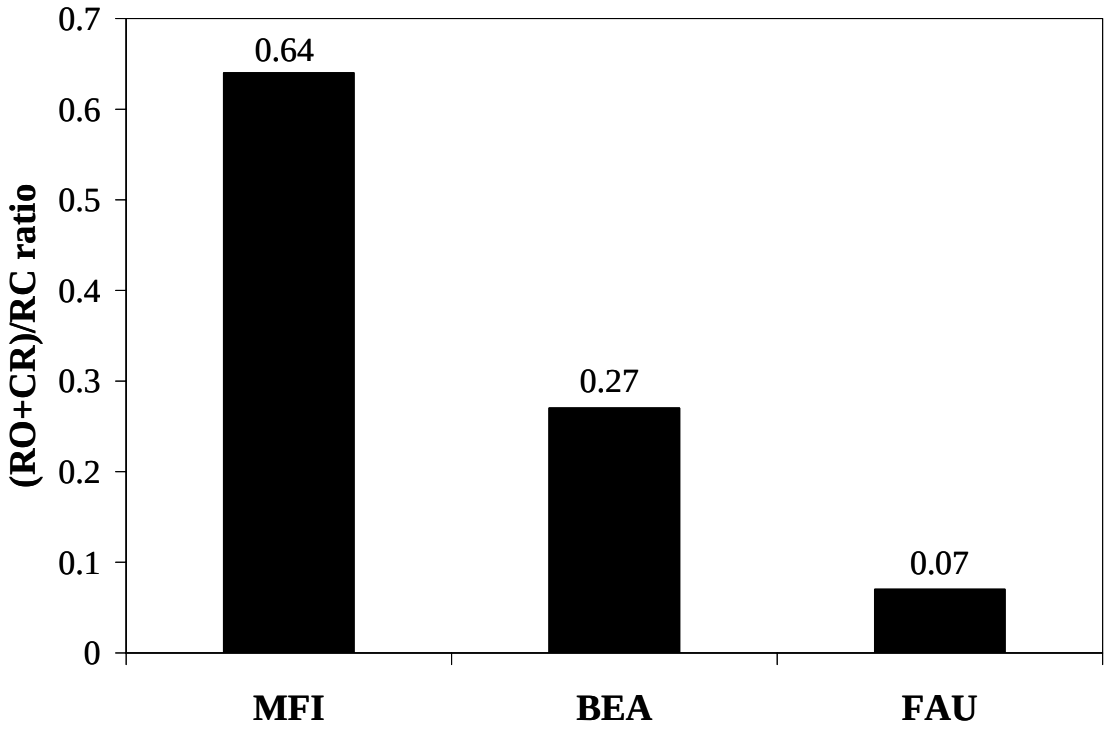

Figure 6.3 The ratio of CR and RO products to RC products on various zeolites (~3% conversion). Reaction conditions: Total pressure = 2 MPa; Temperature = 533 K; H_2/MCH molar ratio = 40.

The strength of acid sites, pore size and pore structure of zeolites are important parameters for product distribution. Thus, it is interesting to investigate the effect of these parameters on the RC isomers, which are the major products at these reaction conditions. The RC isomers found on this study contain *cis*-1,3-dimethylcyclopentane, *trans*-1,3-dimethylcyclopentanes, *trans*-1,2-dimethylcyclopentane, 1,1-dimethylcyclopentane, and ethylcyclopentane, except *cis*-1,2-dimethylcyclopentane. As we discussed in the previous paper [121] the highest yield of RC isomers on the Pt/HY catalyst is at the equilibrium concentration and at this concentration, the amount of *cis*-1,2-dimethylcyclopentane is the lowest. In addition, the formation of *cis*-1,2-dimethylcyclopentane is the most steric hindrance due to the two methyl groups at the same site.

The selectivities to the individual RC isomers as a function of the MCH conversion were plotted in Figs 6.4a (for MFI), 6.4b (for BEA), and 6.4c (for FAU). For strong acid strength zeolites (MFI and BEA), the selectivity to 1,3-dimethylcyclopentane isomers (*cis*-1,3-DMCP and *trans*-1,3-DMCP) are high, and the selectivity to *trans*-1,2-dimethylcyclopentane (*trans*-1,2-DMCP) are low at all conversion ranges. Unlike these zeolites, the selectivity to 1,3-DMCP isomers is high at low conversions and then it decreases with the conversions. Opposite to 1,3-DMCP, the selectivity to *trans*-1,2-DMCP increases toward the conversions. In addition, the selectivity to ECP on FAU zeolite (~ 25%) is very high at low conversions and this value is higher than that on both MFI and BEA (~ 14%). However, the sharp decrease in the selectivity to ECP (from ~25% to ~13%) was

found over FAU zeolite. This showed that the ECP is preceded via the formation of a protonated cyclopropane intermediate. An interesting point is that these three zeolites give the lowest selectivity toward 1,1-dimethylcyclopentane (1,1-DMCP) over all conversion ranges. This difference in selectivity to the individual RC isomers on these three zeolites can be assigned to the difference in the acidic strength and pore geometry of zeolites as well as the residence time of the intermediates.

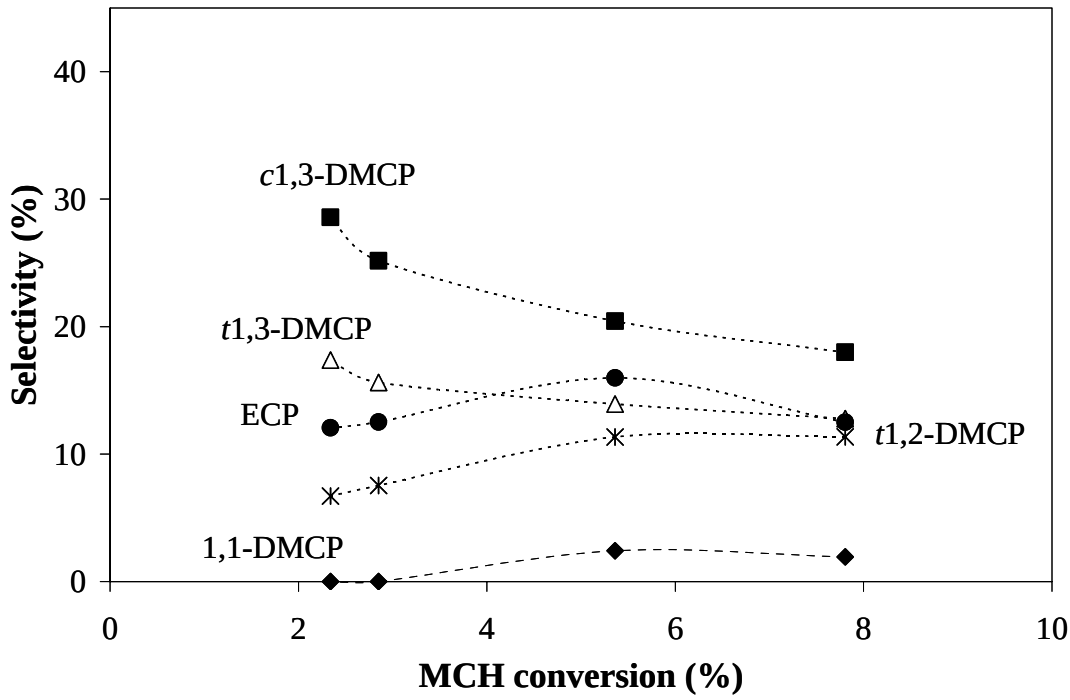

Figure 6.4a Selectivity to RC products vs. MCH conversion over MFI zeolite at different space velocities. Reaction conditions: Total pressure = 2 MPa; Temperature = 533 K; H_2/MCH molar ratio = 40.

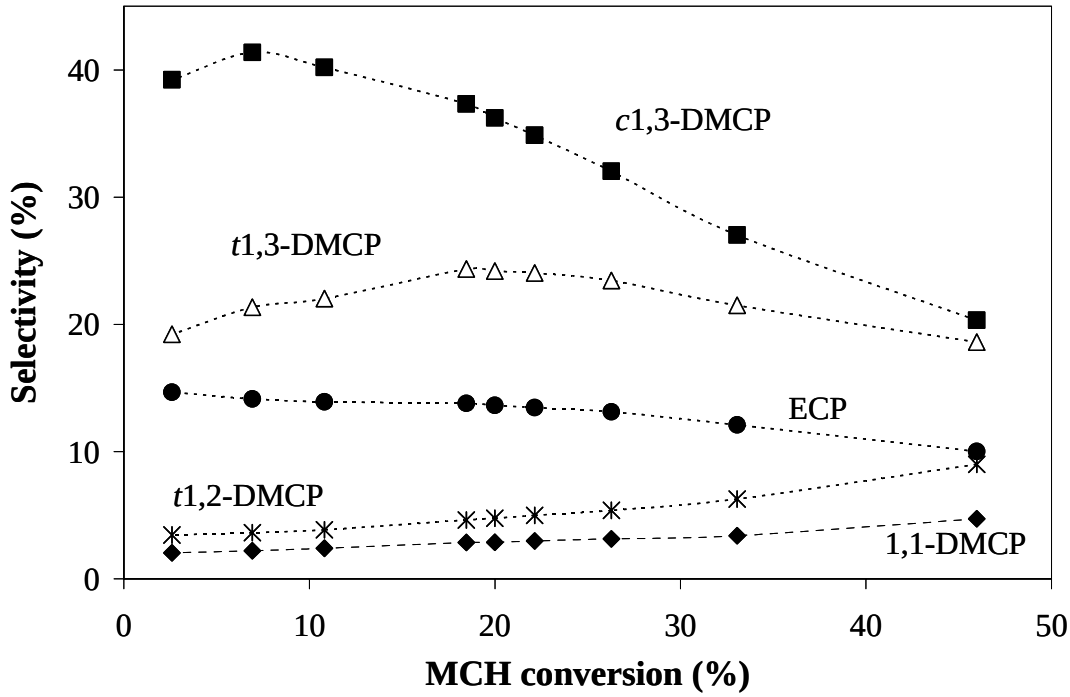

Figure 6.4b Selectivity to RC products vs. MCH conversion over BEA zeolite at different space velocities. Reaction conditions: Total pressure = 2 MPa; Temperature = 533 K; H_2/MCH molar ratio = 40.

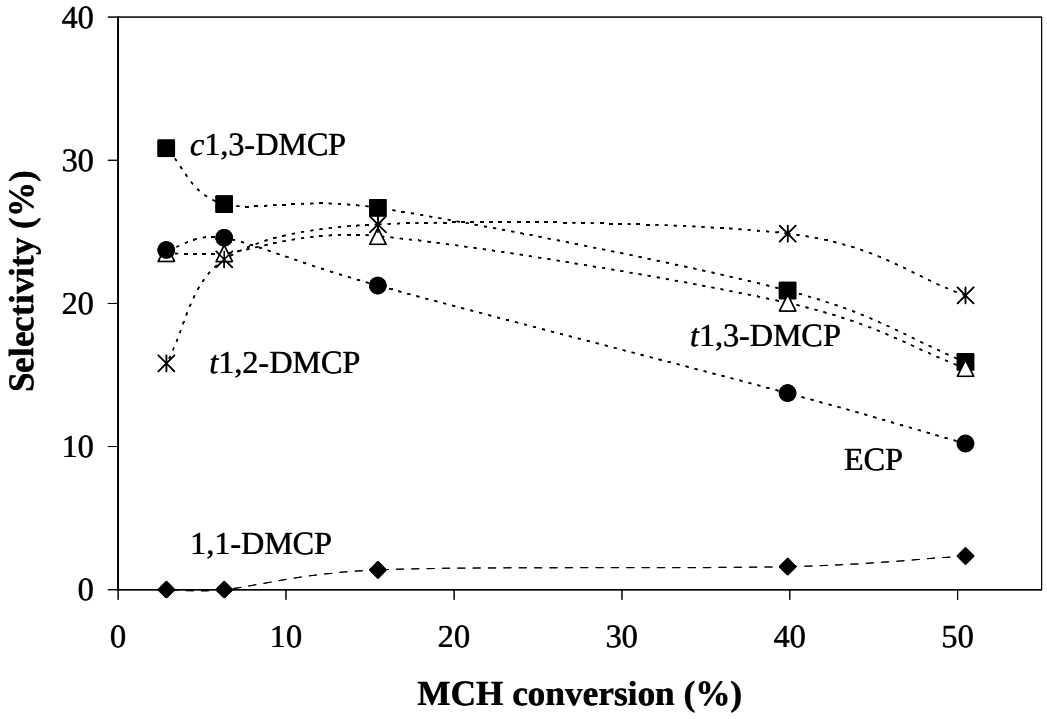

Figure 6.4c Selectivity to RC products vs. MCH conversion FAU zeolite at different space velocities. Reaction conditions: Total pressure = 2 MPa; Temperature = 533 K; H_2/MCH molar ratio = 40.

The acid-catalyzed branching isomerization of naphthenic hydrocarbon compounds on solid acid is generally rationalized by the formation of protonated cyclopropane intermediates after the formation of a carbenium ion [136] and each branching isomer (RC) requires the formation of carbocation at different positions as shown in Fig. 6.5. The monobranched ECP is formed via the rearrangement of a tertiary transition state (intermediate A), which is the most stable transition state, involving the internal alkyl shifts, in which the three C-atoms of the cycloproponium intermediates are involved [82]. High yield of ECP (high selectivity) is due to the easiest formation of this type of an intermediate on the weak acid sites. In addition, the shortening of the residence time will even increase the formation of ECP, resulting in high selectivity to ECP at low conversions (small reactor sizes). Unlike ECP, the dibranched DMCPs are preceded via corner-protonated cyclopropane (CPCP) intermediates (B,C, and D) [82], which have a less stable transition state and require a strong Brönsted acid site (B) [124]. These types of intermediates are least favored. Therefore, the formation of ECP is faster than the formation of DMCPs, and ECP can be produced on the weaker acid sites. In other words, the formation of DMCPs needs stronger acid sites or a longer surface residence time than an ECP, especially 1,3-DMCP isomers [93,124]. As shown from the TPD of ammonia results, the strength of acid sites of the FAU zeolite is weaker than that of MFI and BEA zeolites. These result in a large amount of ECP. Furthermore, it is confirmed by the ratio of DMCPs to ECP as shown in Fig. 6.6.

The DMCP/ECP ratio on the FAU zeolite (3.0) is less than that of the BEA (4.4) and MFI (3.9) zeolites resulting from the relatively weak acid sites of the FAU zeolite.

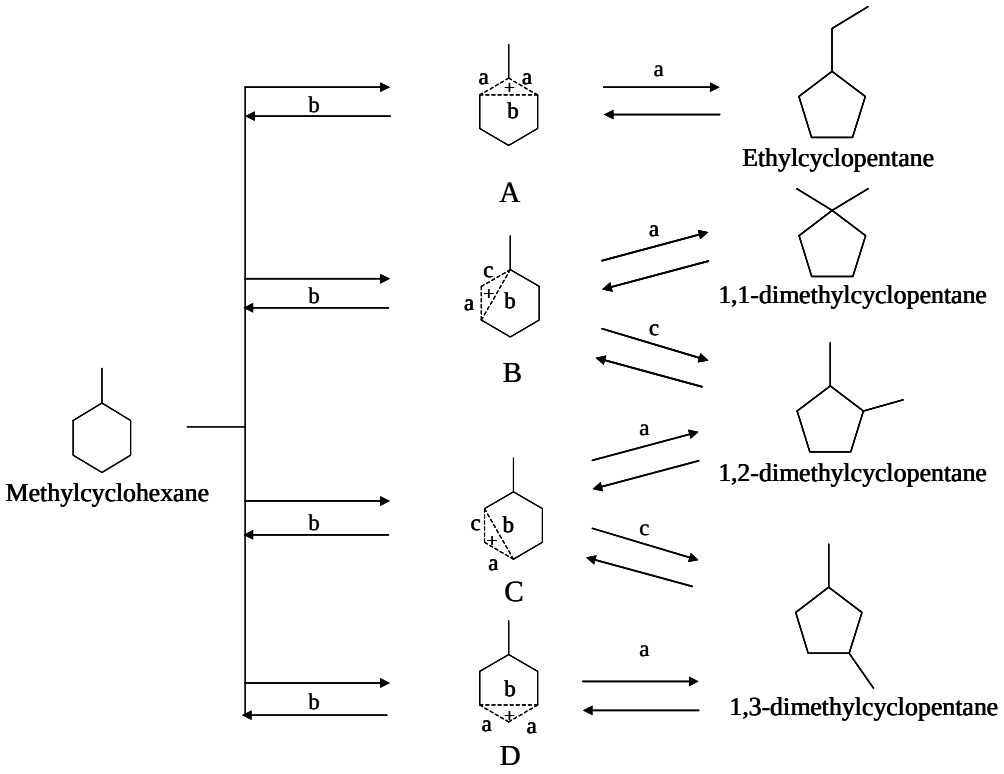

Fig. 6.5 Carbocation chemistry for the ring contraction reactions.

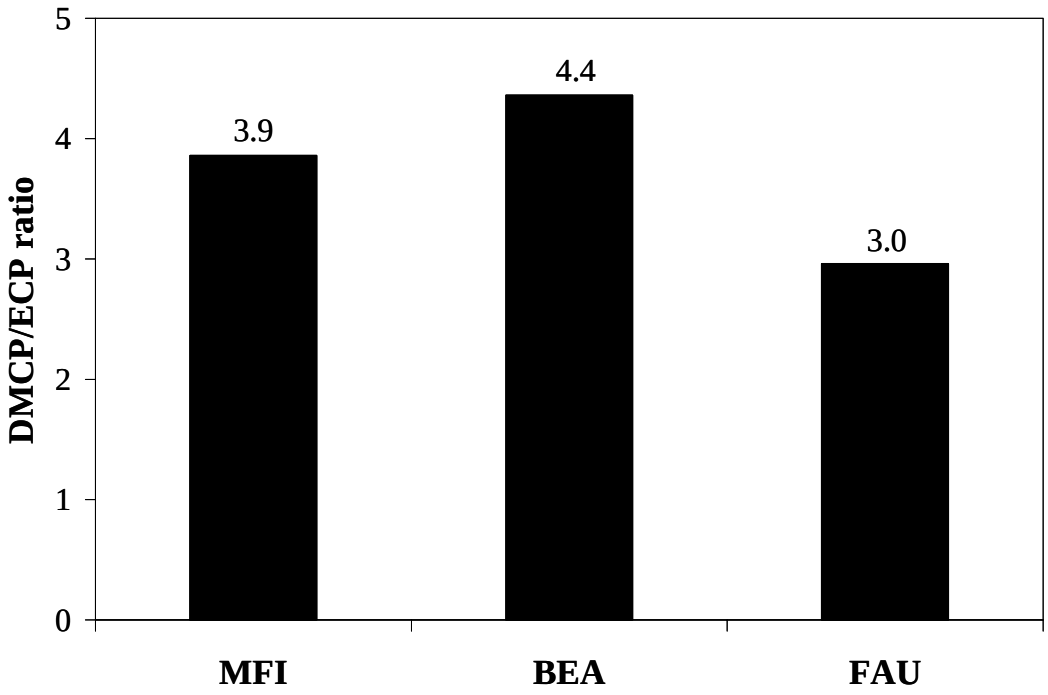

Figure 6.6 The DMCP/ECP ratio over MFI, BEA and FAU zeolites.

As discussed above, an increasing acidic strength of zeolites should enhance the formation of DMCPs. The comparison of selectivity between the most stable intermediate (ECP) and the least stable intermediate (1,3-DMCP) over the large pore zeolites (BEA and FAU) in order to minimize the shape selectivity effect of the medium pore zeolite (MFI) are shown in Fig. 6.4a. It can be seen that the selectivity to 1,3-DMCP is higher on the BEA zeolite than on the FAU zeolite, but the selectivity to ECP is lower on the BEA zeolite than on the FAU zeolite. In addition, a BEA zeolite shows a larger difference between selectivity to 1,3-DMCP and ECP than a FAU zeolite. These results are obviously due to the strong acidic strength of the BEA zeolite. However, when comparing the selectivity of 1,2-DMCP and 1,1-DMCP over BEA and FAU zeolites (Fig. 6.4b), the selectivity to *t*1,2-DMCP on the FAU zeolite is higher than on the BEA zeolite. This suggests that the decrease in the selectivity to *t*1,2-DMCP on the BEA zeolite should be due to the different pore structure of these zeolites. Both the FAU and BEA zeolites are large pore zeolites, but the FAU zeolite contains a supercage. The bulkiest *t*1,2-DMCP exhibits the most difficulty for transport in the channels or pore mouth with a high constraint [127]. In the case of the 1,1-DMCP, both zeolites exhibit low selectivity at all conversion ranges. The formation of both *t*1,2-DMCP and 1,1-DMCP requires the same intermediate (B in Fig. 6.5). This indicates that there should be another effect that plays an important role for this intermediate. A similar situation was found on the isomerization of n-hexane over highly acidic WO_x/ZrO_2-based catalysts by Santiesteban et al. [105]. They found that the 2,2-dimethylbutane isomer was not

formed on this acidic catalyst due to the high kinetic barrier associated with the intermolecular hydride transfer to the sterically-hindered intermediate (i.e., 2,2-dimethyl-3-butyl cation). Therefore, if the same situation occurs on the isomerization of MCH over acid zeolite, it would be due to the suppression of the intermolecular hydride transfer of 2,2-dimethylcyclopent-1-yl cation with an electroneutral molecule [105]. This effect will be explained later.

6.3.2.2 Effect of Metal (Pt) on RC Isomers over Pt/MFI, Pt/BEA and Pt/Y Zeolites

As discussed above, the low amount of 1,1-DMCP found on bare zeolites may be due to the limitation of the hydride/hydrogen transfer. Thus, to elucidate the effect of metal (Pt) on a hydride transfer step, the MCH reaction was performed over the Pt supported on the bare zeolites (MFI, BEA, and FAU) under the same reaction conditions. The Pt loading on zeolites was constant and was at 1 wt% in this study. This value was found to be good enough for the isomerization activity for *n*-heptane [122]. On these Pt catalysts, RC products are the dominant products with a selectivity > 95% at a reaction temperature of 533 K. The selectivity to the individual RC isomers was presented in Figs. 6.7a (for Pt/MFI), 6.7b (for Pt/BEA), and 6.7c (for Pt/FAU). The results obviously showed that the selectivity to the RC isomers over the Pt catalysts (Figs. 6.7a, 6.7b, and 6.7c) differs from the selectivity to the RC isomers over the bare zeolites (Figs. 6.4a, 6.4b, and 6.4c).

These results suggest that Pt metals have an influence on the product distribution of RC isomers. A significant difference was the selectivity to ECP and 1,1-DMCP. High selectivity to ECP was found at a low conversion, and then it decreased as the conversion increased for all Pt catalysts. It can be seen that the selectivity to monobranched isomer (ECP) decreases with conversion, while that to the dibranched isomers (DMCPs) increases. This trend may be explained considering that at low conversions ECP is easily formed via the internal alkyl shifts [82]. The increase in the selectivity to the thermodynamically favored DMCP isomers observed at higher space times may be due to a stepwise isomerization [91,99]. However, this proposed sequence is opposite to the MCH reaction over Pt/H-mordenite [100]. Calemma et al. [37] have shown that both ECP and DMCPs are primary products.

As opposed to ECP, the selectivity to DMCPs increases with conversions, except for high conversions resulting from the secondary reactions. In the case of 1,1-DMCP, it was found in large amounts over Pt supported on large pore zeolites (Pt/BEA and Pt/FAU) but not over Pt supported on medium pore (Pt/MFI) when compared to the corresponding bare zeolites. The production of 1,1-DMCP involves a 2,2-dimethylcyclopent-1-yl cation. With such a bulky intermediate, the hydride transfer from an electroneutral RH molecule is sterically unfavorable and one can expect this step to be slow. As a result, the production of 1,1-DMCP is very low on bare zeolites. This suggests that the Pt metals enhance the isomerization rate and increase the hydride transfer step, except for the medium pore. A similar situation was reported by Santiesteban et al. [105] investigated that the isomerization

of *n*-hexane on highly acidic WO_x/ZrO_2-based catalysts and found that the 2,2-dimethylbutane isomer was not formed in the absence of Pt, but it was produced in significant amounts when Pt was added to the catalyst. They suggested that the presence of Pt gives rise to a high concentration of atomic hydrogen on the surface, enough to overcome the high kinetic barrier associated with the intermolecular hydride transfer to the sterically-hindered intermediate (i.e., 2,2-dimethyl-3-butyl cation). In addition, the presence of Pt seems to accelerate the RC isomers to approach equilibrium [121]. However, the exception was found on the MCH reaction over the Pt/MFI due to the sterical hindered effect

When comparing the selectivity to *t*1,2-DMCP (the bulkiest RC isomer) over MFI (Fig. 6.4a) and Pt/MFI (Fig. 6.7a), the selectivities to these compounds over both catalysts are about the same. The presence of Pt does not enhance the formation of the *t*1,2-DMCP isomer due to a shape selectivity effect of this support (a 10 member-ring medium-pore structure; MFI). Unlike MFI, the selectivity to the *t*1,2-DMCP isomer are different over the Pt containing large pore zeolites (Pt/BEA; Fig. 6.7b and Pt/FAU; Fig. 6.7c) and without Pt (BEA; Fig. 6.4b and FAU; Fig. 6.4c). On the Pt/BEA and Pt/FAU catalysts, the selectivity to *t*1,2-DMCP was the highest, but this value was very low on the BEA zeolite. This confirms that the presence of Pt plays an important role in the hydrogen transfer step.

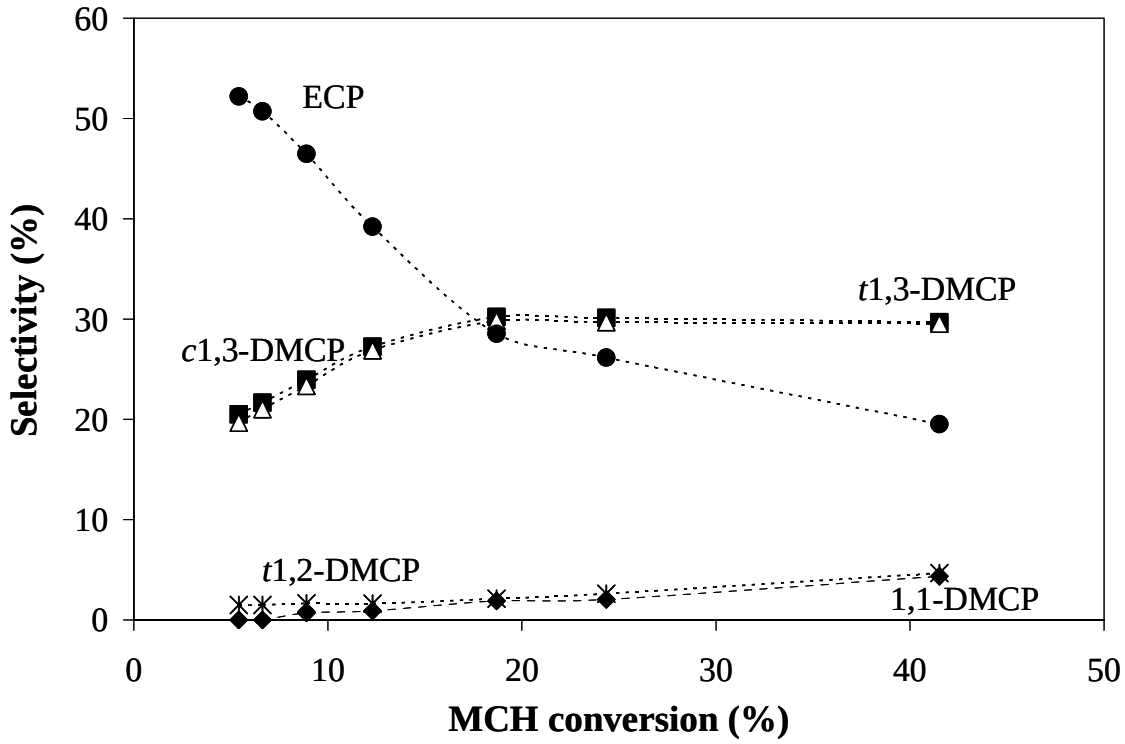

Figure 6.7a Selectivity to RC products vs. MCH conversion over Pt/MFI catalyst at different space velocities. Reaction conditions: Total pressure = 2 MPa; Temperature = 533 K; H_2/MCH molar ratio = 40.

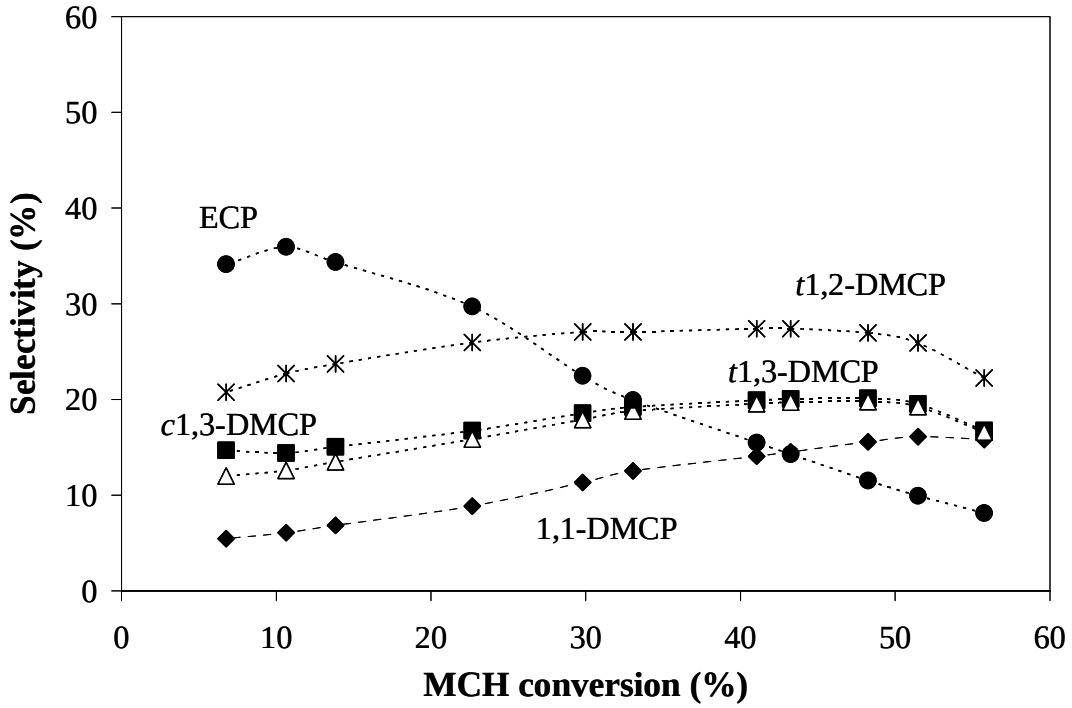

Figure 6.7b Selectivity to RC products vs. MCH conversion over Pt/BEA catalyst at different space velocities. Reaction conditions: Total pressure = 2 MPa; Temperature = 533 K; H_2/MCH molar ratio = 40.

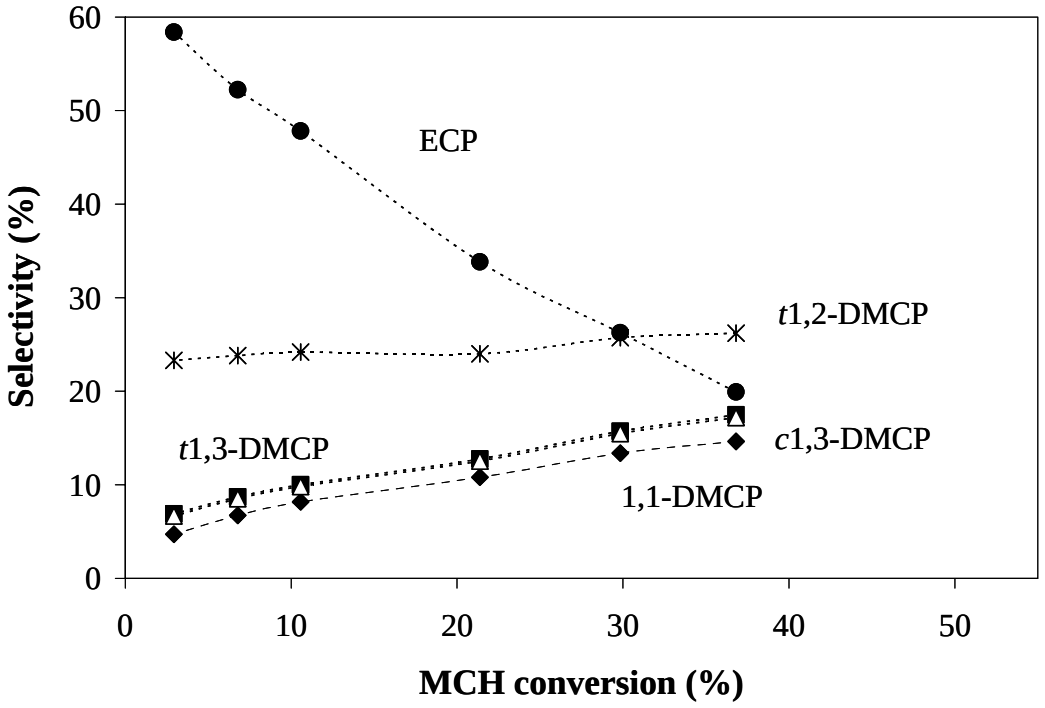

Figure 6.7c Selectivity to RC products vs. MCH conversion over Pt/FAU catalyst at different space velocities. Reaction conditions: Total pressure = 2 MPa; Temperature = 533 K; H_2/MCH molar ratio = 40.

As discussed above, the enhancement of the formation of ECP, *t*1,2-DMCP, and 1,1-DMCP over the Pt supported catalysts should be due to the enhancement of the hydrogen transfer step, which results in decreasing surface residence time of the intermediates [102-104]. On an acid zeolite, the desorption of an intermediate (alkylcarbenium ions) on the surface to form RC isomers occurs by a bimolecular hydride transfer with the electroneutral molecules, mostly reactant. In this case, the hydride transfer step is slow, and it results in the slow desorption of intermediate transition states. On the Pt catalysts, Pt metals are very active for the hygrogenation/dehydrogenation reaction that would accelerate the desorption rate, which decreases the lifetime for the intermediate. These result in the difference in the distribution of RC isomers. In addition, Santiesteban et al. [105] suggested the new pathways in the hydride transfer reaction step for the isomerization reaction for n-hexane over the Pt catalysts. Pt metals activate hydrogen (H_2) to form a large amount of hydrogen atoms on the surface, and these hydrogen atoms accelerate the hydride transfer rate resulting in decreasing surface residence time. So, 1,1-DMCP is merely found because of a high kinetic barrier of 2,2-dimethylcyclopent-1-yl cation in the bimolecular hydride transfer step with an electroneutral molecule.

To clearly understand the influences on the formation of RC isomers, the selectivities of RC isomers over Pt-supported catalysts were plotted together in Figs. 6.8a and 6.8b. Among the Pt supported catalysts, the selectivity to 1,3-DMCP decreases in the order of Pt/MFI > Pt/BEA > Pt/FAU as following the acidic strength. As explained, the formation of 1,3-DMCP requires a stronger acidic

strength than that of ECP. However, the selectivity to ECP is slightly different due to the ease of its formation and the fast desorption rate of the intermediate. The presence of Pt significantly enhances the formation of 1,1-DMCP, which is the most sterically hindered carbenium ion intermediate, except on Pt/MFI (due to the shape selectivity effect). As stated above, Pt metal provides a large amount of surface hydrogen atoms, which readily undergo the hydride transfer with the carbenium ions. In the case of the formation of 1,2-DMCP, Pt metal increases the desorption rate of the carbenium ion intermediate and the isomerization reaction. However, the formation of *t*1,2-DMCP does not increase on Pt/MFI or MFI alone due to shape selectivity. A *t*1,2-DMCP shows the highest difficulty for the diffusion in channels or on pore mouths of the most restricted structure, due to its bulkiest molecule.

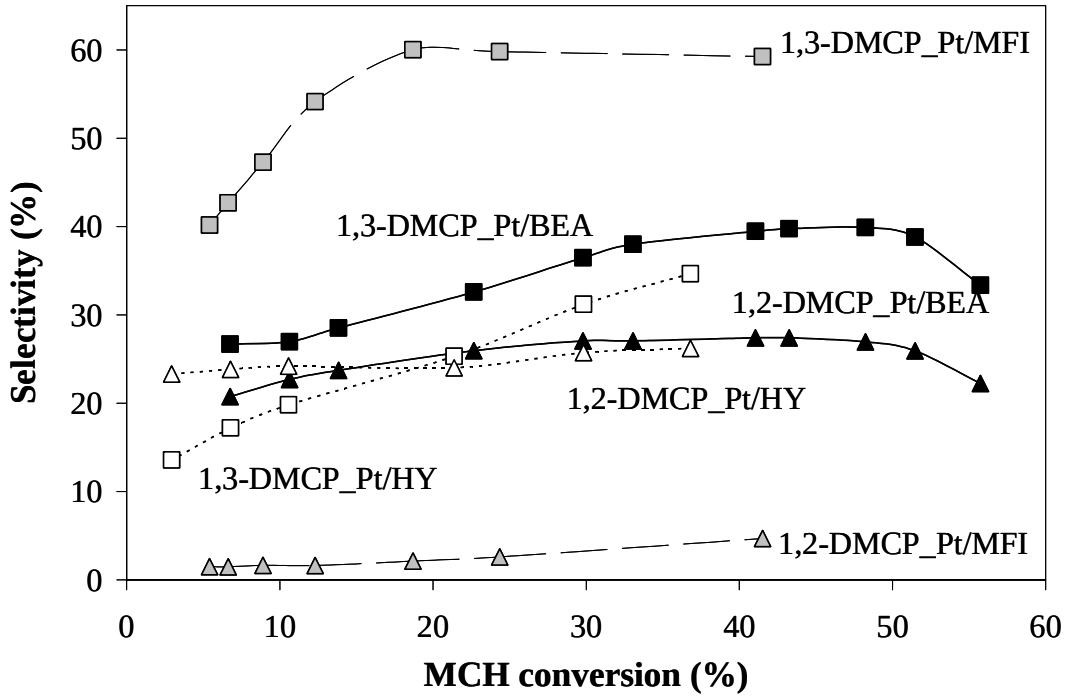

Figure 6.8a Selectivity (%) to RC products (*trans*-1,2-dimethylcyclopentane, *t*1,2-DMCP; 1,3-dimethylcyclopentane, 1,3-DMCP) plotted vs. MCH conversion (%) over Pt/MFI, Pt/BEA, and Pt/FAU catalysts. Reaction conditions: Total pressure = 2 MPa; Temperature = 533 K; H_2/MCH molar ratio = 40.

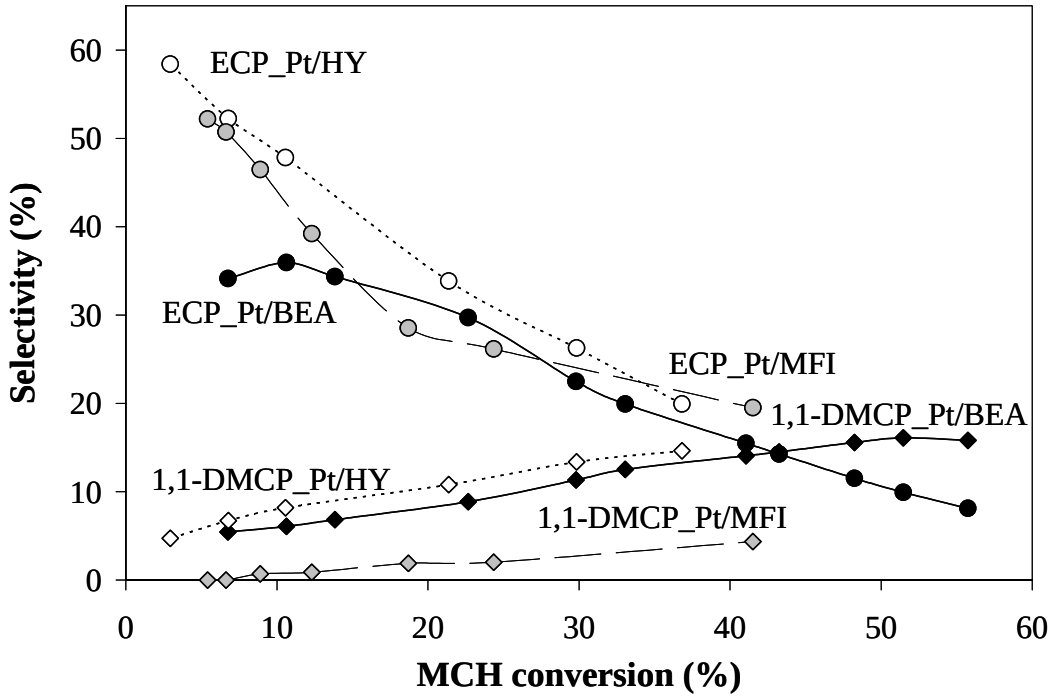

Figure 6.8b Selectivity (%) to RC products (1,1-dimethylcyclopentane, 1,1-DMCP; ethylcyclopentane, ECP) plotted vs. MCH conversion (%) over Pt/MFI, Pt/BEA, and Pt/FAU catalysts. Reaction conditions: Total pressure = 2 MPa; Temperature = 533 K; H_2/MCH molar ratio = 40.

Figs. 6.9a and 6.9b show the ratio of 1,3-DMCP and the sum of 1,1-DMCP and 1,2-DMCP over bare zeolites and Pt supported zeolites. A huge difference was found between zeolites with and without Pt. For large pore zeolites (BEA, FAU, Pt/BEA and Pt/FAU) with a minor or no shape selectivity effect, the 1,3-DMCP/(1,1-DMCP+1,2-DMCP) ratios on Pt catalysts are higher than that on zeolites alone. This result confirms that Pt metal enhances the ability of hydrogen transfer. Opposite to large pore zeolites, this ratio does not decrease but increases on zeolites containing Pt metal, due to the difficulty of the transportation inside the small pores or shape selectivity effect.

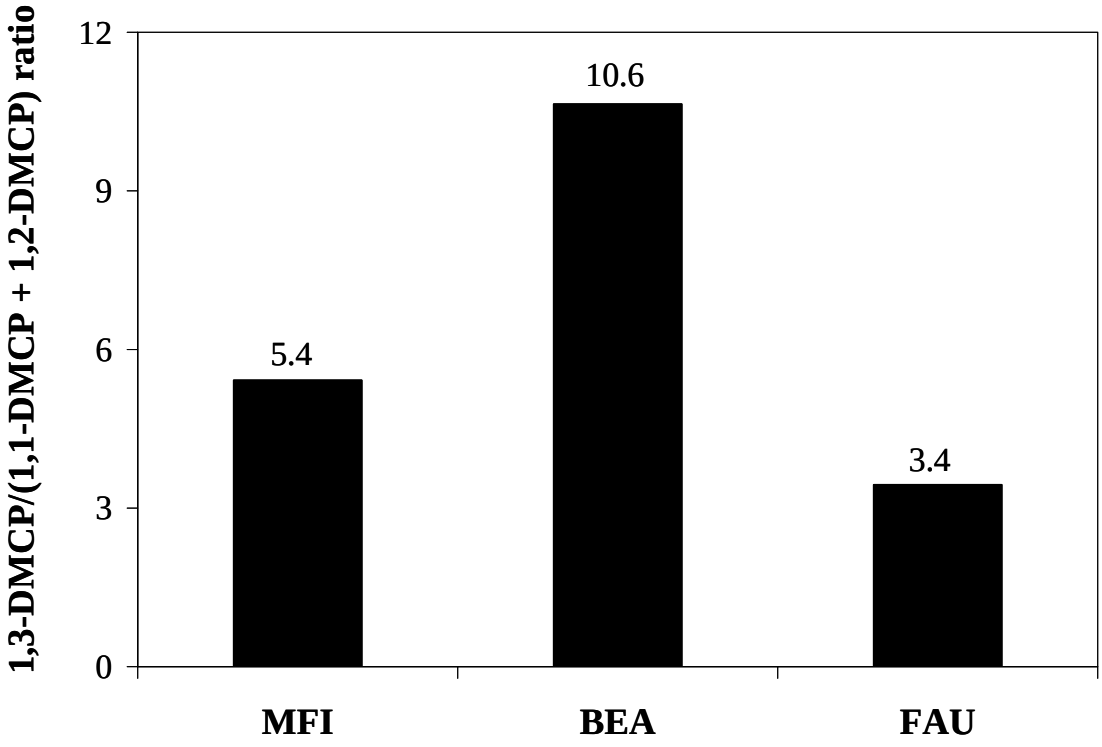

Figure 6.9a The 1,3-DMCP/(1,2-DMCP+1,1-DMCP) ratio over MFI, BEA and Y zeolites at the same conversion (~3%). Reaction conditions: Total pressure = 2 MPa; Temperature = 533 K; H_2/MCH molar ratio = 40.

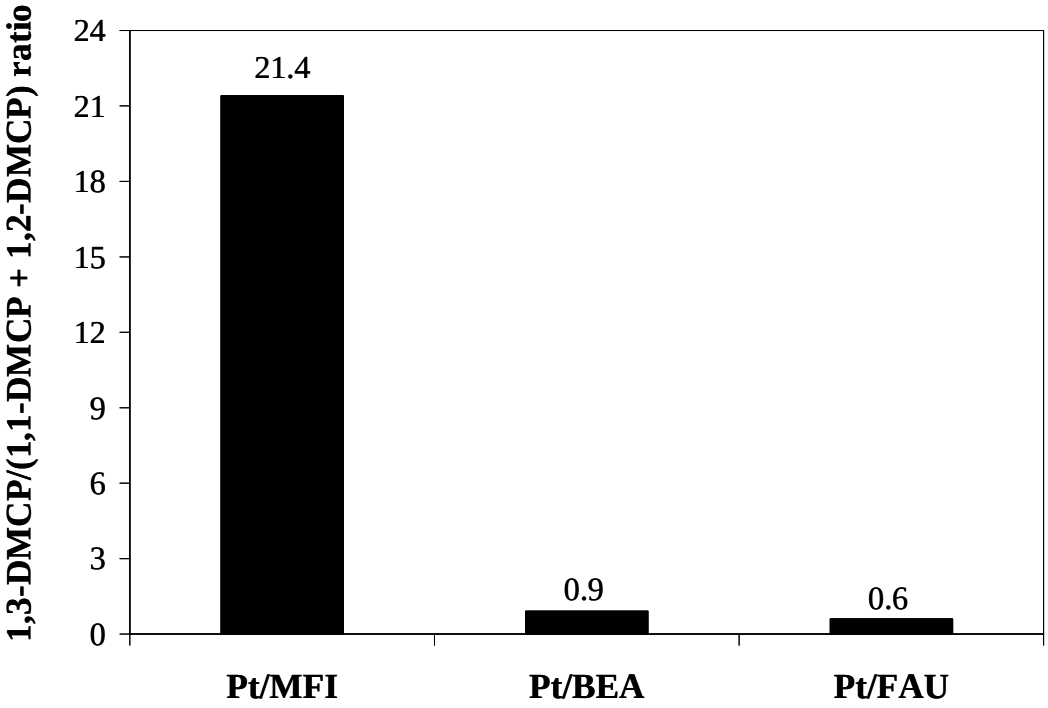

Figure 6.9b The 1,3-DMCP/(1,2-DMCP+1,1-DMCP) ratio over Pt/MFI, Pt/BEA and Pt/FAU catalysts at the same conversion (~13%). Reaction conditions: Total pressure = 2 MPa; Temperature = 533 K; H_2/MCH molar ratio = 40.

An interesting change in the cis/trans 1,3-DMCP ratio was observed in the product between bare zeolites and Pt supported zeolites. In all zeolites, as shown in Figs 6.10a and 6.10b, this ratio was observed to decrease significantly on Pt supported zeolites. This result may be due to both *cis*-to-*trans* isomerization and the enhancement of hydrogen transfer. The formation of *c*1,3DMCP is easier than that of *t*1,3-DMCP, due to its conformation. The methyl groups are both in the equatorial type positions.

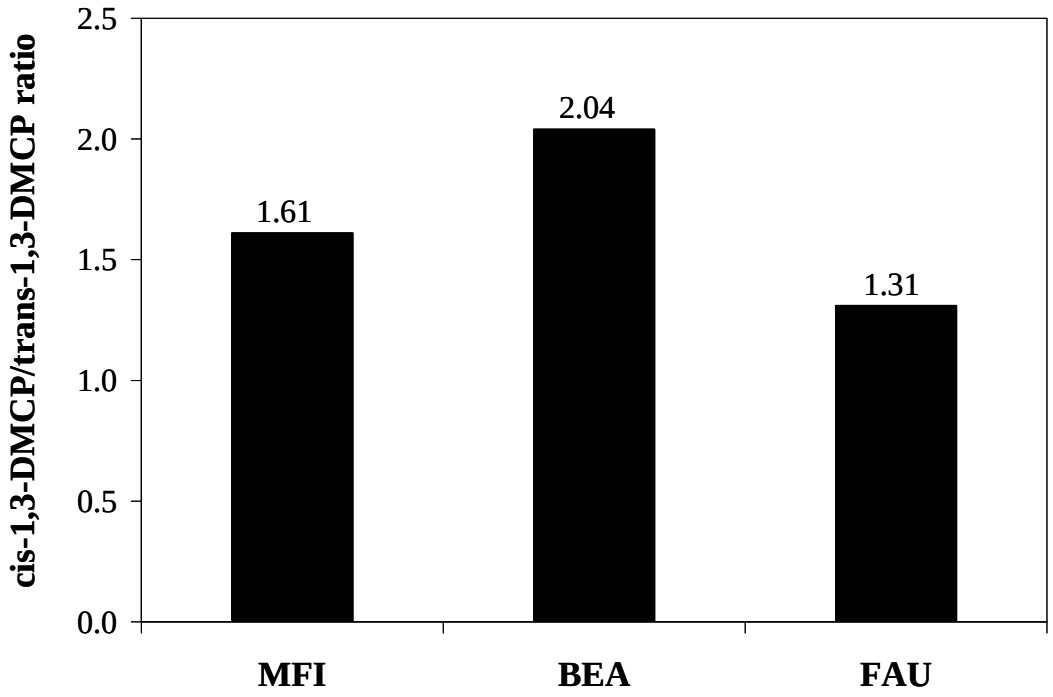

Figure 6.10a The *cis*-1,3-DMCP/*trans*-1,3-DMCP ratio over MFI, BEA and FAU zeolites at the same conversion (~3%). Reaction conditions: Total pressure = 2 MPa; Temperature = 533 K; H_2/MCH molar ratio = 40.

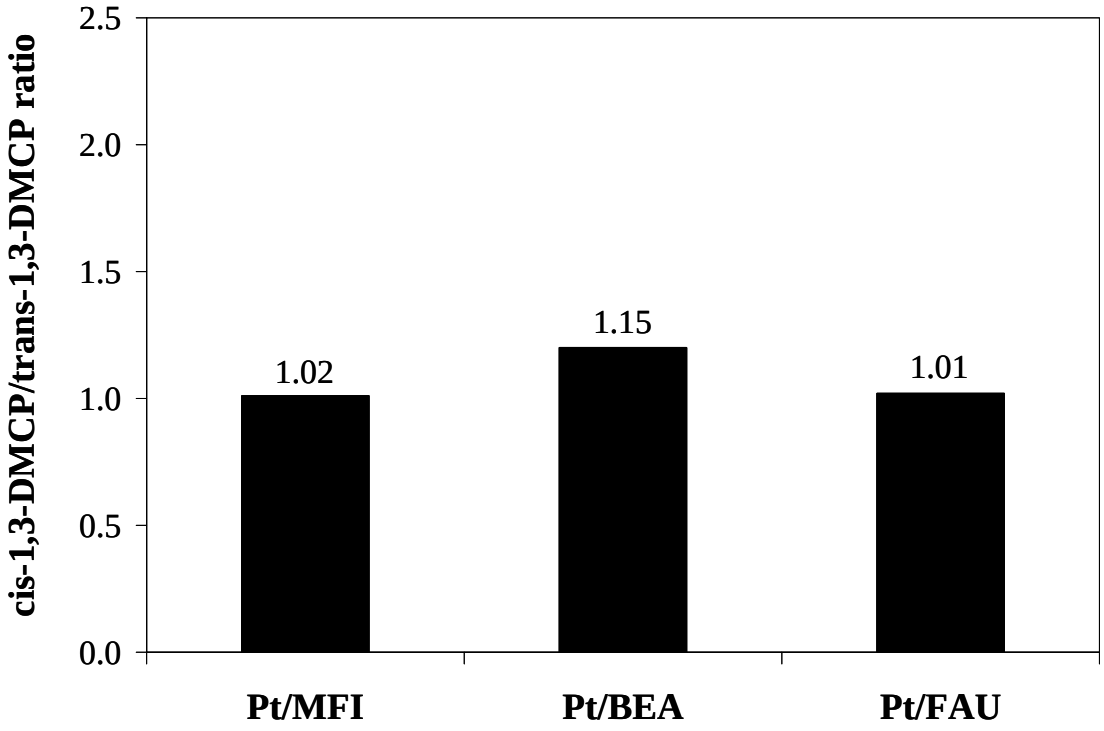

Figure 6.10b The *cis*-1,3-DMCP/*trans*-1,3-DMCP ratio over Pt/MFI, Pt/BEA and Pt/FAU catalysts at the same conversion (~13%). Reaction conditions: Total pressure = 2 MPa; Temperature = 533 K; H_2/MCH molar ratio = 40.

6.3.2.3. Effect of the Reaction Temperature on the RC Isomers

To study the effect of the reaction temperatures, the MCH reactions were performed over the Pt supported catalysts at 533 K and 563 K (Table 6.3). Comparing the product distribution over the Pt-free catalysts (Table 6.2) and the Pt-supported catalysts (Table 6.3) reveals that the major difference is the suppression of the secondary reactions to yield the RO and CR products over the catalysts containing Pt. This implies that Pt metals decrease the surface residence times of intermediates. As shown in Table 6.3, the secondary products increase with the reaction temperatures for all catalysts. Among the Pt containing catalysts, Pt/MFI shows the highest selectivity to cracking products at 533 K, due to its restricted pore structure. However, the cracking products on Pt/BEA greatly increase when the reaction temperature increases, whereas the cracking products on Pt/FAU only slightly increase; instead, the RO products significantly increase. It can be concluded that the RO products tend to undergo cracking faster on Pt/BEA than on Pt/FAU, due to its structure.

Table 6.3 The catalytic conversion of MCH over various catalysts at 533 K and 563 K. Reaction conditions: total pressure = 2 MPa; H_2/feed molar ratio = 40

Catalyst		**Pt/MFI**		**Pt/BEA**		**Pt/FAU**	
Temperature (K)		533	563	533	563	533	563
Total conversion (%)		18.7	41.6	49.9	64.0	31.6	55.4
RC/RO ratio		38.3	16.6	17.9	6.3	74.3	40.6
MCH (wt%)		81.3	58.4	50.1	36.0	68.4	44.6
Products		Selectivity to (%)					
Cracking Products		5.0	6.9	2.5	19.1	1.7	3.3
RC products	(RON)	Selectivity to (%)					
1,1-DMCP	(92.3)	1.9	4.4	15.8	13.8	13.6	15.7
Cis -1,3-DMCP	(79.2)	30.2	29.6	19.8	14.5	16.4	20.5
Trans -1,3-DMCP	(80.6)	29.8	29.5	19.5	14.6	16.1	20.1
Trans -1,2-DMCP	(86.5)	2.1	4.7	26.4	19.0	26.2	27.1
ECP	(67.2)	28.5	19.5	10.7	7.9	24.4	10.9
RO products		Selectivity to (%)					
2,2,3-TMB	(100.0)	-	-	-	0.2	-	-
3,3-DMP	(80.8)	-	-	0.3	0.6	-	0.1
2,2-DMP	(92.8)	-	-	0.5	0.9	-	0.2
2,4-DMP	(83.1)	-	0.7	1.0	2.7	0.4	0.6
2,3-DMP	(91.1)	-	0.2	0.5	1.1	0.0	0.2
n-heptane	(0.0)	1.0	1.7	1.0	2.0	0.4	0.4
2-MH	(42.4)	1.4	2.8	1.9	3.6	0.4	0.8
3-MH	(52.0)	-	-	-	-	-	-
3-EP	(65.0)	-	-	-	-	-	-
Heavy products		-	-	-	0.4	-	-

6.3.2.4 Effect of Acid Density on RC Isomers

Both CBV400 and CBV720 zeolites were used to study the effect of acid density on the MCH reaction. Table 6.4 summerizes the conversion of MCH and product distribution after an hour time on stream. The conversion showed the order CBV400 > CBV720 and Pt/CBV400 > Pt/CBV720, which is the same order of the acid density. The main products are RC isomers. The selectivity to RC isomers for the MCH reaction over Pt free catalysts is shown in Figs. 6.11a and 6.11b. Both catalysts show a slightly different selectivity to RC isomers. This implies that the acid density has merely an effect on isomerization if there are no other effects involved (i.e., shape selectivity). In addition, the selectivity to RC isomers for the MCH reaction on the Pt supported catalysts is presented in Figs 6.12a and 6.12b. There is no change in the selectivity to RC isomers, which suggests that Pt metals enhance isomerization.

Table 6.4 The catalytic conversion of MCH over acidic catalysts and bifunctional catalysts

Catalyst		**CBV400**	**CBV720**	**Pt/CBV400**	**Pt/CBV720**
Conversion (%)		25.3	10.5	36.0	21.7
MCH (wt%)		74.7	89.5	64.0	78.3
Products			Yield (wt%)		
Cracking Products		0.2	0.1	0.3	0.2
RC products	(RON)		Yield (wt%)		
1,1-DMCP	(92.3)	0.4	0.1	5.4	2.5
Cis -1,3-DMCP	(79.2)	6.8	3.1	6.2	2.8
Trans -1,3-DMCP	(80.6)	6.3	2.6	6.1	2.7
Trans -1,2-DMCP	(86.5)	6.3	2.0	9.5	5.3
ECP	(67.2)	5.1	2.7	7.3	7.6
RO products			Yield (wt%)		
2,2,3-TMB	(100.0)	-	-	0.0	0.0
3,3-DMP	(80.8)	-	-	0.1	0.0
2,2-DMP	(92.8)	-	-	0.1	0.0
2,4-DMP	(83.1)	0.1	-	0.3	0.2
2,3-DMP	(91.1)	-	-	0.1	0.0
n -heptane	(0.0)	-	-	0.3	0.1
2-MH	(42.4)	0.2	0.1	0.4	0.3
3-MH	(52.0)	-	-	0.0	0.0
3-EP	(65.0)	-	-	0.0	0.0

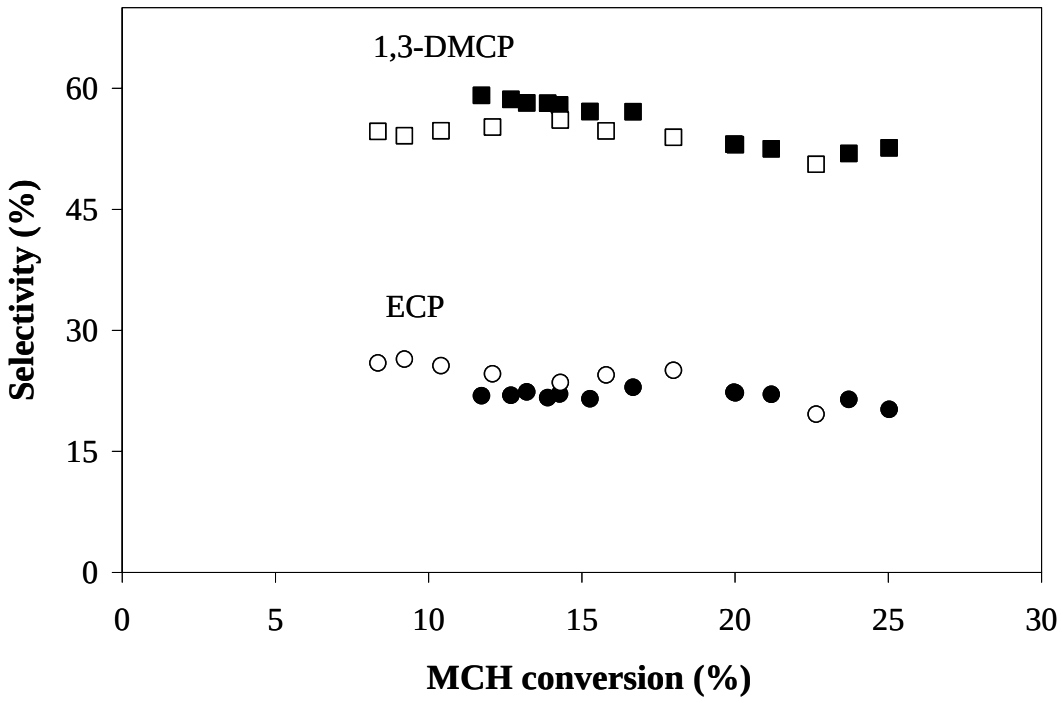

Figure 6.11a Selectivity (%) to RC products (ethylcyclopentane,ECP; 1,3-dimethylcyclopentane, 1,3-DMCP) plotted vs. MCH conversion (%) over CBV400 (solid) and CBV720 (open).

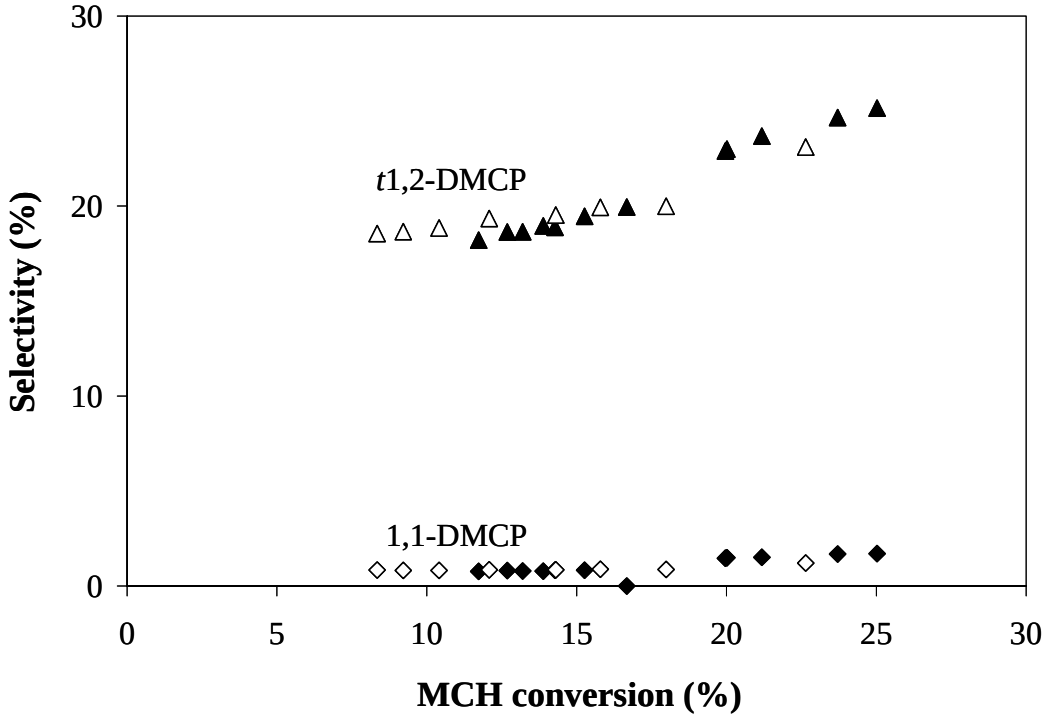

Figure 6.11b Selectivity (%) to RC products (1,1-dimethylcyclopentane, 1,1-DMCP; *trans*-1,2-dimethylcyclopentane, *t*1,2-DMCP) plotted vs. MCH conversion (%) over CBV400 (solid) and CBV720 (open).

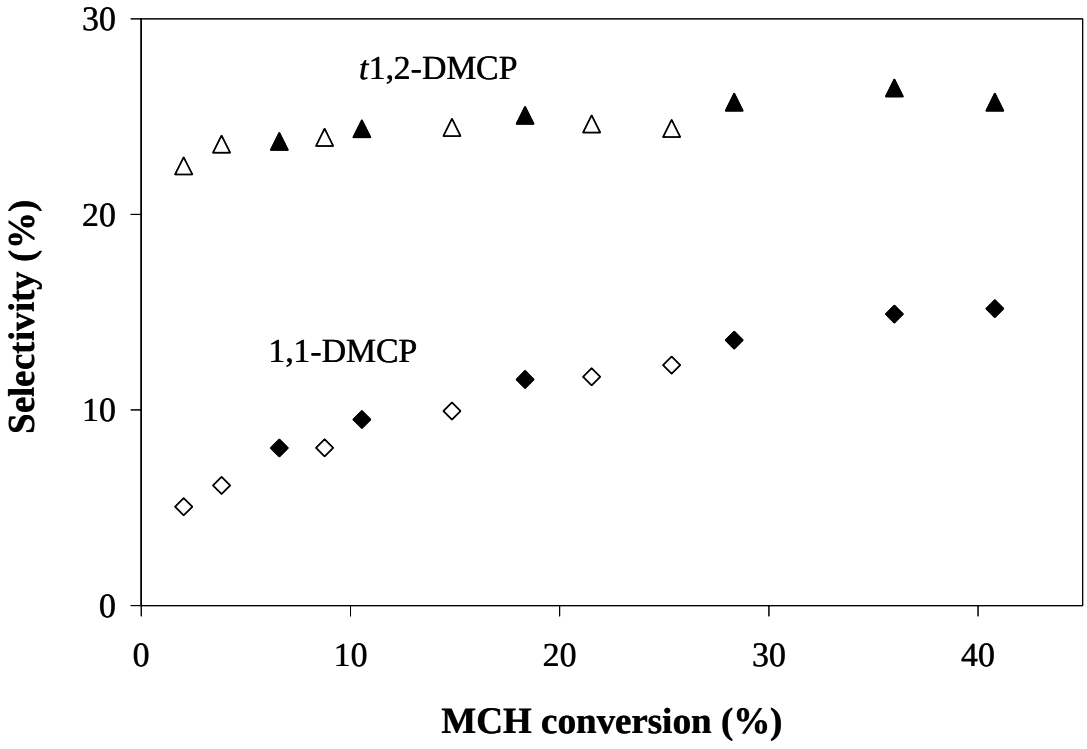

Figure 6.12a Selectivity (%) to RC products (ethylcyclopentane,ECP; 1,3-dimethylcyclopentane, 1,3-DMCP) plotted vs. MCH conversion (%) over Pt/CBV400 (solid) and Pt/CBV720 (open).

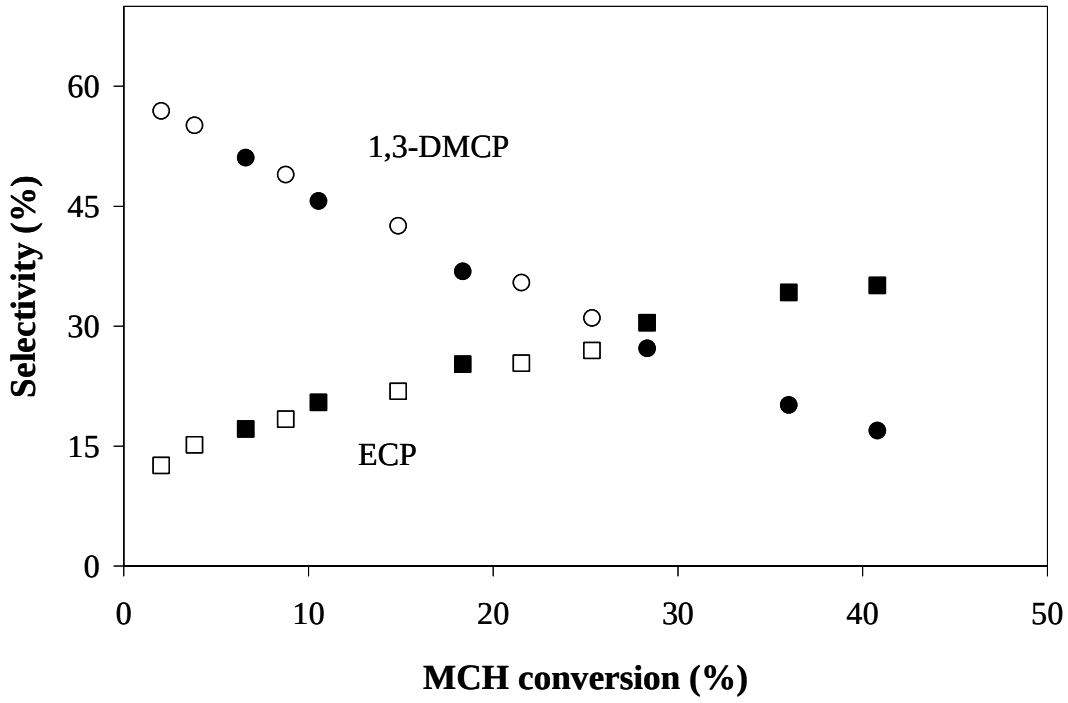

Figure 6.12b Selectivity (%) to RC products (1,1-dimethylcyclopentane, 1,1-DMCP; *trans*-1,2-dimethylcyclopentane, *t*1,2-DMCP) plotted vs. MCH conversion (%) over Pt/CBV400 (solid) and Pt/CBV720 (open).

6.4 Conclusions

The main conclusion of this work can be summarized as follows:

- A high acidic zeolite can be an effective catalyst for the ring contraction of the MCH compound, but the presence of Pt is better because of the suppression of the secondary reactions and low deactivation, as well as a large amount of 1,1-DMCP, which has a very high octane number.

- Large pore zeolites (FAU and BEA) are better for isomerization of the MCH reaction than the medium pore zeolite (MFI) because of less cracking products. This is due to a less restricted pore structure.

- The selectivities to RC isomers is highly dependent on the acidic strength but not the density of acid. The dibranching molecules (DMCPs) require a higher acid strength than monobranching molecule (ECP). However, the catalytic activity depends on the density of acid. The lower the acid density, the lower the MCH conversion.

- The presence of Pt enhances the formation of 1,1-DMCP, which is the most sterically hindered carbenium ion intermediate, due to providing surface hydrogen atoms that are readily used for the hydride transfer reaction.

Acknowledgments

We would like to acknowledge Oklahoma Center for Advancement of Science and Technology (OCAST) and ConocoPhillips for financial support of the ConocoPhillips Catalysis Lab at the University of Oklahoma.

LITERATURE CITED

1. Owen, K. and Coley, T.; *in* "Automotive Fuels Reference Book," 2nd Ed., Soc. Autom. Engin. Inc., Warrendale, PA (1995).
2. Absi-Halabi, M., Stanislaus, A. and Qabazard, H., *Hydrocrab. Process* **76**, 45 (1997).
3. Stanislaus, A. and Cooper, B.H., *Catal. Rev. Sci. Eng.* **36**, 75 (1994).
4. Corma, A., Gonzalez-Alfaro, V. and Orchilles, A.V., *J. Catal*. **200**, 34 (2001).
5. Eastwood, D., de Van, V. and Venne, H., *NPRA Annual meeting*, San Antonio, TX, (1990).
6. Lee, S.L., de Wind, M., Desai, P.H., Johnson, C.C. and Asim Mehmet, Y., *Fuel Reformulation* **5**, 26 (1993).
7. Khan, M.R. and Reynolds, J.G., *Chemtech* **26**, 56 (1996).
8. Unzelman, G.H., *Fuel Reformulation* **5**, 38 (1993).
9. http://journeytoforever.org/biodiesel_stana.html
10. Rhead, M.M. and Hardy, S.A., *Fuel* **82**, 385 (2003).
11. Schuetzle, D., *Environ. Health Perspect*. **47**, 65 (1983).
12. Maxwell, T.T. and Jones, J.C.; *in* " Alternative Fuels: Emissions, Economics, and Performance" p. 12, Society of Automotive Engineers, Inc. Warrendale, PA (1995).
13. Guru, M., Karakaya, U., Altiparmak, D. and Alicilar, A., *Energy Conversion and Management* **43**, 1021 (2002).
14. Knothe, G., Matheaus, A.C. and Ryan III, T.W., *Fuel* **82**, 971 (2003).
15. http://en.wikipedia.org/wiki/Steam_cracking
16. McVicker, G. B., Daage, M., Touvelle, M. S., Hudson, C. W., Klein, D. P., Baird, Jr., W. C., Cook, B. R., Chen, J. G., Hantzer, S., Vaughan, D. E. W., Ellis, E. S. and Feeley, O. C., *J. Catal*. **210**, 137 (2002).

17. Edmonds, T.; *in* "Catalysis and chemical process, (Pearce R. and Patterson W.R., editors)", p. 90. John Wiley & Sons, Inc., New York (1981).
18. Song, C. and Ma, X.L., *Appl. Catal. B* **41**, 207 (2003).
19. Kubicka, H. and Okal, J., *Catal. Lett.* **25**, 157 (1994).
20. Fu, J., *Chem. J. Chin. Univ.-Chin.* **16**, 461 (1995).
21. Tam, N.T., Cooney, R. P. and G. Curtheoys, *J. Catal.* **68**, 81 (1976).
22. Abbot, J. and Wojciechowski, B. W., *Canad. J. Chem. Eng.* **66**, 637 (1988).
23. Iglesia, E., Soled, S. L. and Kramer, G. M., *J. Catal.* **144**, 238 (1993).
24. Sato, K., Iwata, Y., Yoneda, T., Nishijima, A., Miki, Y. and Shimada, H., *Catal. Today* **45**, 367 (1998).
25. Miki, Y.and Sugimoto, Y., *Fuel Proc. Tech.* **43**, 137 (1995).
26. Kubicka, D., Kumar, N., Maki-Arvela, P., Tiitta, M., Niemi, V., Salmi, T. and Murzin, D.Y., *J. Catal.* **222**, 65 (2004).
27. Arribas, M.A. and Martınez, A., *Appl. Catal. A* **230,** 203 (2002).
28. Vasina, T. V., Masloboischikova, O.V., Khelkovslaya-Sergeeva, E.G., Kustov, L.M. and Zeuthen, P. *Stud. Surf. Sci. Catal.* **135** (2001).
29. Onyestyak, G., Pal-Borbely, G. and Beyer, H. K., *Appl. Catal. A* **229**, 65 (2002).
30. Schulz, H., Weitkamp, J. and Eberth, H., *Proc. 5th Internat. Congr. Catal.* **2**, 1229 (1973).
31. Kustov, L.M., Yu. Stakheev, A., Vasina, T.V., Masloboishchikova, O.V., Khelkovslaya-Sergeeva, E.G. and Zeuthen, P., *Stud. Surf. Sci. Catal.* **138,** 307 (2001).
32. Arribas, M.A., Concepción, P. and Martínez, A., *Appl. Catal. A* **267**, 111 (2004).
33. Arribas, M.A. and Martínez, A., *Stud. Surf. Sci. Catal.* **130**, 2585 (2000).
34. Arribas, M.A. and Martínez, A., Sastre, G., *Stud. Surf. Sci. Catal.* **142** 1015 (2002).

35. Rodriguez-Castellon, E., Diaz, L., Braos-Garcia, P., Merida-Robles, J., Maireles-Torres, P., Jimenez-Lopez, A. and Vaccari, A., *Appl. Catal. A* **240,** 83 (2003).
36. Zubin, C., Xianlun, X., Yutai, Q., Shuwen, L. and Bangfeng, Q, *J. Fuel Chem. Tech.* **29**, 12 (2001).
37. Paal, Z. and Tetenyi, P., *Nature* **267**, 234 (1977).
38. Sarkany, A., Gaal, J. and Toth, L., *Proc. Int. Congr. Catal. 7th*, p. 291, Tokyo (1980) Kodansha Ltd, Elsevier, Tokyo (1981)
39. Paál, Z. and Tétényi, P.; in "*Catalysis"* Vol. **5**, p. 80, Royal Society of Chemistry, London (1982).
40. Liberman, A.L., *Kinet. Catal.* **5**, 128 (1964).
41. Du, H., Fairbridge, C., Yang, H. and Ring, Z., *Appl. Catal. A* **294**, 1 (2005).
42. Bragin, O.V., Helkovskaya-Sergeeva, E.G., Preobrazhensky, A.V. and Liberman, A.L., *Dokl. Akad. Nauk SSSR* **214**, 103 (1974).
43. Gualt, F.G., *Adv. Catal.* **30**, 1 (1981).
44. Gualt, F.G., Amir-Ebrahimi, V., Garin, F., Parayre, P. and Weisang, F., *Bull. Soc. Chim. Belges* **88**, 475 (1979).
45. Paál, Z., *Adv. Catal.* **29**, 273 (1980).
46. Du, H., Fairbridge, C., Yang, H.and Ring, Z., *Appl. Catal. A* **294**, 1 (2005).
47. Chow, M., Park, S.H. and Sachtler, W.M.H., *Appl. Catal.* **19**, 349 (1985).
48. Zimmer, H. and Paal, Z., *J. Mol. Catal.* **51**, 261 (1989).
49. Zhuang, Y. and Frennet, A., *Appl. Catal. A* **134**, 37 (1996).
50. van Senden, J.G., van Broekhoven, E.H., Wreesman, C.T.J. and Ponec, V., *J. Catal.* **87**, 468 (1984).
51. Weisang, F. and Gault, F.G., *Chem. Comm.*, 519 (1979).
52. Galperin, L.B., Bricker, J.C. and Holmgren, J.R., *Appl. Catal. A* **239**, 297 (2003).
53. Teschner, D., Matusek, K. and Paal, Z., *J. Catal.* **192**, 335 (2000).
54. Figueras, F., Coq, B., Walter, C. and Carriat, J.Y., *J. Catal.* **169**, 103 (1997).

55. Kijenski, J. and Baiker, A., *Catal. Today* **5**, 1 (1989).
56. Emeis, C.A., *J. Catal.* **141**, 347 (1993).
57. Rossino, S., *Catal. Today* **77**, 467 (2003).
58. Santana, R.C., Do, P.T., Santikunaporn, M., Walter, W.E., Taylor, J.D., Sughrue, E.L. and Resasco, D.E., *Fuel* **85**, 643 (2006).
59. Kubička, D., Kumar, N., Mäki-Arvela, P, Tiitta, M., Niemi, V., Karhu, H., Salmi, T. and Yu. Murzin, D., *J. Catal*. **227**, 313 (2004).
60. Augusto, C.C.C., Zotin, J.L. and da Costa-Faro, A., *Catal. Lett.*, **75**, 37 (2001).
61. Le Bihan, L. and Yoshimura, Y., *Fuel*, **81**, 491 (2002).
62. Vaarkamp, M., Miller, J.T., Modica, F.S. and Koningsberger, D.C., *J. Catal.* **163**, 294 (1996)
63. de Graaf, J., van Dillen, A.J., de Jong, K.P. and Koningsberger, D.C., *J. Catal.* **203**, 307 (2001)
64. Lai, W.C. and Song. C., *Catal. Today* **31,** 171 (1996).
65. Mostad, H.B., Riis T.U. and Ellestad, O.H., *Appl. Catal.*, **58** 105 (1990).
66. Falabella Sousa-Aguiar, E., Mota, C.J.A., Murta Valle, M.L., Pinhel da Silva, M. and Forte da Silva, D., *J. Mol. Catal.* **104**, 267 (1996).
67. Jongpatiwut, S., Li, Z., Resasco, D.E., Alvarez, W.E., Sughrue, E.L. and Dodwell, G.W., *Appl. Catal.* **262**, 241 (2004)
68. Fenoglio, R.J., Nuñez, G.M. and Resasco, D.E., *Appl. Catal.* **63**, 319 (1990).
69. Schepers, F.J., can Senden, J.G., van Broekhoven, E.H. and Ponec, V., *J. Catal* **94**, 400 (1985).
70. Teschner, D. and Paál, Z., *React. Kinet. Catal. Lett.* **68**, 25 (1999).
71. Barron, Y., Maire, G., Muller, J.M. and Gault, F.G., *J. Catal.* **5**, 428 (1966).
72. Kramer, R. and Zuegg, H., *J. catal.* **80**, 446 (1983).
73. Gates, B.C., Katzer, J.R. and Schuit, G.C.A.; *in* "Chemistry of Catalytic Processes", p. 246, McGraw-Hill, New York (1995).

74. Santikunaporn, M., Herrera, J.E., Jongpatiwut, S., Resasco, D.E., Alvarez, W.E. and Sughrue, E.L., *J. Catal.* **228**, 100 (2004).
75. Weitkamp, A.W.; *in* "Advances in Catalysis and Related Subjects (Eley, D.D., Pines, H. and Weisz P.B., editors)" vol. 18, p.1, Academic Press, New York (1968).
76. Martens, J.A., Jacobs, P.A. and Weitkamp, J., *Appl. Catal.* **20**, 239 (1986).
77. Nakamura, I., Zhang, A. and Fujimoto, K., *Stud. Surf. Sci. Catal.* **94**, 464 (1995).
78. Nakamura, I. and Fujimoto, K., *Stud. Surf. Sci. Catal.* **100**, 235 (1996).
79. Corma, A., Miguel, P.J. and Orchillés, A.V., *J. Catal.* **145**, 171 (1994).
80. Jentoft, F.C. and Gates, B.C., *Top. Catal.* **4**, 1 (1997).
81. Ono, Y., *Catal. Today* **81**, 3 (2003).
82. Martens, J.A. and Jacobs, P.A., *Stud. Surf. Sci. Catal.* **137**, 663 (2001).
83. Corma, A., Planelles, J., Sánchez-Marín, J. and Tomás, F., *J. Catal.* **93** (1985).
84. Song, C.S. and Ma, X.L., *Int. J. Green Energy* **1**, 167 (2004).
85. Ringelhan, C., Burgfels, G., Neumayr, J. G., Seuffert, W., Klose, J. and Kurth, V., *Catal. Today* **97**, 277 (2004).
86. Weitkamp, J., Raichle, A., Traa, Y., Rupp, M. and Fuder, F., *Chem. Commun.*, 1133 (2000).
87. Raichle, A., Traa, T., Fuder, F., Rupp M. and Weitkamp, J., *Angew. Chem Int. Ed.* **40**, 1243 (2001).
88. Wang, J., Li, Q. and Yao, J., *Appl. Catal. A* **184**, 181 (1999).
89. Weitkamp, J., Raichle, A., Traa, Y., Rupp, M. and Fuder, F., *Chem. Commun.*, 403 (2000).
90. Raichle, A., Traa Y. and Weitkamp, J., *Appl. Catal. B.* **41**, 193 (2003).
91. Mignard, S., Caillette, Ph. and Marchal, N., *Chem. Ind.* **58**, 447 (1994).
92. Figueras, F., Coq, B., Walter C. and Jean-Yves Carriat, *J. Catal.* **169**, 103 (1997).

93. Belatel, H., Al-Kandari, H., Al-Khorafi, F., Katrib, A. and Garin, F., *Appl. Catal. A* **275**, 141 (2004).
94. Weitkamp, J., Jacobs, P.A. and Ernst, S.; *in* "Structure and Reactivity of Modified Zeolites" p. 279, Elsevier Sci. Publ., Amsterdam (1984).
95. Do, P.T., Alvarez, W.E. and Resasco, D.E., *J. Catal.* **238**, 477 (2006).
96. Miller, J.T., Meyers, B.L., Modica, F.S., Lane, G.S., Vaarkamp, M. and Koningsberger, D.C., *J. Catal.* **143**, 563 (1993).
97. Kip, B.J., Van Grondelle, J., Martens, J.H.A. and Prins, R., *Appl. Catal.* **26**, 353 (1986).
98. Kip, B.J., Duivenvoorden, F.B.M., Koningsberger, D.C. and Prins, R., *J. Catal.* **105**, 26 (1987).
99. Weitkamp, J., Jacob P.A. and Ernst, S., *Stud. Surf. Sci. Catal.* **18**, 279 (1984).
100. Calemma, V., Carati, A., Flego, C., Giardino, R. and Millini, R., *Prepr. Pap.-Am. Chem. Soc., Div. Fuel Chem.* **50**, 116 (2005).
101. Cid R. and Lopez Agudo, A., *React. Kinet. Catal. Lett.* **22**, 13 (1983).
102. Barton, D.G., Soled, S.L., Meitzer, G.D., Fuentes, G.A. and Iglesia, E., *J. Catal*. **181**, 57 (1999).
103. Iglesia, E., Soled, S.L. and Kramer, G.M., *J. Catal.* **144**, 230 (1993).
104. Pellet, R.J., *J. Catal.* **177**, 40 (1998).
105. Santiesteban, J.G., Calabro, D.C., Change, C.D., Vartuli, J.C., Fiebig, T.J. and Bastian, R.D., *J. Catal*. **202**, 25 (2001).
106. Ghosh, P., Hickey, K.J. and Jaffe, S.B., *Ind. Eng. Chem. Res.* **45**, 337 (2006).
107. Knocking characteristics of pure hydrocarbon. Special Technical Publication No. 225; American Society for Testing and Materials: West Conshohocken, PA (1958).
108. API Technical Data Book on Petroleum Refining, API: Washington, DC, (1986).
109. Foger, K., *J. Catal*. **78**, 406 (1982).
110. Foger, K. and Jaeger, H., *J. Catal.* **120**, 465 (1989).

111. Schtler, W.M.H. and Zhang, Z.C.; *in* "Advances in Catalysis, (Eley, D.D., Pines, H. and Weisz, P.B. (editors)" Vol. 39, p. 129, Academic Press, New York (1993).
112. Olah, G.A. and Molnár, A.; in "Hydrocarbon Chemistry" Wiley, New York (1995).
113. Blekkan, E.A., Cuong, P.H., Ledoux, M.J. and Guille, J., *Ind. Eng. Chem. Res.* **33**, 1657 (1994).
114. Paal, Z., Rath, M., Zhan, Z. and Gombler, W., *J. Catal*. **147**, 342 (1994).
115. Cuming, K. A. and Wojciechowshi, B.V., *Cata. Rev. Sci. Eng.* **38**, 101 (1996).
116. Wojciechowshi, B.V., *Cata. Rev. Sci. Eng.* **40**, 209 (1998).
117. Schulz, H.F. and weitkamp, J.H., *Ind. Eng. Chem. Prod. Res. Develop.,* **11**, 46 (1972).
118. Miyaji, A. and Okuhara, T., *Catal. Today* **81**, 43 (2003).
119. Schulz, H., Weitkamp, J.H. and Eberth, H.; in "Proc. 5th Int. Congr. Catal., (Hightower, J.W., editor)" Vol. 2, p. 1229, North-Holland Publishing Co., Amsterdam (1973).
120. Patrigeon, A., Benazzi, E., Travers, Ch. and Bernhard, J.Y., *Catal. Today* **65**, 149 (2001).
121. Santikunaporn, M., Alvarez, W.E. and Resasco D.E., (to be published).
122. Pope, T.D., Kriz, J.F., Stanciulescu, M. and Monnier, J., *Appl. Catal. A*. **233**, 45 (2002).
123. Valyon, J., Engelhardt, J., Lónyi, F., Kalló, D. and Gömöry, A., *Appl. Catal. A.* **229**, 135 (2002).
124. McVicker, G.B., Feeley, O.C., Ziemiak, J.J., Vaughan, D.E.W., Strohmaier, K.C., Kliewer, W.R. and Leta, D.P., *J. Phys. Chem. B* **109**, 2222 (2005).
125. Niwa, M. and Katada, K., *Catal. Surv. Jpn.* **1**, 215 (1997).
126. Seo, G., Kim, M.-Y. and Kim, J.-H., *Catal. Lett.* **67**, 207 (2000).

127. Nakao, R., Kubota, Y., Katada, N., Nishiyama, N., Kunimori, K. and Tomishige, K., *Appl. Catal. A* **273**, 63 (2004).

128. Katada, N., Igi, H., Kim, J.H. and Niwa, M., *J. Phys. Chem. B* **101**, 5969 (1997).

129. Lonyi, F., Valyon, J., *Thermochim. Acta* **373**, 53 (2001).

130. Kunieda, T., Katada, N. and Niwa, M.; *in* "Proceedings of the 12th IZC" Vol. 4, p. 2549, MRC (1999).

131. Miyamoto, Y., Katada, N. And Niwa, M., *Micropor. Mesopor. Mater.* **40**, 271 (2000).

132. Cerqueira, H.S., Rodrigues, M.G.F., Magnoux, P., Martin, D. and Guisnet, M. Stud.Surf. Sci. Catal. 130 (2000) 2477.

133. Satoh, D., Matsuhashi, H., Nakamura, H. and Arata, K., *Catal. Letters.* **89**, 105 (2003).

134. Câmara, L.D.T., Cerqueira, H.S., Aranda, D.A.G. and Rajagopal, K., *Catal. Today* **98**, 309 (2004).

135. Lacombe, S., Patrigeon, A. and Benazzi, E., *Stud. Surf. Sci. Catal.* **135**(Zeolites and Mesoporous Materials at the Dawn of the 21st Century), 4272 (2001).

136. Martens, J.A. and Jacobs, P.A.; *in* "Handbook of Heterogeneous Catalysis : Reaction mechanisms in acid catalysed hydrocarbon raction on zeolites, (. Ertl, G, Knozinger, H., Weitkamped, J., editors)", p.1137, VCH (1997).

PUBLICATIONS, PRESENTATION AND POSTERS

PUBLICATTIONS (PUBLISHED AND IN PROGRESS)

1. *"Catalytic Strategies for Improving Specific Fuel Properties"* Phuong T. Do, Steven Crossley, **Malee Santikunaporn**, Daniel E. Resasco (summitted in May 2006)
2. "*Ring Contraction and selective ring opening of naphenic molecules for octane number improvement*", **Malee Santikunaporn**, Walter E. Alvarez, Daniel E. Resasco. (in process)
3. *"Influence of the zeolite structure and acidity on the hydroisomerization of MCH"*, **Malee Santikunaporn**, Walter E. Alvarez, Daniel E. Resasco. (in process)
4. *"Enhancing the Selectivity of Decalin Ring Contraction Vs. Ring Opening by Tailoring the Acid Density and Pt particle location in Pt/HY Catalysts*", **Malee Santikunaporn**, Walter E. Alvarez, Daniel E. Resasco. (in process)
5. *"Evaluation of different reaction strategies for the improvement of cetane number in diesel fuels"*, Roberto Santana, Phuong T. Do, **Malee Santikunaporn**, Walter E. Alvarez, Joshua D. Taylor, Edward L. Sughrue, Daniel E. Resasco, *Fuel* 85 (2006) 643.
6. *"Combined deep hydrogenation and ring opening of poly-aromatic hydrocarbons for diesel quality improvement"*, Daniel E. Resasco, Phuong Do, Roberto Santana, Siriporn Jongpatiwut, **Malee Santikunaporn**, Andrea Beltramone, *Abstracts of Papers*, 229th ACS National Meeting, San Diego, CA, US, March 13-17, 2005.
7. *"Ring Opening of Decalin and Tetralin on HY and Pt/HY zeolite catalysts"*, **Malee Santikunaporn**, Jose E. Herrera, Siriporn Jongpatiwut, Daniel E. Resasco, Walter E.Alvarez, Ed L.Sughrue, *J. Catal.* 228 (2004) 100.

PRESENTATION AND POSTERS

1. *"Ring opening of Decalin and Tetralin on HY and Pt/HY catalysts"*, **Malee Santikunaporn**, Jose E. Herrera, Siriporn Jongpatiwut, Daniel E. Resasco, 51st Annual Pentasectional Meeting, Oklahoma Sections of American Chemical Societ, ConocoPhillips Technology Center, Bartlesville, OK, April 1, 2006. Final Program & Abstracts of Papers.
2. *"Enhancement of octane number in non-aromatic components of gasoline"*, **Malee Santikunaporn**, Daniel E. Resasco, 2006 Graduate Student Research & Creativity Endeavors/Poster Session, Oklahoma Memorial Union Beaird Lounge, University of Oklahoma, Norman, Oklahoma, US, March 30, 2006.
3. *"Strategies to maximize cetane number in diesel fuels"*, Phuong Do, Roberto Santana, **Malee Santikunaporn**, Siriporn Jongphatiwut, Daniel E. Resasco, Joshua Taylor, Walter E. Alverez, Ed L. Sughrue, 19th North American society of Catalysis Meeting, Philadelphia, Pennsylvania, US, May 22-27, 2005.
4. *"Ring opening of Decalin and Tetralin on HY and Pt/HY catalysts"*, **Malee Santikunaporn**, Jose E. Herrera, Siriporn Jongpatiwut, Daniel E. Resasco, Walter E.Alvarez, Ed L.Sughrue, Laurence Leid Gas Conditioning Meeting, Sam Noble Oklahoma Museum of Natural History, Norman, Oklahoma,US, Feb 28, 2005 (poster).
5. *"Combined deep hydrogenation and ring opening of poly-aromatic hydrocarbons for diesel quality improvement."*, **Malee Santikunaporn**, Jose E. Herrera, Siriporn Jongpatiwut, Daniel E. Resasco,Walter E. Alvarez, Ed L. Sughrue, AIChE National Annual Meeting. Austin, US, November 7-12, 2004.
6. *"Improving Diesel Fuel Using Combined Deep Hydrogenation and Ring-Opening"*, Siriporn Jongpatiwut, **Malee Santikunaporn**, Walter E. Alvarez, Ed L. Sughrue, Glenn W.Dodwell, Daniel E. Resasco. AIChE National Annual Meeting, Austin, US, November 7-12, 2004.

7. *"Combined deep hydrogenation and ring opening of poly-aromatic hydrocarbons for diesel quality improvement"*, Siriporn Jongpatiwut, **Malee Santikunaporn**, Jose E. Herrera, Daniel E. Resasco, Walter E. Alvarez, Ed L. Sughrue, Glenn W. Dodwellb. 13th International Congress in Catalysis, Paris, July 11-16, 2004.
8. *"Combined deep hydrogenation and ring opening of poly-aromatic hydrocarbons for diesel quality improvement"*, **Malee Santikunaporn**, Jose E. Herrera, Siriporn Jongpatiwut, Daniel E. Resasco, Walter E. Alvarez, Ed L. Sughrue, Hydroprocessing and Refining session. 18th Canadian Symposium on Catalysis. Montreal, Canada. May 23-28, 2004.

APPENDIX

Table A1 Product distribution and conversion of decalin over PtPdIr supported on different acidities of HY zeolites. Reaction conditions: Total pressure = 2 MPa, Temperature = 533 K, LSV = 1.89 h^{-1}, and H_2/HC molar ratio = 65

	PtPdIr/HY1	**PtPdIr/HY2**	**PtPdIr/HY3**
Trans -decalin (wt%)	90.9	54.1	65.8
Cis -decalin (wt%)	5.0	2.8	9.8
Conversion*	4.2	43.1	24.4
Products		Yield (wt%)	
C1-C5	0.1	1.1	0.7
C6-C9	0.4	13.9	7.5
C10			
Ring opening products	0.9	14.9	8.7
Ring contraction products	2.7	13.2	7.4
Heavy products	0.0	0.0	0.0

* Conversion based on *trans*-decalin and *cis*-decalin

Table A2 Product distribution and conversion of decalin over various metals supported on HY zeolite. Reaction conditions: Total pressure = 2 MPa, Temperature = 533 K, LSV = 1.89 h^{-1}, and H_2/HC molar ratio = 65

	Ir/HY	**Pd/HY**	**PdPt/HY**	**PtIr/HY**	**PdPtIr/HY**
Trans-decalin (wt%)	70.7	75.7	72.3	67.5	78.9
Cis-decalin (wt%)	13.3	20.1	10.7	10.0	10.2
Conversion*	16.0	4.1	17.0	22.5	10.9
Products	Yield (wt%)				
C1-C5	1.4	0.9	0.2	1.8	0.9
C6-C9	4.1	1.0	4.5	4.3	2.7
C10					
Ring opening products	5.4	0.7	4.5	9.4	5.7
Ring contraction products	5.1	1.6	7.9	7.1	5.1
Heavy products	0.0	0.0	0.0	0.0	0.0

* Conversion based on *trans*-decalin and *cis*-decalin

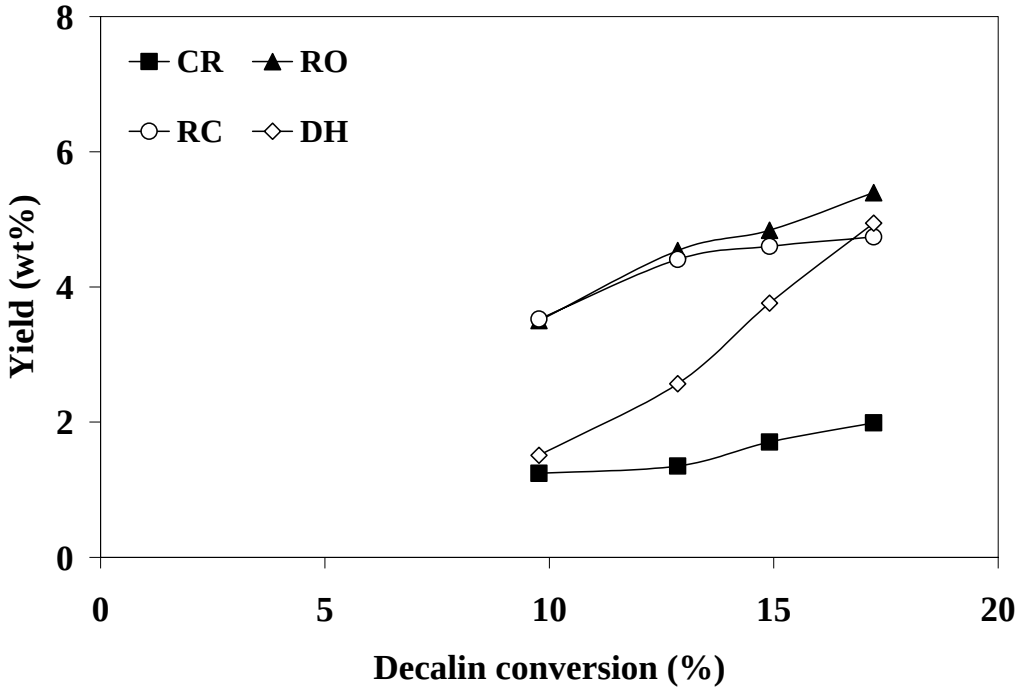

Figure A1. Product distribution of decalin ring opening on PtPdIr/HY3 at different space velocities (different conversions). Reaction conditions: Total pressure = 0.27 MPa, Temperature = 533 K, and H_2/HC molar ratio = 65 after time on stream = 270 min. (CR: Cracking Products; RO: ring opening products; RC: ring contraction products; DH: dehydrogenation products).

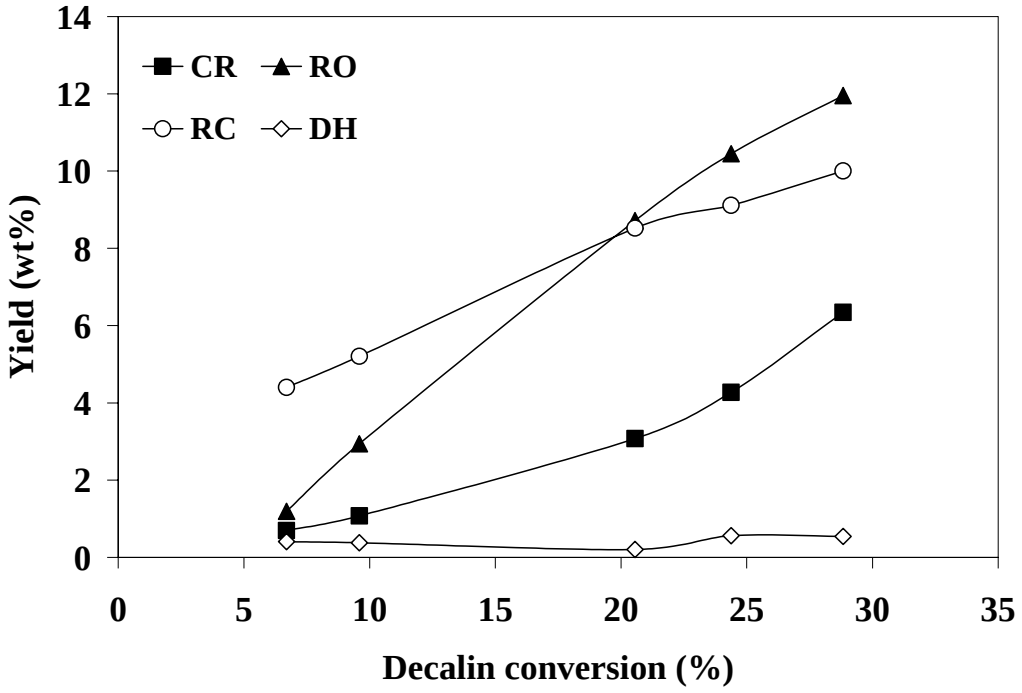

Figure A2. Product distribution of decalin ring opening on PtPdIr/HY3 at different space velocities (different conversions). Reaction conditions: Total pressure = 2 MPa, Temperature = 533 K, and H_2/HC molar ratio = 65 after time on stream = 270 min. (CR: Cracking Products; RO: ring opening products; RC: ring contraction products; DH: dehydrogenation products).